Affimer Inhibition of Verona Integron-encoded Metallo-β-Lactamase 1

Trent McLean-Ash

201146988

Submitted in part fulfilment of the requirements of the degree of

Master of Science in Programme of Study

MRes Molecular and Cellular Biology

Faculty of Biological Sciences Undergraduate School

University of Leeds, Leeds, LS2 9JT

June 2022

Word count: 23686

The candidate confirms that the work submitted is his own and that appropriate credit has been give where reference has been made to the work of others.

Acknowledgements

I would like to express my sincere thanks to Dr Darren Tomlinson for affording me this opportunity and for his support throughout this project. Thanks also to Dr Christian Tiede who is always willing to share his extensive knowledge of Affimers, and to Professor Alex O'Neill for his support and supervision.

My thanks to everyone in the Tomlinson lab for their friendship, support and guidance. Thanks to Annie Herbert for being an endless source of knowledge and encouragement. To my family and friends, I am constantly thankful for your help, patience, and willingness to pretend to understand me when I talk to you about what I do. Thanks to Dr Matt Lees for always reminding me to dot my i's and cross my T's. Thanks to Ashley for always telling me to get back to work whenever he sees me.

Abstract

Metallo-β-lactamases (MBLs) are a class of enzyme that hydrolyse the β-lactam ring in β-lactam antibiotics through their active site Zn^{2+} rendering them inactive. Verona Integron-encoded metallo-β-lactamase 1 (VIM-1) is a class B1, group 3, carbapenemase which is easily disseminated through the plasmid $bla_{VIM,}$ and offers bacteria broad-spectrum resistance to almost all known β-lactam antibiotics. A combination of β-lactamase inhibitors with β-lactam antibiotics is currently the most reliable method of dealing with resistant pathogens, but there are currently no clinically available inhibitors of this class of MBL.

Affimers, a class of non-antibody binding proteins could potentially offer an alternative source of novel MBL inhibitors. An Affimer that binds and inhibits New Delhi metallo-β-lactamase (NDM-1), a structurally similar MBL to VIM-1, has previously been identified. It was proposed that utilising similar screening methods, Affimer reagents could be raised against VIM-1 also to bind and modulate its activity. Though further study is needed, as a result of this work, an Affimer (Affimer61) was identified that was capable of reducing VIM-1's hydrolysis of nitrocefin substrate by 47%.

Contents

Abbreviations

2TY	2x Tryptone and Yeast
ABC	ATP-Binding Cassette
Aff	Affimer
AMR	Antimicrobial Resistance
BAP	Biotin Acceptor Peptide
BSA	Bovine Serum Albumin
BSTG	BioScreening Technology Group
DMSO	Dimethyl SulfOxide
DNA	Deoxyribonucleic Acid
E. coli	*Escherichia coli*
EDTA	EthyleneDiamineTetraacetic Acid
EPI	Efflux pump inhibitor
ELISA	Enzyme-Linked Immunosorbent Assay
ESBL	Extended-Spectrum β-Lactamase
EU	European Union
HEPES	4-(2-hydroxyethyl)-1-piperazineethanesulfonic acid
HRP	Horse Radish Peroxidase
IC50	Inhibitory concentration – 50%
IMP	Imipenemase
IPTG	IsoPropyl β-D-1 ThioGalactopyranoside
K. pneumoniae	*Klebsiella pneumoniae*
Kb	Kilobase
LB	Luria Broth
MATE	Multidrug and Toxic Compound Extrusion
MBL	Metallo-β-Lactamase
MDR	Multi-Drug Resistance
MGE	Mobile Genetic Element
MIC	Minimum Inhibitory Concentration
MRSA	Methicillin-Resistant *Staphylococcus aureus*
NDM-1	New Delhi Metallo-β-lactamase
NMR	Nuclear Magnetic Resonance
NPs	Natural Products
OD	Optical Density
OM	Outer Membrane
OXA	Oxacillinase
PBP	Penicillin Binding Protein
PCR	Polymerase Chain Reaction
PDB	Protein Data Bank
RNA	Ribonucleic Acid
SBL	Serine β-lactamase
SDS-PAGE	Sodium Dodecyl Sulphate-Polyacrylamide Gel Electrophoresis
SEC	Size Exclusion Chromatography
SMR	Small Multidrug Resistance
SOE	Splicing by Overhang Extension
UK	United Kingdom
VIM	Verona Integron-encoded Metallo-β-lactamase
VR	Variable Region
WHO	World Health Organisation

1. Introduction

1.1. Antibiotic Discovery

The complete history of antibiotics is long and well documented. The "modern era" of antibiotics is often identified by two distinct discoveries, that of Paul Ehrlich in the 1880's, and that of Alexander Fleming in 1928 and, while ground-breaking, they certainly are not alone in deserving of accolades.

A German physician at various universities, Paul Ehrlich's training included the use of different dyes to stain cells selectively. Having access to various different dyes, he noticed that they would affect variants of cells in different ways. This indicated to Ehrlich that divergent cellular processes must be occurring across cell types. He surmised that there must be a way to target bacterial cells alone; this famously became his "Zauberkugel" or "magic bullet" theory [1]. In 1904 he began an early iteration of a systematic screening program on infected rabbits to identify a drug against syphilis, an incurable disease at the time[2]. Working with Alfred Bertheim and Sahachiro Hata, they synthesised organoarsenic derivatives of Atoxyl. In their 600th series of testing, they discovered number 606, which cured the syphilis-infected rabbits and entered limited human trials. Later named Salvarsan, it was a highly prescribed drug until penicillin replaced it twenty years later [2]. This screening method was adopted by the pharmaceutical industry and has been used to identify a number of drugs – including antimicrobials.

Though Salvarsan is regarded as one of the first prescribed drugs to fit under the broad header "antimicrobial", attention should be paid to another antibacterial drug, belonging to the sulphonamide group, Prontosil. In 1932, German pathologist Gerhard Domagk and his fellow colleagues demonstrated the use of sulphonamides to counteract the bacteria that resulted in instances of blood poisoning, even going so far as to administer it to his own daughter who was suffering from a streptococcal infection – saving her life[3]. For this discovery, Domagk was awarded the Nobel Prize in Physiology or Medicine 1939, but was forced by the Nazi party to refuse the award, and was arrested and detained. It wasn't until 1947, after the conclusion of the Second World War that he received his prize but was not awarded the monetary portion due to the time elapsed[3].

Some years later Alexander Fleming, a persistent Scottish physician and microbiologist, took advantage of a rather fortuitous event to discover penicillin – the first broad spectrum antibiotic. Though what followed was 12 years of attempting to expound the advantages of penicillin to chemists, he eventually gave up in 1940[4]. Fortunately, that year, this antibiotic was purified and eventually synthesised by the chemists Florey and Chain in sufficient quantities for clinical testing, which allowed for its commercial success. For this, all three shared the Nobel Prize in Physiology or Medicine in 1945[5].

Fleming's discovery was not the only one that brought about this era, however. The work of Selman Waksman throughout the 1930's had focused on the systematic production of antimicrobials sourced from actinomycetes[6], and natural products (NPs) by the genus *Streptomyces*. It was through his endeavours that a novel screening platform was popularised – dubbed the Waksman platform - which consists of identifying zones of inhibition on an agar plate by placing soil-borne antibiotic producers over a field of bacteria [7]. Waksman himself described an antibiotic as "inhibiting the…activities of bacteria…by a chemical substance of microbial origin"[8].

This series of new screening techniques heralded what is commonly referred to as the "golden age" of antibiotics, described generally between the late 1940's and 1960's, wherein discoveries were

made swiftly, antibiotics and derivatives were rapidly identified, purified, then placed on the market for consumption, though it should be noted that new antibiotics continued to be marketed by pharmaceutical companies at a lower frequency into the 1990's. The reason for this moniker being such that heretofore unknown or unidentified antibiotics could be discovered by way of the Waksman platform, and the throughput methods of Ehrlich. Figure 1.1.1 shows an inexhaustive list of the discoveries made since the 1900's. An earlier use of an arguable antibiotic was Pyocyanase, from what is now called *Pseudomonas aeruginosa.* Emmerich and Löw used prepared extracts from this bacterium against a variety of diseases in a clinical setting, having noticed both their effects against pathogenic bacteria. However, the treatment was discovered to be inconsistent and toxic to the human host, and was thus abandoned [9].

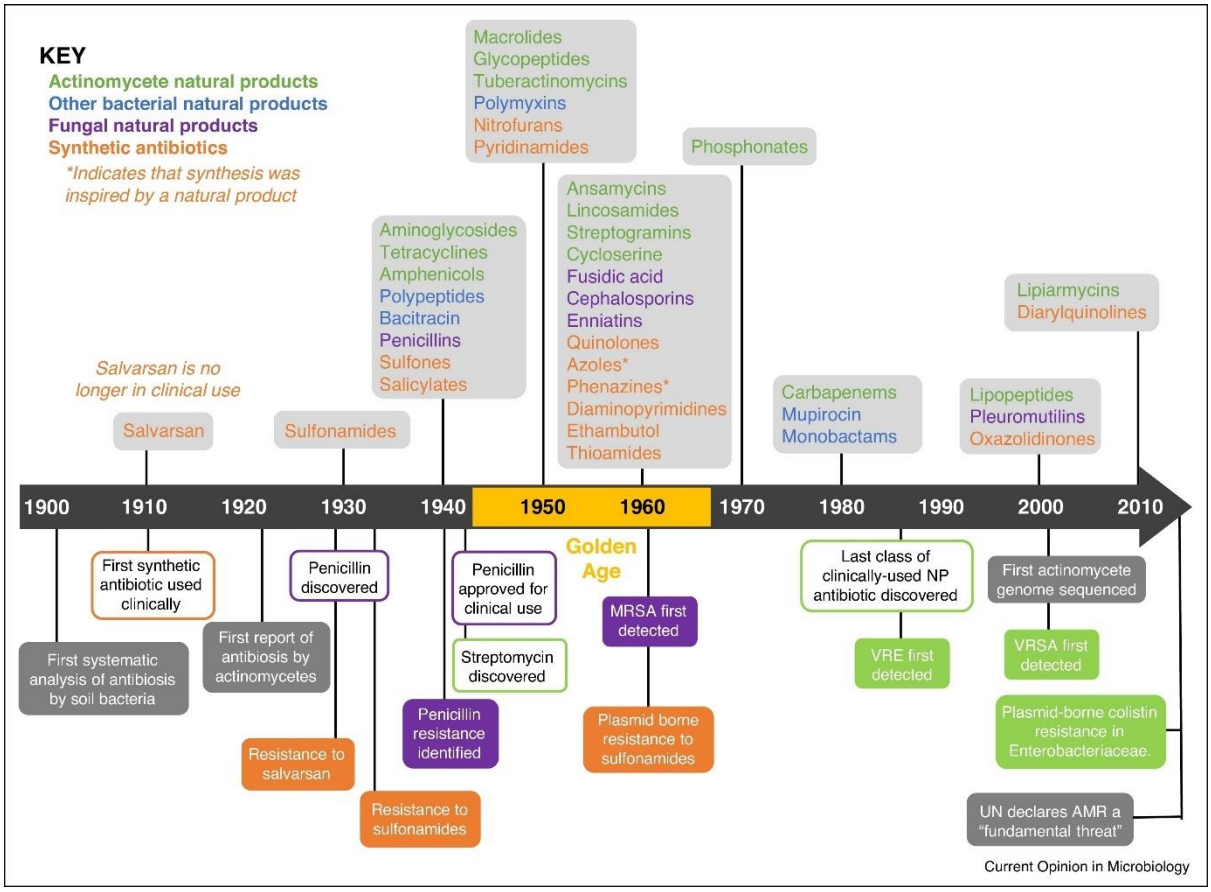

Figure 1.1.1. Antibiotic discovery spanning 1900-2010. This timeline demonstrates an inexhaustive list of antibiotics, from whence they were sourced, and the decade they became clinically available, as well as when resistances were developed. Image sourced from Hutchings et al., 2019[10].

1.1.2. Antibiotic Resistance

During the period in which antibiotics were discovered and utilised, so too was evidence shown of bacterial resistance to these treatments. Dubbed antibiotic resistance but held under a wider umbrella of antimicrobial resistance (AMR), these terms describe the numerous ways in which bacteria have mutated or otherwise evolved mechanisms to avoid inhibition by these chemotherapeutic techniques. There are numerous ways in which they accomplish this, the primary four general categories of resistance mechanism are; efflux, target mutation, target bypass, and antibiotic inactivation[11]. Excessive use and prescription of the plethora of new drugs elicited

selective pressure resulting in mechanisms of resistance in bacterial pathogens. Reductions in permeability, efflux pumps specific for antibiotics, mutations in transpeptidases as well as β-lactamase enzymes all function to restore cellular function in the presence of antibiotics [11].

Mutation in either target genes or proteins for antibiotics can result in a change in susceptibility, coupled with this, mutations that result in upregulation of certain proteins can also aid resistance [11]. In 2014, a study of clinical isolates of *Klebsiella pneumoniae* showed a change in resistance to Colistin, whereby only a single amino acid change in protein PmrB was responsible for upregulation of downstream operons that gave colistin resistance in *K. pneumoniae* [12]. VIM-4, a variant of the resistance enzyme Verona Integron-encoded metallo-β-lactamase (VIM) has one amino acid mutation, and one insertion (Arg44 and Ser265Arg respectively) and increases resistance to carbapenems [13][14]. A well-documented antibiotic resistance strain is methicillin-resistant *Staphylococcus aureus* (MRSA). MRSA is a strain of *S. aureus* which historically acquired a *MecA* gene that encodes a class B penicillin binding protein, PBP2a which is able to catalyse cell-wall crosslinking even in in the presence of β-lactam antibiotics [15]. It manages to retain its function as well as its resistance by having a closed active site covering its active-site serine in a tight groove to which the β-lactam cannot gain access, but undergoing allosteric modulation which opens the active site to perform transpeptidation [15].

Porins are protein channels found in Gram-negative bacteria that allow passive entry from the outer membrane into the periplasmic space to hydrophilic compounds, including several β-lactams and licosamides, but not glycopeptides which, due to their size, are unable to pass through. Through porin upregulation, cellular permeability can be mitigated. Choi and Lee found that by assessing *omp* gene mutants (*ompA, ompC, ompF*) they could analyse *E. coli*'s susceptibility to various antibiotics [16]. Deletion of the *ompC* gene resulted in MICs for some antibiotics decreasing, and others increasing. Deletion of the *ompA* gene showed the OmpA protein was important in membrane integrity but had little effect on antibiotic resistance[16]. Lastly, the deletion of the *ompF* gene showed a significant increase in resistance to β-lactam antibiotics[16].

Efflux pump systems in Gram-negative bacteria work to bestow resistance by pumping antibiotics out of the cytosol into either the periplasmic space or through the outer membrane outside of the bacterial cell. There are five classes that function against antimicrobials; the ATP-binding cassette (ABC) family, the major facilitator superfamily (MFS), the small multidrug resistance family (SMR), resistance-nodulation-division (RND) family, and the multidrug and toxic compound extrusion (MATE) family [17]. In *K. pneumoniae* it has been demonstrated that inactivation of efflux pumps by an efflux pump inhibitor (EPI) can increase susceptibility to a host of antibiotics [18]. By using phenylalanine-arginine β-naphthylamide (PaβN) to inactivation efflux pumps, and in combination with various antibiotics Pages et al., decreased MICs of *K. pneumoniae* of ofloxacin, erythromycin, and chloramphenicol substantially[18]. *S. aureus* has also been shown to upregulate expression of *norB* in acidic pH, and so too increase resistance to moxifloxacin, demonstrating that environmental variables can have an effect on antibiotic resistance when referring to efflux pumps[19].

Horizontal gene transfer was discovered as early as the 1950's in Japan and is now understood to be the transference of mobile gene elements (MGEs) between bacteria either through transformation, conjugation, or transduction. One such example is the resistance Integron; these are segments of dsDNA which carry drug-resistant genes within a gene cassette. Localised to a transferrable plasmid, they can be disseminated in both inter- and intra-bacterial species. This process is summarised in Figure 1.1.2.1 [20].

Observations in an internal medicine unit in France in 2011 showed a nosocomial outbreak of *Enterobacter cloacae* producing bla_{OXA-48} suggesting that not only did this plasmid transfer to other patients within the wing within 3-16 days, but to other bacteria within the primary patients gastrointestinal carriage, as verified by PCR [21]. This is merely a single example of how swiftly MGEs can transfer.

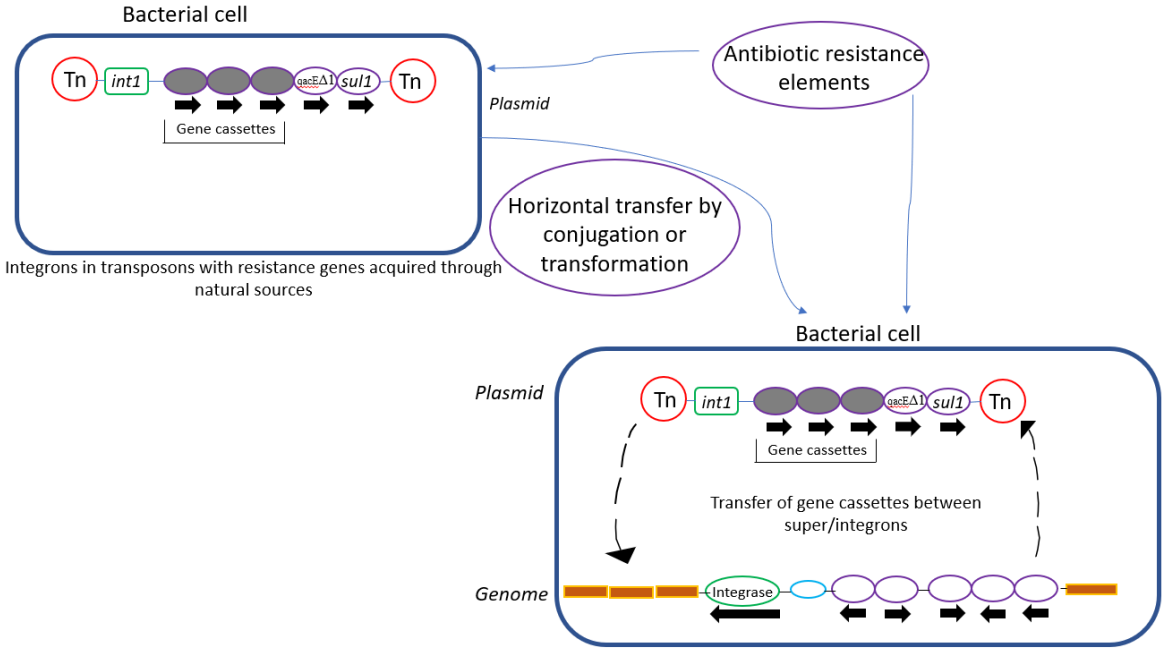

Figure 1.1.2.1. Integrons with antibiotic resistance elements being transferred between cells. Mobile integrons (top left) feature a promoter region *Pc,* a recombination site *attI,* and a gene for integrase *intI*, and have capacity for only a few antibiotic resistance cassettes. Super-integrons (bottom right), owing to their larger size, have the capability to store upwards of 200 cassettes and are found in many different bacterial species. Figure shown here has deleted transposon genes so is not self-mobilizable but can be integrated onto a plasmid for transmission. Image based upon Akrami et al., 2019[20].

It can also be noted that while horizontal gene transfer seems to be the a preferred method of antibiotic resistance development for certain organisms such as *P. pneumoniae*, mutation appears to be more important for others, such as mycobacteria which appears to be unable to acquire new DNA as efficiently as other organisms[22].

All of these factors cultivate a bleak view for the near future, with a government-backed report predicting that by the year 2050, 10 million people will die from drug-resistant infections per year [23]. Coupled with this, the expected cost of treatment for low-case to high-case scenarios could run anywhere from $300 billion - $1200 billion respectively by the same year [24]. This points towards a need for both new and alternative technologies that can mitigate this spread. Moreover, the relative cost/reward model of attempting to discover new antibiotics is prohibitive, extensive and labour-intensive, leading many companies to avoid making an investment. Ryan Chapman from Wellcome reported “it can take 10-15 years and over $1 billion to develop a new antibiotic”[25]. As governments are taking steps to reduce the number of antibiotics being prescribed, this also reduces the relative monetary gain from discovering a new antibiotic, when compared to the sale of “quality-of-life” drugs[26].

1.2. Gram-negative Bacteria

One of the difficulties in the use and identification of antimicrobials is the difference between bacteriological species. Separating bacteria into two distinct categories is one of the easiest ways to swiftly categorise them, based on their response to Gram stain. This technique was created by the Danish bacteriologist Hans Gram, and works to differentiate bacteria based on the composition of their cell walls [27]. Gram-positive cells have a layer of thick peptidoglycan, in which a crystal violet stain can be sequestered, shown best in Figure 1.2.1. On the other hand, Gram-negative cells possess a thinner 7-8 nm layer, which does not hold the stain as well and allows it to be washed off in the presence of ethanol.

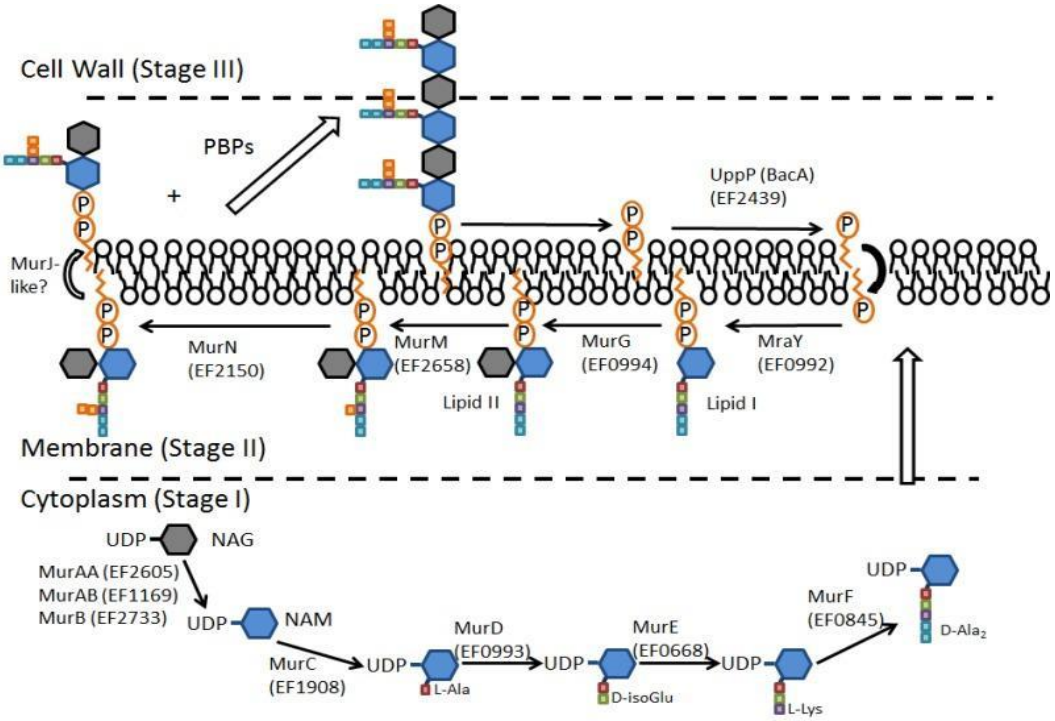

Figure 1.2.1. The biosynthesis of peptidoglycan and construction of cell wall. Initial steps of the cell wall biosynthesis occur in the cytoplasm, with UDP-sourced N-acetyl glucosamine (UDP-NAG) converted through MurA and MurB along with pyruvate into UDP-NAM. Three amino acids are then added to the stem peptide in a stepwise reaction, L-alanine, D-isoglutamine and L-lysine, the synthetases MurC, MurD, and MurE responsible for these, respectively. The MurF transferase is then responsible for the addition of the final two D-alanines. This finished molecule, referred to as Park's nucleotide, is then used in the second stage of cell wall synthesis. It is transferred to the cytoplasmic face of the cell membrane by undecaprenol, and MraY catalyses a transfer to the C55-isopenoid carrier. MurG then adds UDP-NAG to this generated lipid I, resulting in lipid II. From here, MurM and MurN sequentially add cross-bridge peptides and L-Ala to the precursor. The transference to the outer face of the membrane is then accomplished through precisely unknown - but speculated to be different - mechanisms dependent upon the strain of bacteria. Once in the outer facing membrane, penicillin binding proteins (PBPs) catalyse the final stage of assembly by removing the peptidoglycan precursor through transglycosylation from the lipid carrier onto the nascent peptidoglycan chain. Cross-linking new glycan chains to existing peptidoglycan is reliant upon the D-Ala terminus [28]–[30]. Image sourced from Hancock et al., 2014 [31].

This thicker layer of peptidoglycan can work as a protective barrier against some antibiotics, limiting the ability of some broad-spectrum antimicrobials. Its monomeric structure and linkage can be seen in Figure 1.2.2. It can also serve well as protection from osmotic pressure from extraneous sources,

but vital steps in its synthesis also work as targets for certain antibiotics. This difference between bacterial species provides another challenge in finding an appropriate broad spectrum antimicrobial agent.

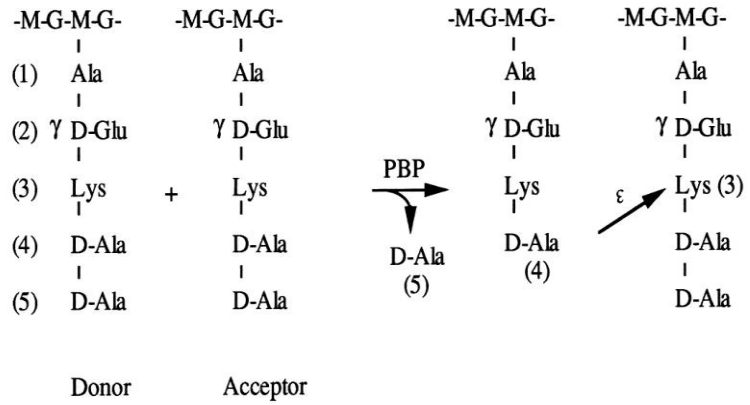

Figure 1.2.2. Structure of a peptidoglycan monomer and the mechanism of its linkage through transpeptidation. The high specificity of transpeptidase forms a peptide bond between a donor carboxyl group in position 4 (D-alanine) and an acceptor peptide (L-lysine), subsequently releasing the donor. Image sourced from van Heijenoort et al., 2000 [32].

1.3. β-lactam Antibiotics

β-lactam antibiotics are currently the best-selling and most prescribed antimicrobial drugs – due to their broad spectrum and relative safety profile [33]. The structural similarity of β-lactam antibiotics is in the presence of a (at minimum) four-member β-lactam ring which mimics the stem peptide's D-Ala structure used in the creation of the peptidoglycan cell wall, shown in Figure 1.3.1.1. This similarity allows the antibiotic to mimic the structure of a stem peptide, and thereby sequester penicillin binding proteins and bind them, rendering them ineffective. This, in high enough numbers, leads to the cell's death through osmotic pressure or through cell lysis. β-lactam antibiotics are generally separated into four different classes; penicillin's such as penicillin and ampicillin, cephalosporins such as cefotetan and cefepime, monobactams such as aztreonam, and carbapenems such as imipenem and meropenem. Despite all featuring the same β-lactam ring, they are not interchangeable, and each have their own minimum inhibitory concentrations (MIC's) and indications for use in a clinical setting. Even variants of the same MBL can have different susceptibilities, for example VIM-2 has an MIC of 64 and 128 (μg/mL) against ampicillin and cefoxitin respectively, against those same antibiotics a W87F mutation has an MIC of 8 and 8 μg/mL[34]. This, coupled with reports that therapeutic drug monitoring is not routinely reported for MIC's can work against efforts to track how well our current spectrum of antibiotics is working [35].

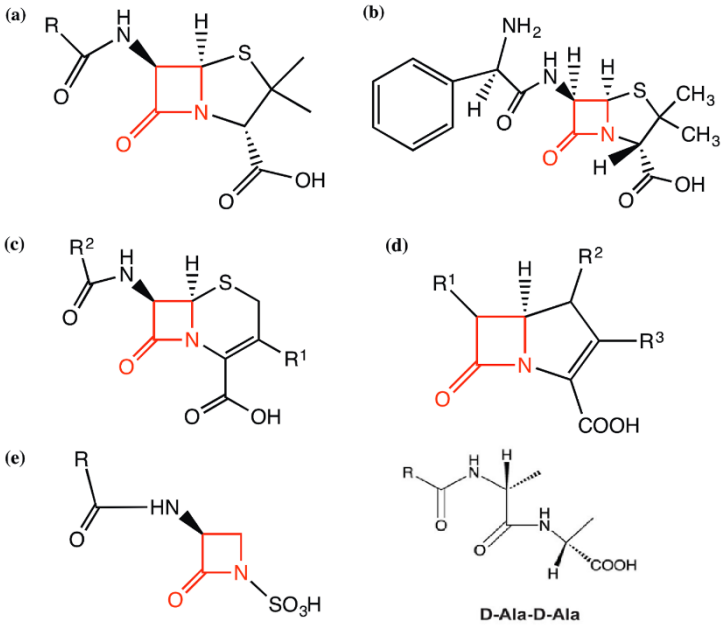

Figure 1.3.1.1. Basic structure of the major groups of β-lactam antibiotics. (A) penicillin's, (B) ampicillin, (C) cephalosporins, (D) carbapenem's, (E) monobactams. Of particular import is the red β-lactam ring which represents the D-Ala of the stem peptide which is featured bottom right. Image sourced from Lee et al., 2016 [36].

1.4. β-lactamase Enzymes

A bacterial cell's ability to avoid cell lysis from β-lactam antibiotics stems from their use of β-lactamase enzymes, which recognise β-lactams as substrates. β-lactamases are proteases that dissociate peptide bonds, targeting the -CO-NH structure within the β-lactam ring, giving them specificity for the mimic of a stem peptide, and leaving stem peptides unharmed. Some evidence points towards a co-evolution of PBP and class A β-lactamase, due to their similar structure and mechanistic characteristics, including their active site motifs [37]. There are two methods of classification for β-lactamases, by their molecular structure – Ambler classes – and their functional classification – Bush-Jacobi-Medeiros [38]. These are summarised in Figure 1.3.2.1.

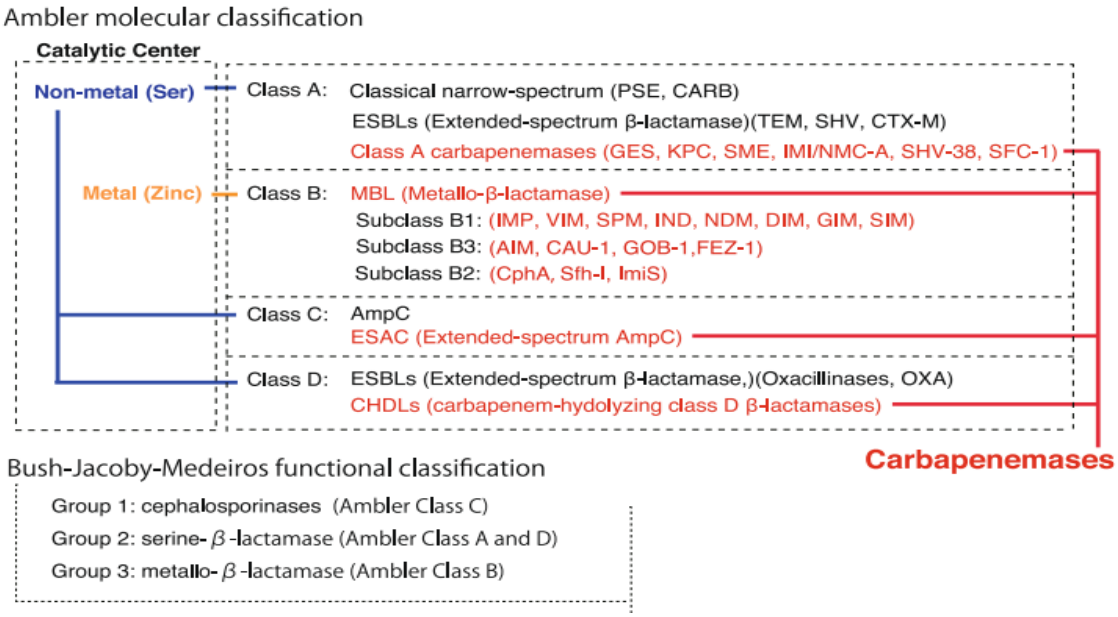

Figure 1.3.2.1. Ambler and Bush-Jacoby-Mederios classifications and where each β-lactamase fall into them. VIM-1 is a class B, subclass B1, group 3 enzyme. Image sourced from Sawa et al., 2020[38].

The motifs of the Ambler classes are defined by the primary sequences of the proteins. Classes A, C, and D utilise an active site serine as a nucleophile to hydrolyse β-lactams via a covalent acyl-enzyme intermediate [40]. Class B Ambler class fall under Group 3 of Bush-Jacoby-Mederios and commonly utilise either one or two Zn^{2+} ions in their active site - and are thus referred to collectively as metallo-β-lactamases (MBLs). The hydrolytic mechanism used by this class of β-lactamases indicates that an -OH group from a molecule of water is coordinated by the zinc ions and used to hydrolyse the amide bond in a β-lactam. The preferred substrates of these MBLs include most β-lactams, including carbapenems, which are generally considered a last resort when treating Gram-negative bacterial infections [41].

There are currently several different MBLs identified, with variants within each familial group. These include; imipenemase (IMP), New Delhi (NDM), Germany imipenemase (GIM), Sao Paulo (SPM), Florence imipenemase (FIM), and Verona Integron-encoded (or integrated-encoded) MBL (VIM). The vast spread of MBLs comes from their ability to be encoded on MGEs, whether that be plasmids, chromosomes, integrons, or transposons.

Within the MBL classifications, there are three further subclasses; B1 (VIM, IMP, NDM, SPM), B2 (Sfh-1, ImiS), and B3 (CAR, BAU, GOB). The subclasses are based on the amino acid sequences in

each protein, though similarity between them can be as low as 20%[42]. Despite this, their structural layout when viewed through X-ray is similar. A distinctive αβ/βα sandwich fold that holds an active site between these domains [14].

1.5. Verona Integron-encoded Metallo- β-lactamase (VIM)

Verona Integron-encoded Metallo-β-lactamase (VIM) is a Bush-Jacoby-Mederios group 3, Ambler class B β-lactamase. First described in the Verona University Hospital, Italy in 1999, VIM-1 was found in a clinical isolate of *P. aeruginosa* [43]. Initially only of minor concern, due to the prevalence of this MBL in species of only minor clinical relevance, and when compared to the spread of other MBLs such as NDM-1 (VIM was initially prevalent only in Italy and Greece), over time the promiscuity of this class 1 Integron encoded bla_{VIM} has seen its relevance greatly increase, along with the discovery of multiple other variants. Figure 1.4.1 shows VIM-expressing dissemination in enterobacteria as of 2011. Of particular concern is this MBLs ability to hydrolyse not only standard β-lactams, but also carbapenems (though efficiency can differ between variants), which are commonly used against multi-drug resistant infections, often as a last resort [44].

A study in 2019 in a hospital in the Netherlands over a period of eight years found that VIM positive *P. aeruginosa* nosocomial infections had a direct link to mortality. Of 198 patients with an identified positive culture, 48% died, and of these 22.4% were judged to have a definite relation to the infection, 25.4% were judged to have been probably or possibly related to infection [45]. While acquisition of MBLs is of course of concern when dealing clinically with *P. aeruginosa,* it should be noted that its carbapenem resistance is commonly found to be instead due to expression of an inherent AmpC β-lactamase and overexpression of efflux pumps. Of 190 isolates of *P. aeruginosa* isolates collected from nosocomial outbreaks in Spain in 2008, only two were found to produce VIM-2, whereas 39% were found to have some form of overexpression resulting in increased resistance to a host of combination antibiotic therapies [46].

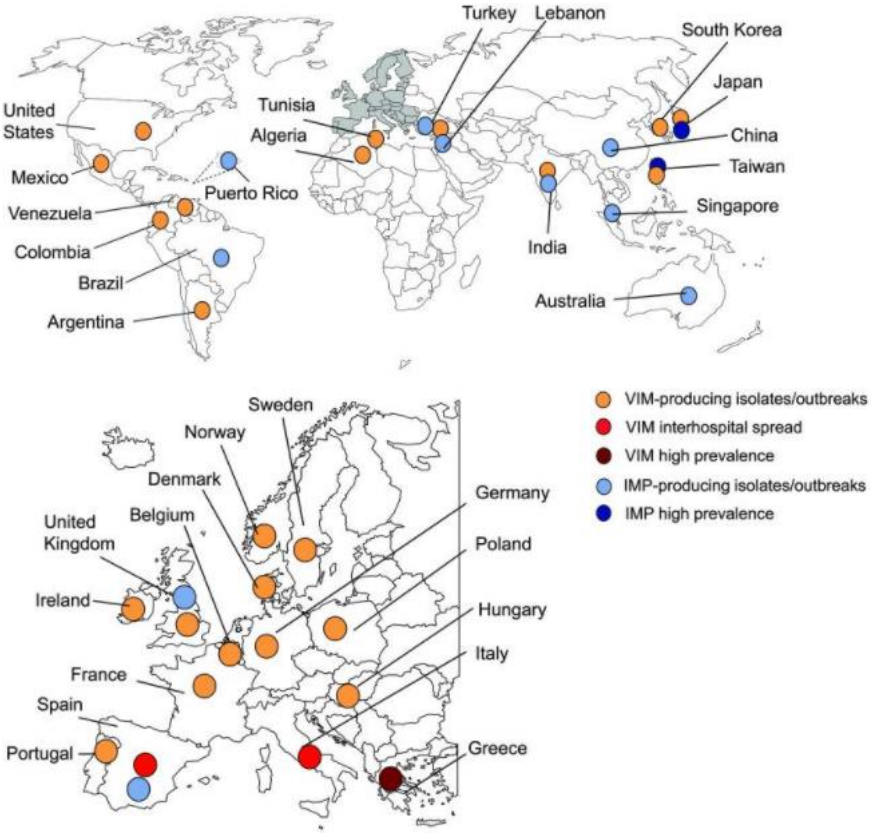

Figure 1.4.1. Dissemination of VIM-1 and IMP enterobacterial producers in Europe and the rest of the world. Image sourced from Nordmann et al., 2011 [47].

1.5.1. VIM Genetics

As stated, the *bla*$_{VIM}$ gene encodes VIM, and was discovered in *P. aeruginosa* initially, though being housed on a MGE has the ability to be transferred to other species of bacteria, as well as being transformed into strains such as *E. coli* for growth and study [43]. The spread of this MBL is further assisted by its association with a variety of broad range plasmids, such as incompatibility group (Inc) N, H12, and A/C2 [48], [49].

Depending upon the variant gene, resistance is conferred to various β-lactams as well as carbapenems such as; doripenem, imipenem, meropenem to varying degrees, as well as this, variants have also been described as having differences in their thermal stability [50].

1.5.2. VIM Categorisation

As of January 2022, 79 variants of VIM have been described [51]. Though all have a similar phenotype of 3a, the difference in variants has led to the development of a subfamily classification, three of which are currently described, that is; VIM-1-like, VIM-2-like, and VIM-7-like [52]. These subfamilies are characterised by a VIM variants sequence identity and summarised in Figure 1.4.3.1.

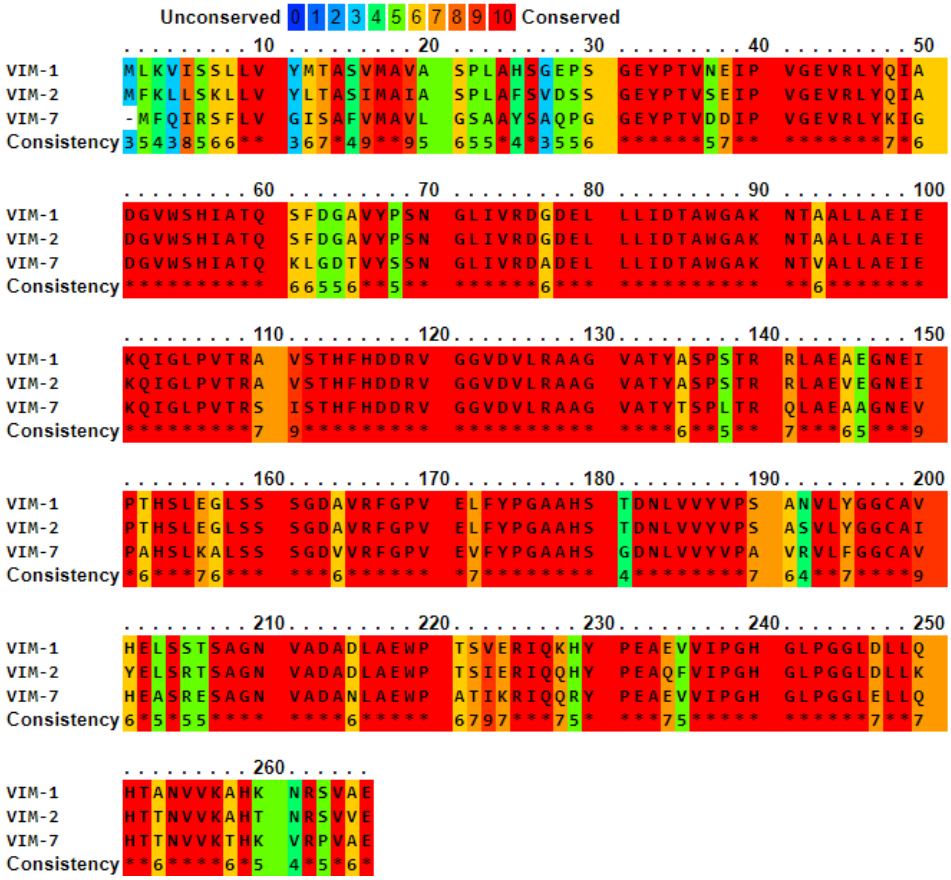

Figure 1.4.3.1. Three major VIM subfamilies and their amino acid differentiation. Here is shown the three heads of the subfamilies – VIM-1, VIM-2, and VIM-7 - and the amino acid conservation between them VIM-1 to VIM-2 and VIM-7. Sequence similarity is 90.6% and 77.9% respectively. VIM-2 to VIM-7 sequence similarity is 74.4%. Colour change from red to blue indicates conserved to non-conserved residues between VIM proteins. Image generated by PRALINE multiple sequence alignment tool [53].

1.5.3. VIM Structural and Mechanistic Characteristics

Despite the variance between VIM, the structure and therefore presumably mechanisms remain the same for MBLs of their classification. Though only eight variants have yet had crystal structures accepted, the similarity in their sequences would perhaps justify the assumption that they function in the same way, just with varying results in their kinetics, as previously observed by Makena et al. [50].

That is a classic αβ/βα sandwich fold with two active Zn^{2+} ions flanked by flexible loops and held in place by three surrounding histidine residues, that give the MBL its specificity. These ions are utilised to activate a water molecule – if coordinated to the zinc – to act as a nucleophile, or to use the zinc ion itself as a Lewis acid, resulting in an electron-deficient carbonyl carbon through coordinating to the peptide carbonyl oxygen of a β-lactam ring, resulting in the facilitation of a nucleophilic attack as shown in Figure 1.4.4.1 [54]. H_2O (Wat3 (see Figure 1.4.4.2)) appears to hold an important role within VIM and known variants activation, mediating substrate and inhibitor interactions in a similar way to NDM-1's Lys224 [55].

It is not known precisely what all of the effects are of differing amino acids at various points in VIM-variants, whether the conserved regions are solely for structure stability or precisely the effect they have on activity of the enzyme. Though more research needs to be done to say for sure, certain evidence points towards changes in VIM's activity as residues change. For example, a study by Borgianni et al. in 2010 used mutagenesis to demonstrate the critical importance Trp-87 had in VIM's ampicillin resistance [34]. Located close to the active site, but not involved in its catalytic activity, it was found in *E. coli* that comparisons between native and mutated W87F variants resulted in the same amount of enzyme being produced, but that difference in activity was affected by up to 60-fold [34].

A study comparing VIM-1/2/4/5/38 noted small differences in their catalytic efficiencies against a range of β-lactam substrates, but larger disparities in their thermal stabilities (melting points of 60-80°C), and IC_{50} against isoquinoline (>1000 - 2 μM respectively) and pyridine-2-carboxylates 50/100/125/50/50 μM respectively) [50]. The authors suggested that the substitutions of single residues on the L10 loop alter the space in the active sites of the VIM variants, increasing susceptibility to larger tryptophan side chains on inhibitors in the case of smaller residues such as leucine at 224 in VIM-5 [56].

Clearly the considerable variations between residues within VIM variants poses an increased challenge in either attempting to find a single inhibitor for them all, or a one-size-fits-all inhibitor that would neutralise this MBL threat altogether.

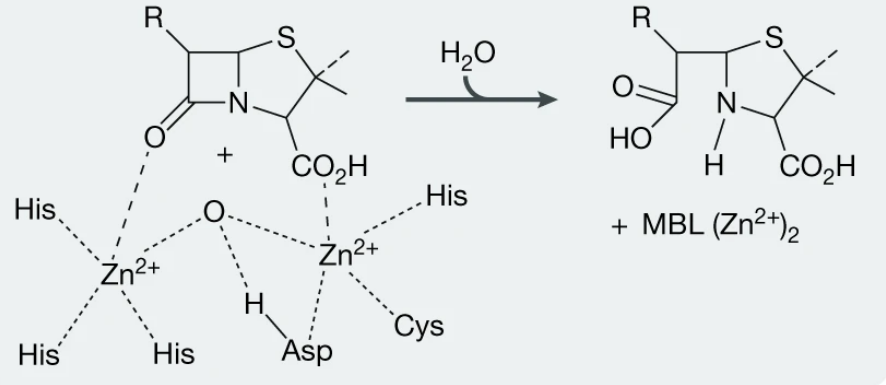

Figure 1.4.4.1 Schematic representation of hydrolysis by a metallo-β-lactamase. Image sourced from Bush et al., 2019 [57].

Variations of VIM can also pose unique challenges between them, related though they may be. VIM-2 for example is disseminated almost exclusively in *P. aeruginosa* and seems to struggle to be expressed in other bacterial strains. Of the 77 structures for VIM-2 currently hosted on the protein data bank, all but one originated from *P. aeruginosa,* the other isolated from *K. pneumoniae.* VIM-1 however can be quite easily expressed in strains of *E. coli* resulting in a greater potential for increased infection rates given the prevalence of *E. coli* in the human microbiome, and the relative absence of *P. aeruginosa* (~3% normally with increases to ~20% in a clinical setting) [58].

With regards to VIM-2 variations, it can also be noted that in the case of a virulent *P. aeruginosa* strain "ST325" 99.6% isolates containing MBL genes (including bla_{VIM-2}) increased from 4.5% in 2002-04, to 99.6% in 2010[59]. These isolates were gathered throughout Russia initially in the study, and then later included both Belarus and Kazakhstan. Analysis of these isolates also showed that in this case of bla_{VIM-2} spread it was more closely linked to clonal dissemination rather than that of horizontal gene transfer between isolates[59].

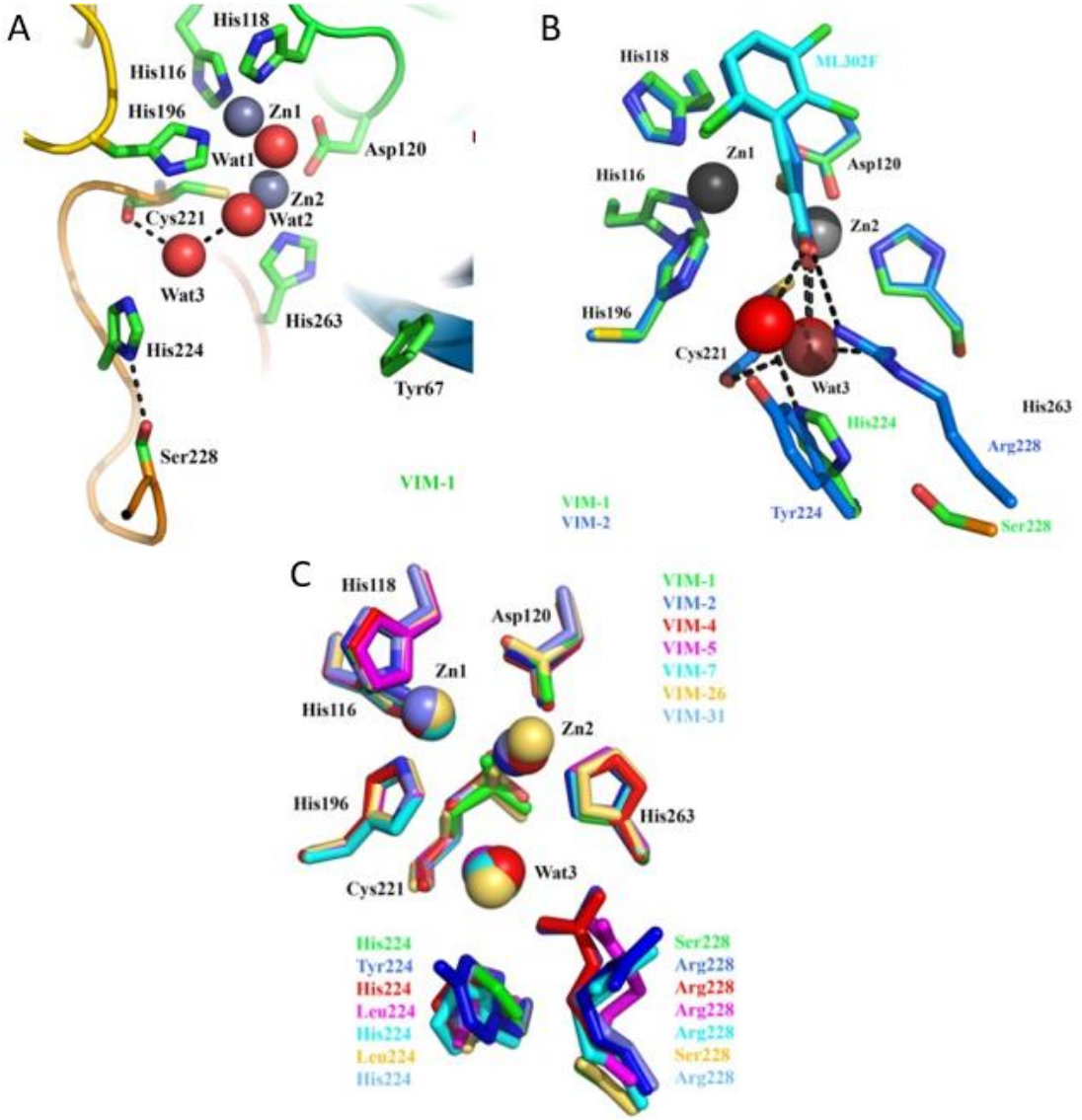

Figure 1.4.4.2. Structures of VIM. (A) The active site of VIM-1 showing contacts to zinc ions, water molecules shown as red spheres[55]. **(B)** Electron density map for VIM-1 with hydrolysed meropenem bound[55]. **(C)** Overlay of VIM structures showing conserved Wat3 location[55].

1.5.4 VIM Localisation Within the Cell

Though VIM has not yet been fully characterised, and is certainly an avenue for further research, a system similar to that of MBL NDM-1 would suggest travel through the SecA/SecYEG pathway, and transportation into the periplasmic space, either untethered or bound to in the inner envelope [60].

1.6. β-lactamase Inhibitors in Current Use

Inhibitors of β-lactamases of all varieties are administered along with the β-lactam antibiotics to counteract the antimicrobial action of these enzymes, thereby rendering the target susceptible to the presence of antibiotic. These combinations are shown in Table 1.6.1.1 and follow one of two mechanisms of action, although all work to do essentially the same thing - draw out the longevity of our current host of β-lactam antibiotics [61]. Some β-lactamase inhibitors act as substrates for β-lactamases, binding with high specificity and forming steric interactions that are unfavourable to the enzyme, such as avibactam and relebactam [61]. Others function as so-called "suicide inhibitors" which utilise secondary chemical reactions to the enzyme's active site, and render it permanently inactive, such as clavulanic acid [62].

Inhibitor composition	% protein bount at $t_{1/2}$
Piperacilin-tazorbactam	pip 30, taz 30
Ampicillin-sulbactam	amp 28, sul 28
Amoxicillin-clavulanate	amo 18, clav 25
Ticarcilin-clavulanate	tic 45, clav 25
Cefoperazone-sulbactam	No data

Table 1.6.1.1. Combination β-lactam-β-lactamase inhibitors clinically available. Currently Cefoperazon-sulbactam is not in use outside of Europe, India, and Japan. Data and information sourced from [61].

Certain virulent bacteria, such as *P. aeruginosa* are capable of producing extended-spectrum β-lactamases (ESBLs) that are able to hydrolyse antibiotics containing an oxyimino group, resulting in them confering further resistance against antimicrobials such as the ability to hydrolyse penicillins, extended-spectrum cephalosporins, and certain monobactams [63], [64]. These ESBLs exceed 200 as it stands in January 2022, and though they are importantly still inhibited by clavulanic acid, their ability to hydrolyse aztreonam and third generation cephalosporins certainly makes them a threat worth considering[65]. ESBLs are commonly plasmid-mediated, and these transferable elements can be found to contain a combination of resistance enzymes, rather than just a singular one[66].

Of concern is the evident way in which bacteria can not only develop resistance, but also share these developments with other bacterial species. As such, the existence of enzymes capable of rendering the last line β-lactamase inhibitors obsolete as well as developing further resistances would indicate that without new innovations in antimicrobials, the potential efficacy of the current clinical arsenal could be lessened over time.

1.6.1. β-lactamase Inhibitors in Clinical Development

In order to counteract this increase in, and still developing resistance there are many inhibitors that are currently undergoing or will soon enter clinical trials. The issue with many of these is that they are still reliant upon, in many cases, currently existing antibiotics used in combination with other therapies or are derived from currently existing moieties in such a way that the development of resistance is a very tangible concern. The stages of clinical trial and source of these inhibitors are listed in Table 1.6.2.1.

Derivation	Clinical phase			
	I	II	III	IV
Diazabicyclooctane	18	2	7	1
Boronic acid	6	0	1	0
β-lactam	4	1	1	0

Table 1.6.2.1 Derivations of Carbapenemase antibiotic/inhibitor combination, and clinical phase they are in. Data sourced from [67].

From Table 1.6.1.1, two have direct relevance to VIM. Taniborbactam (VNRX-5133) was the first pan spectrum β-lactamase inhibitor which entered clinical development in 2019 [67]. Its design was based on a previously low-activity boronic-acid derivative by Burns et al. and during testing was shown to inhibit both serine and metallo-β-lactamases to a degree that was either comparable, or exceeded inhibition when compared to current clinical examples, as shown in Table 1.6.2.2. It was also shown to be able to rescue Cefepime activity against a host of bacterial strains [68]. Taniborbactam entered Phase 3 clinical trials in 2019 for the treatment of urinary tract infections (*n* = 582), and the study was completed in December 2021, although results are yet to be published as of January 2022.

	IC50 (μM)		
Entry	NDM-1	VIM-2	IMP-1
Taniborbactam	0.19	0.026	39.8 (2.51)
avibactam	>100	>100	>100
vaborbactam	>100 (631)	>100 (316)	>100 (126)
clavulanic acid	>100	>100	>100
tazobactam	>100	>100	>100

Table 1.6.2.2. Taniborbactam inhibitory activity shown in comparison to clinically relevant β-lactamases. Of particular interest is the inhibitory activity against the class B MBLs, including VIM-2, which far exceed the IC_{50} of the other β-lactamases. Previously reported IC_{50} values are shown in parentheses. Image adapted from Lu et al., 2020 [68].

QPX7728 is a structurally modified boronic acid which showed fast on-fast off kinetics with the class B MBLs *in vitro* and presented a K_i of less than 100 nM for both NDM-1 and VIM-1 [67], [69]. Coupled with this, when using imipenem as a substrate they showed greater K_i values than both vaborbactam and avibactam against VIM-1, IMP-1, and NDM-1, all clinically relevant MBLs, presented in Table 1.6.2.3 [69]. QPX7728 entered Phase 1 clinical trials in 2020 for the treatment of bacterial infections (*n*=64), and the study is due to be completed in late 2021.

enzyme	QPX7728	vaborbactam	avibactam
VIM-1	0.0080 ± 0.0035	>40	>40
NDM-1	0.032 ± 0.014	>40	>40
IMP-1	0.22 ± 0.05	>40	>40

Table 1.6.2.3. QPX7728 K_i values against class B enzymes aside comparators vaborbactam and avibactam using imipenem as a substrate. Data sourced from [69].

1.6.2. Metallic and Covalent Inhibitors

Zinc (Zn^{2+}) and zinc oxide have been shown in various systems to have antibacterial effects on a broad range of Gram-positive and -negative bacteria, as well as fungi, biofilms, and plant life, which is thought to be due to their generation of reactive oxygen species [70], [71]. In cases where they show bacteriostatic rather than bactericidal effects, they have been shown to increase the effectiveness of other antimicrobials when used in combination [71]. Their effectiveness is marred, however, with their tendency towards cyto- and genotoxicity of mammalian cells, reducing their effectiveness as a pharmaceutical antimicrobial.

Less prevalent but still effective are synthesised nanoparticles made of silver, titanium, copper, gold, and magnesium [70], [72]–[74]. The use of these is impaired by similar factors to those involving zinc and

zinc oxide, in that there is a strong link between their antibacterial properties and their relative toxicity. Recent studies have shown that gold may be selectively fabricated to impart favourable antibacterial properties [75].

Zinc chelating compounds have shown to be effective inhibitors of metallo-β-lactamase, but their tendency to bind to free zinc ions precludes their clinical use for MBL inhibitors. As an example, thiol-containing inhibitors such as thiomandelic acid have been shown to inhibit broad ranges of MBL's [61], [76]. *In vitro* studies from the early 2000's demonstrated that the *Ki* against VIM-1 and VIM-2 were 0.230 and 0.220 μM respectively [76], [77].

1.6.3. Novel Inhibitors

Peptide antimicrobials have demonstrated some efficacy against certain MBLs. The peptide Thanatin was shown to inhibit NDM-1 and NDM-1 producing *E. coli* by targeting both cations in the cellular outer membrane - disrupting stability - and the active site zinc within NDM-1 itself, displacing the ion and inhibiting in a dose-dependent manner [78].

In vitro allosteric inhibition of VIM-4 has been observed through the use of a Camelid nanobody, dubbed NbVIM_38, which achieved an IC_{50} of 10 μM. This was found to function through allosteric inhibition, which could relate back to the study by Borgianni et al. which demonstrated a vital residue in VIM-2 situated outside of the active site, and could suggest that inhibitors that do not bind in the active site are viable[34][79]. However, only one such nanobody was discovered from a host of 43 specifically screened sequences [79]. Evidently, these proteins have properties that can be targeted with a variety of different reagents.

Despite the existence of these MBL inhibitors, the apparent diversity in the primary sequence of MBL families results in a distinct lack of a "one size fits all" inhibitor [50]. As can be seen from Table 1.6.2.1, the majority of clinical trials are still in the early phases and will not be available – if they are successful – for nearly a decade. Coupled with the relative success of finding a single inhibitor this does however demonstrate both the potential discovery and absolute need for a novel biologic which can be utilised as a highly specific inhibitor.

1.7. Affimer Reagents

Originally called Adhirons, but later licensed by Avacta Life Sciences Ltd under the name Affimers, Affimers are separated into two types based on protein conformations. Type I were created in 2005, and were designed based upon Stefin A, a human protease inhibitor [80]. Type II - the type used in the present thesis - are small protein synthetic scaffolds that are based on the plant-derived cysteine protease inhibitors phytocystatins [81].

Utilising the stable aspects conserved in the sequence and replacing the protease regions with two random variable loops, a library of 1.3×10^{10} has been created of proteins with various elements that make them potentially good reagents for protein binding. These include their stable scaffold, capable of maintaining structure both at 101°C, and across a range of pH's, and the two nine-amino acid variable region random loop structures mean that the potential is good to find a suitable reagent to bind to a target protein [81]. The structure of an Affimer, shown in Figure 1.7.1.1 demonstrates an α-helix resting on an anti-parallel β-sheet, the variable loops contain a randomised sequence which give the Affimer a potential for good specificity against potential targets [82].

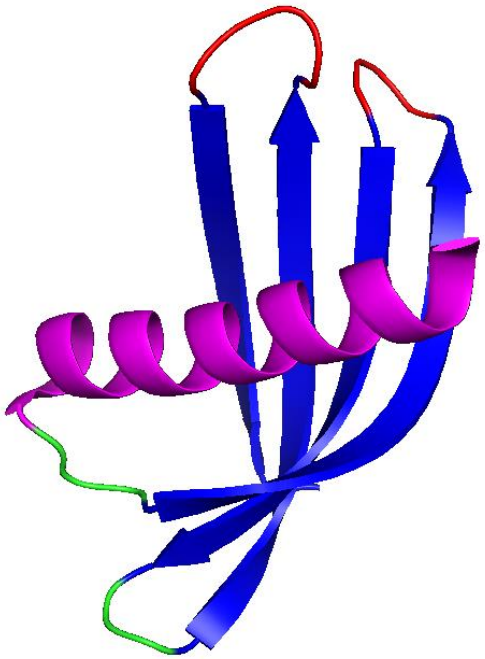

Figure 1.7.1.1. Crystal structure of Affimer (PDB: 4N6T). Resolution at 1.75 Å. Shown in red are the variable loops, in magenta the α-helix, and in blue the anti-parallel β-sheet [81].

Differentiating Affimers from antibodies as a study for protein interactions and biological processes is a host of characteristics that serve to make them a potential alternative. Expressing easily in *E. coli,* they can be rapidly and cheaply synthesised - with production volume of up to 100 mg/L, with no batch-to-batch variation as found in animal-sourced antibodies, coupled with the ethical considerations of not having to use animals for diagnostic tool production [81], [82]. They are monomers of roughly 12 kDa making them ideal for the study of protein interactions, with an ability to potentially bind to pockets too small for a conventional antibody, and their lack of cysteines ensure no disulphide bonds that may provide interference when binding to a target [81].

1.7.1. Affimer Technology

Affimers are highly adaptable and have been used for; imaging – as demonstrated against F-actin [83], immunoassays – as demonstrated against human interleukin-8 [84], and biosensors – for example small organics such as methylene blue [82].

1.7.2. Affimers as Inhibitors

Affimers have also been previously identified as potential inhibitors of proteins, lending credence for their use in identifying potential interactions with VIM.

Affimers have been raised to bind specifically to FcγRIIIa and were shown to reduce the IgG immune complex binding to it, showing an allosteric mode of inhibition, however the specificity is so high for FcγRIIIa that FcγRIIIb was not affected [85]. In 2020, three Affimers were found to inhibit SOS1-mediated nucleotide exchange - a process essential in RAS activation – with the greatest of these having an IC_{50} of 144± 94 nM, their small size also enabled them to find druggable pockets within a

previously undruggable site [86]. There is a rationale for using Affimers in this thesis, in unpublished work, Affimers have been raised against another MBL, NDM-1 and effected inhibition in nitrocefin hydrolysis assays by over 80% at five-fold the enzyme concentration (500 nM Affimer to 100 nM NDM-1)[87], [88].

1.7.3. Phage Display and Library Generation

Phage display has been a prominent *in vitro* method for screening since 1985, devised by George Smith, and securing him the Nobel Prize for Chemistry in 2018. This system utilises *E. coli* filamentous bacteriophages f1, fd and M13 which present polypeptides on their surface, and have physically linked phenotype and genotype. Housing a gene which codes for the molecule presented in a single-stranded DNA (ssDNA) virion as well as both non-structural proteins, and the phage coat protein [89]. This ensures that whichever affinity methods are used to identify the polypeptides present on the surface of the bacteriophage will be replicated exactly from the *E. coli* clone. This system can be used to select for various sizes of protein, from fragments of antibody or biotin bound to smaller phage proteins, to larger polypeptides, correctly folded and bound to several surface proteins [90].

From these bacteriophages vast libraries can be created, featuring around 1.3 x 10^{10} variants that can be used for a whole host of screening techniques.

For the purposes of Affimer identification, and to ensure a high specificity, an Affimer phage library is needed. These were created by manipulating the M13 filamentous phage, to display Affimer products on the coat protein pIII, cloned into phagemid vector pBSTG1 (GenBank KJ474865) giving an amber (TAG) codon, C-term half of gene III of the M13 bacteriophage, a DsbA signal peptide, as well as the Affimer which collectively is known as pBSTG1-Aff [81]. The TAG codon allows for an interruption of translational readthrough resulting in a fused Affimer-truncated-pIII protein amalgam in suppressor *E. coli* strains, ER2738 for example. Figure 1.7.3.1 displays the relevant features of pBSTG1-Aff.

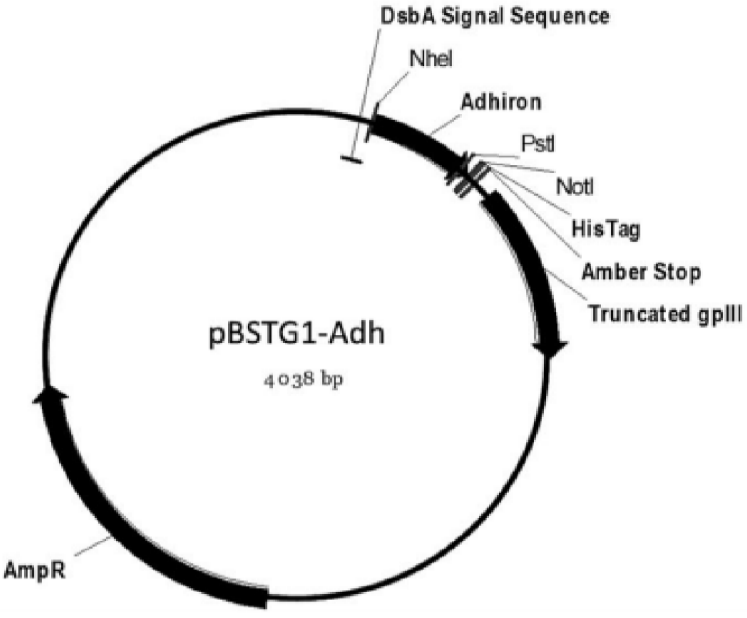

Figure 1.7.3.1. Phagemid vector pBSTG1 containing Affimer (previously known as Adhiron). This pBSTG1-Aff features NheI and NotI restriction sites, as well as ampicillin resistance markers [81].

This library of Affimer reagents was created through the use of splice overlap extension (SOE) of two PCR products popularised by

Horton et al which allows the recombination of sequences of DNA without the use of restriction sites [91]. This process is summarised in Figure 1.7.3.2.

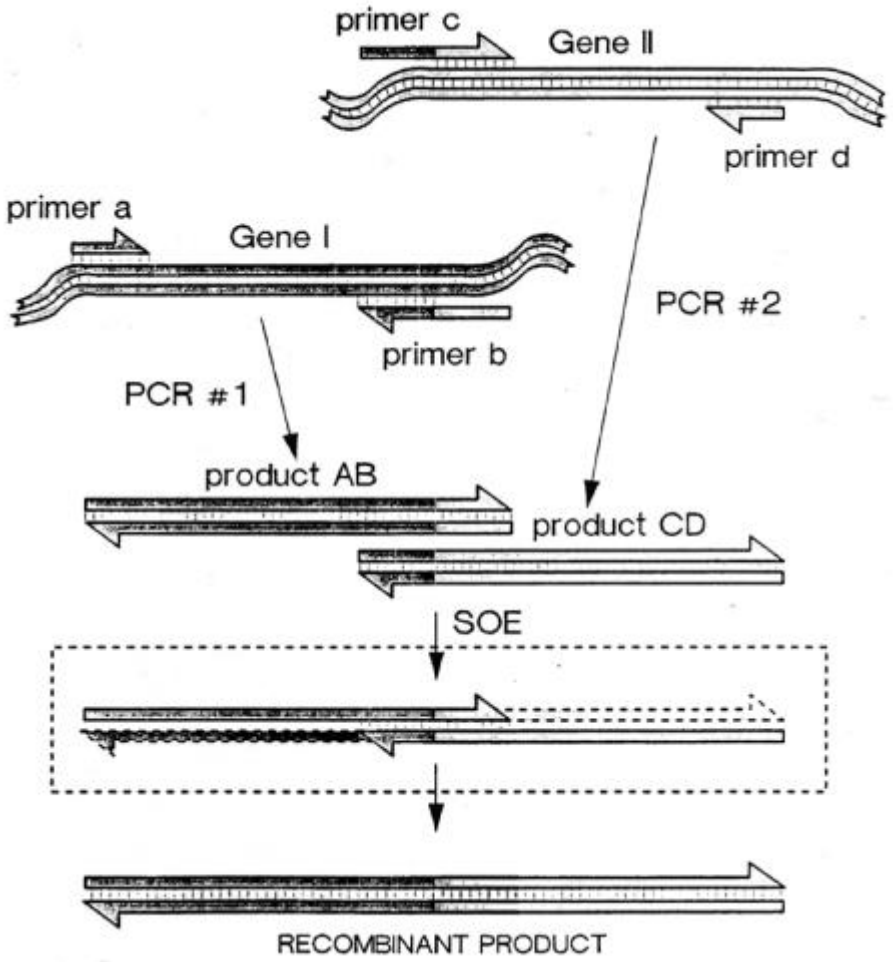

Figure 1.7.3.2. Example of splice overlap extension (SOE). Using this process with Affimers, product AB was generated through the extension of the DsbA coding sequence and included the first variable loop, product CD houses two variable regions (VR) of nine amino acids each. These VRs were incorporated through the use of degenerate positions as trimers and contained a codon for all amino acids except cysteine. Image sourced from Horton., 2013 [91].

1.7.4. M13 Bacteriophage, Infection, and Life Cycle

The bacteriophage utilised for Affimer display is M13. M13 is a chronic, F-pilus specific phage and has a genome that encodes both its five modifiable coat proteins and six non-structural within its ssDNA, demonstrated in figure 1.7.4.1 [92]. Using a bacterial cells pili as primary receptors, a secondary receptor is the conserved TolQRA complex found within inner membrane proteins. Generally, upon initial binding these pili will draw the phage towards the cell surface and allow binding to this secondary receptor within the periplasm [93]. Through an -as yet- poorly defined mechanism, this allows both pIII and the virion cap through the outer membrane, and results in entry of the major coat protein and the phage ssDNA into the inner membrane [94]. Following this, the positive strand genome will enter replication, serving as a template for production of a negative

strand, lacking any sequences for host integration this is reliant upon host mechanisms and enzymes for replication and proliferation [94]. This process is summarised in figure 1.7.4.2.

Figure 1.7.4.1. Basic structure of M13 filamentous phage. In blue pIII, in pink pVI, in yellow pVIII, in red pVII, in orange pIX. Circular singe stranded DNA genome packaged within the body.

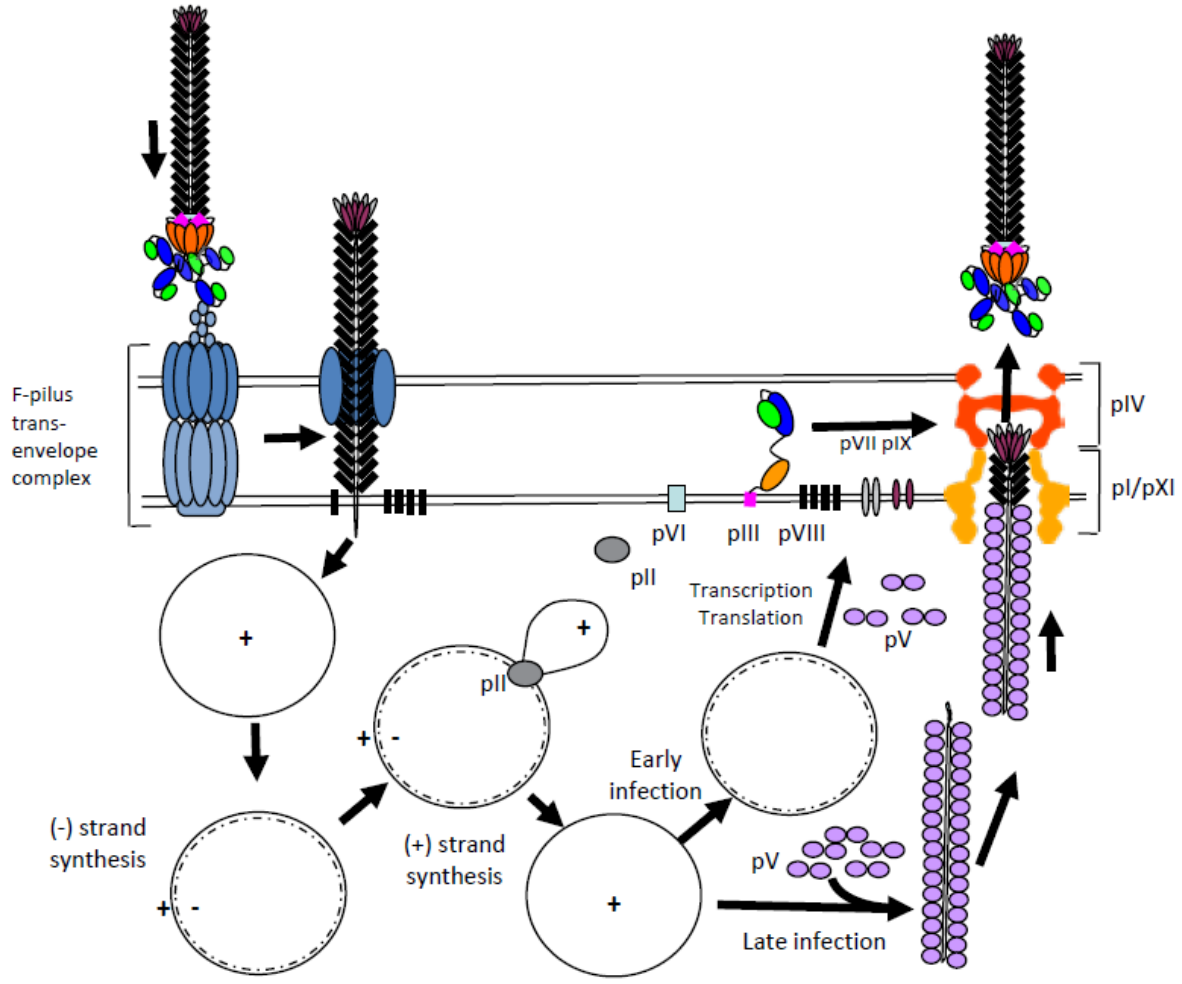

Figure 1.7.4.2. Infection and replication of M13 filamentous phage. Seen here the primary binding between phage and cell receptors, resulting in secretion of both coat proteins and ssDNA into the cell. Positive strand serves as a template for continued replication, later coat proteins assist assembly within the cell, and transported to the cell membrane export complex for release. Image sourced from Rakonjac, 2011 [93].

1.7.5. Phage Display and Screening

The possession of a library housed in a variety of M13 filamentous phage, to allow identification of Affimers that have potentially high affinity to a desired target requires a systematic process of biopanning with the ability to change various conditions to carefully select the strongest binders. The target is biotinylated and immobilised on streptavidin, in order to expose it to the phage library [95]. After exposure unbound phage are washed away, and bound phage can then be eluted by a change in pH. These can then be taken forward to infect specific suppressor *E. coli* strains, such as ER2738, resulting in their amplification [95]. From this further screening can be performed to ensure only the binders with the highest affinity are selected. Enzyme-linked immunosorbent assays (ELISA) can then be performed to verify Affimer-bound target, and these can be sequenced for analysis [95]. This process is summarised in Figure 1.7.5.1.

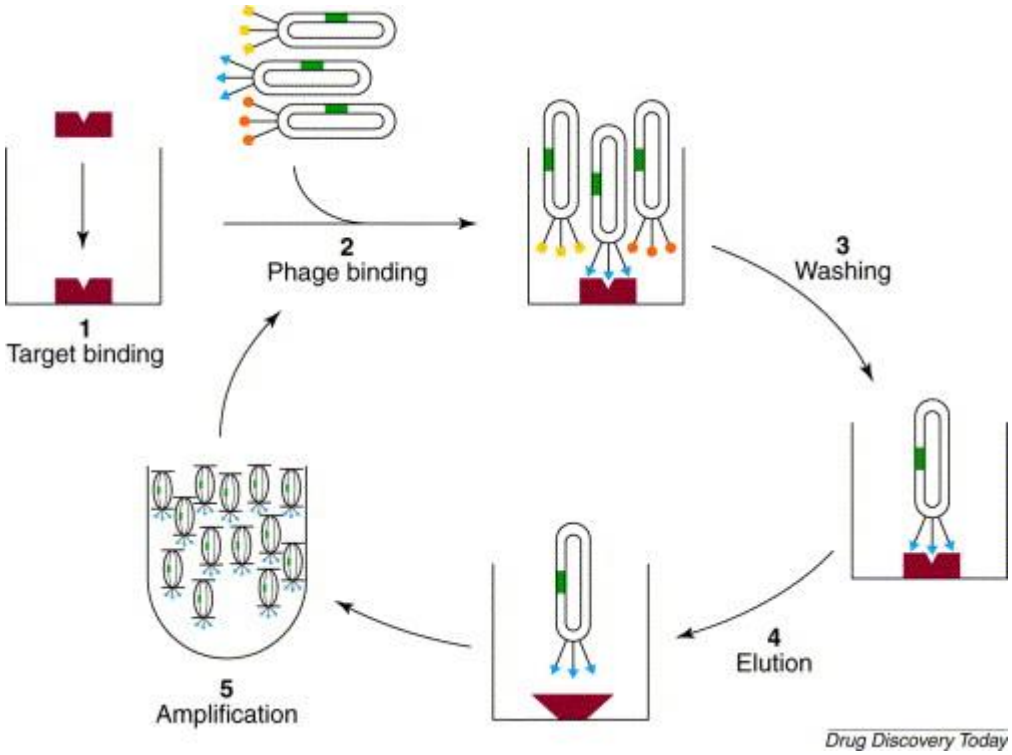

Figure 1.7.5.1. Individual steps of phage display. 1, Biotinylated target is immobilised and (2) incubated with phage library. 3, Unbound phage is washed off. 4, Phage is eluted through pH change. 5, ER2738 cells are infected, and phage is propagated. Then the process is repeated, after which phage with target bound is assessed against a control (homologous protein only) and verified with ELISA. After 5, remaining phage is sent off for sequencing to establish composition of the variable loops. Image sourced from [96].

1.8. Project Objectives

There is a need for novel inhibitors of β-lactamases to combat antimicrobial resistance globally. In an effort to find reagents that can modulate metallo-β-lactamase activity - specifically that of Verona Integron-encoded metallo-β-lactamase – Affimers will be identified and characterised using a range of structural, biochemical, molecular, and cellular assays.

2. Materials and Methods

2.1. Materials

2.1.1. Bacterial Strains and Cloning Vectors

BL21 Star™(DE3) *E. coli* chemically competent expression strain (genotype; F- ompT hsdSB (rB-mB-) gal dcm rne131 (DE3) encoding for a T7 RNA polymerase and ampicillin resistance gene were used for propagation of protein from plasmid DNA (Invitrogen).

XL1-Blue Supercompetent *E. coli* cells (genotype; recA1 endA1 gyrA96 thi-1 hsdR17 supE44 relA1 lac [F proAB lacIqZΔM15 Tn10 (Tetr)]) were used for propagation of plasmid DNA for Sanger sequencing (Agilent Technologies).

AVB101 chemically competent *E. coli* cells (genotype; hsdR, lon11, sulA1) containing a *birA* gene, IPTG-inducible, were used for production of biotinylated protein from plasmid DNA (Avidity).

ER2738 electrocompetent *E. coli* cells (genotype; [F'proA+B+ lacIq Δ(lacZ)M15 zzf::Tn10 (tetr)] fhuA2 glnVΔ(lac-proAB) thi-1Δ(hdS-mcrB)5)) were used for the propagation of phage during phage display (Lucigen).

JM83 chemically competent *E. coli* cells (addgene, produced in Tomlinson lab by Dr Christian Tiede) were used to propagate Affimer proteins from phagemid vectors.

2.1.1.1 Cloning Vectors used During this Study

pET11a containing a T7 promoter, ampicillin resistance gene, and *lac* repressor gene (Novagen).

pBSTG-Aff phagemid vector encoding; an Affimer sequence, C-terminal coding region for domain two and three from gene III of M13 bacteriophage, *dsbA* secretion signal, and ampicillin resistance (Tiede et al., 2014, originally known as pDHisII).

2.1.2. Growth Media and Buffer recipes

2TY broth

Per litre of deionised water; Tryptone (Oxoid) (16 g), yeast extract (Oxoid) (10 g) and NaCl (Fisher Scientific) (5 g) were dissolved and adjusted to pH 7.0 followed by autoclaving at 121°C, 15 psi for 20 minutes.

LB broth

Per litre of deionised water; LB broth powder (Invitrogen) (20 g) was dissolved followed by autoclaving at 121°C, 15 psi for 20 minutes.

Terrific Broth Autoinduction Media

Per litre of deionised water; Terrific broth powder including trace elements (FisherScientific) (50.8 g) was dissolved followed by autoclaving at 121°C, 15 psi for 20 minutes.

TYH Media

Per litre of deionised water; Tryptone (Oxoid) (20 g), yeast extract (Oxoid) (10 g), HEPES (Sigma) (11 g), NaCl (Fisher Scientific) (5 g) and $MgSO_4$ (Fisher Scientific) (1 g) were dissolved, followed by pH adjustment to 7.3 with KOH, and autoclaving at 121°C, 15 psi for 20 minutes.

LB Agar Plates

Per litre of deionised water; LB agar powder (Invitrogen) (32 g) was dissolved followed by autoclaving at 121°C, 15 psi for 20 minutes. Following cooling to 50°C, appropriate antibiotic for the purpose of the plate was added at the appropriate concentration followed by allocating 25 mL per petri dish in aseptic conditions.

2.1.2.2. Buffer Recipes

2x Blocking buffer 10x blocking buffer diluted in PBS-T at a ratio of 1:5

4x loading buffer 200 mM Tris-HCL, pH 6.8, 20% (v/v) glycerol, 8% (w/v) SDS, 0.4% (w/v) bromophenol blue, 20% (v/v) β-mercaptoethanol

β-lactamase assay buffer 50 mM HEPES pH 7, 20 µM $ZnSO_4$, 10 µg/mL bovine serum albumin

Lysis buffer 50 mM NaH_2PO_4, 300 mM NaCl, 30 mM Imidazole, 10% glycerol, pH 7.4

Periplasmic lysis buffer 100 mM Tris, 20% (w/v) sucrose, 1 mM EDTA, pH 8

Wash buffer 50 mM HEPES, 500 mM NaCl, 20 mM Imidazole, pH 7.4

Phosphate buffered saline 137 mM NaCl, 4.3 mM Na_2HPO_4, 1.47 mM KH_2PO_4, 2.7 mM KCl, pH 7.4

SDS-Page running buffer 25 mM Tris, 200 mM glycine, 0.1% (w/v) SDS, pH 8.3

TE buffer 10 mM Tris, 1 mM EDTA, pH 8

Destain buffer 50% (v/v) deionised H_2O, 40% (v/v) methanol, 10% (v/v) acetic acid

TAE running buffer 40 mM Tris-acetate, 1 mM EDTA, pH 8.3.

10x Orange G loading dye 30% glycerol, 0.2% orange G, deionised H_2O

Elution buffer 50 mM NaH_2PO4, 500 mM NaCl, 30 mM Imidazole, 10% glycerol, pH 7.4

PBS-T 1% (v/v) solution of Tween-20 in PBS

PEG-NaCl 20% (w/v) PEG 8000, 2.5 M NaCl

Coomassie Blue stain 45% (v/v) methanol, 7% (v/v) acetic acid, 0.25% (w/v) Coomassie Brilliant Blue R-250

Transfer buffer Tris 0.1 M, glycine 0.192 M, 20% (v/v) methanol

2.1.3. Antibiotics and Additional Media

2.1.3.1. Antibiotics

Stock solutions of antibiotics were made in deionised water, these were then filter sterilised through syringe-end filter sterilisation (0.2 µM) and stored in 1 mL aliquots at -20°C. Table 2.1 shows both the stock and final concentrations used in both cultures and agar plates.

Antibiotic	Stock concentration	Working concentration	Manufacturer
Chloramphenicol	34 mg/mL	10 µg/mL	FisherScientific
Ampicillin	100 mg/mL	100 µg/mL	Sigma Aldrich
Carbenicillin	100 mg/mL	100 µg/mL	FisherScientific
Tetracycline	12 mg/mL	12 µg/mL	Sigma Aldrich
Kanamycin	25 mg/mL	50 µg/mL	Sigma Aldrich

Table 2.1. Antibiotics Used and the Stock or Working Concentration used

2.1.3.2. Additional Media

IPTG 1M stock solution stored at -20°C (Sigma-Aldrich)

Biotin A stock solution of biotin was prepared by taking 5 mM d-biotin (Invitrogen), adding to 10 mM warmed bicine buffer, pH 8.3 (Sigma) this was then syringe-end filter sterilised (0.2 µM). 1 mL aliquots were prepared in tubes and frozen at -20°C.

2.2. Methods

2.2.1. DNA Manipulation

2.2.1.1. Polymerase Chain Reaction (PCR)

VIM-1 coding regions were amplified by PCR from pET11 vectors. Affimer DNA sequences were amplified from a Phagemid vector. All PCR reactions utilised a (T100 BioRad) and were incubated in a 0.2 mL tube (Sarstedt). A master mix was made with Phusion High-Fidelity (HF) DNA polymerase (ThermoFisher), the specifications of which are shown in Table 2.2.

Component	Volume (µL)	Final concentration
5x Phusion HF Buffer	10	1x
dNTP mix, 25 mM	0.4	200 µM of each
Forward primer, 10 µM	4	0.8 µM
Reverse primer, 10 µM	4	0.8 µM
DMSO	1.5	3%
Deionised water	Y	to a final volume of 25 µL
Phusion DNA polymerase	0.5	0.02 U/µL
Template DNA	X	1 ng/µL
Total volume	50 µL	

Table 2.2. Components for PCR.

Reactions were then transferred to a T100 bioRad under the thermocycler conditions shown in Table 2.3.

Cycle step	Temperature (°C)	Time (s)	Cycles
Initial denaturation	98	30	1
Denaturation	98	20	30
Annealing	54	20	
Extension	72	20	
Final extension	72	600	1
Hold	4	∞	

Table 2.3. Thermocycler conditions for PCR.

After final PCR step, to each reaction was added 0.5 µL *DpnI* (New England BioLabs) and incubated at 37°C for one hour. PCR products were purified using a NucleoSpin® Gel and PCR clean-up kit (Macherey-Nagel) following the manufacturers guidance, with exception the last elution step, for which 50 µL of nuclease free H_2O was used.

2.2.1.2. Thermocycler Settings for overlapping PCR Mutagenesis

SOE reactions were accomplished using PCR in VIM-1 pET11 vectors. All reactions utilised a T100 bioRad thermocycler (bioRad) and were incubated in a 0.2 mL tube (Sarstedt). Equal amounts of the two primers were added to the reaction for ratio of 1:1. A master mix was made with KOD Hot Start DNA polymerase (Millipore) the specifications of which are shown in Table 2.4.

Component	Volume (uL)	Final concentration
10 x KOD buffer	5	1x
dNTPs	5	200 µM of each
Forward primer 10 µM	4	0.8 µM
Reverse primer 10 µM	4	0.8 µM
Template DNA	X	10 ng
25 mM $MgSO_4$	3	1.5 mM
Deionised water	Y	to a final volume of 25 µL
KOD DNA polymerase	1	0.02 U/µL
Total volume	50	

Table 2.4. SOE Components using KOD Hot Start DNA Polymerase

Reactions for SOE were then transferred to a T100 bioRad under the thermocycler conditions show in Table 2.5.

Cycle step	Temperature (°C)	Time (s)	Cycles
Polymerase activation	95	120	1
Denaturation	95	20	20
Annealing	60	20	
Extension	70	20	
Final extension	70	300	1
Hold	4	∞	

Table 2.5. SOE Thermocycler Conditions

After final PCR step, 0.5 µL *DpnI* (New England BioLabs) was added to each reaction and incubated at 37°C for one hour. PCR products were purified using a NucleoSpin® Gel and PCR clean-up kit (Macherey-Nagel) following the manufacturers guidance, with exception the last solution step, for which 50 µL of nuclease free H_2O was used.

2.2.1.3. Biotin Acceptor Peptide (BAP) tag Cloning

To facilitate biotinylation of VIM-1, a BAP sequence (G-L-N-D-I-F-E-A-Q-K-I-E-W-H-E) was added subsequent to the *PelB* signal sequence of VIM-1 contained on pET11. The procedure shown in segment 2.2.1.2 was utilised to accomplish this. The method by which this was accomplished is shown in Figure 2.1.

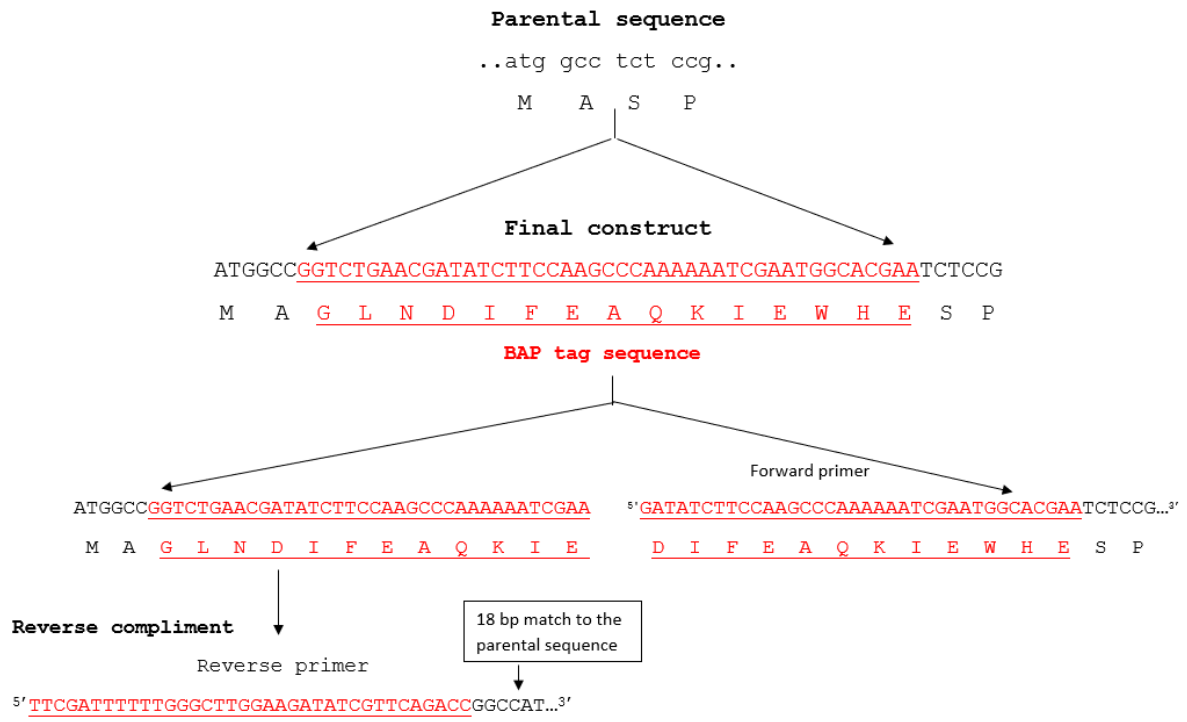

Figure 2.1. Design of primers to facilitate Biotin Acceptor Peptide addition to VIM-1 using an overlapping PCR mutagenesis method.

Primers were designed to allow overlap of 30 bp and include 18 bp that matched to the parental sequence. They are shown below, BAP tag sequence is underlined in red, both primers were synthesised by Sigma.

Forward primer –

5′ GATATCTTCCAAGCCCAAAAAATCGAATGGCACGAATCTCCGCTGGCTCACTCT 3′

Reverse primer –

5′ TTCGATTTTTTGGGCTTGGAAGATATCGTTCAGACCGGCCATCGCCGGCTGGGC 3′

Following *DpnI* digestion and PCR clean-up, DNA was transformed using Supercompetent XL1-Blue cells. After growth, a single colony was picked and inoculated in 5 mL of 2TY broth containing appropriate antibiotic and grown overnight at 230 rpm, 37°C. From this, plasmid was purified using QIAprep Spin Miniprep (Qiagen) according to manufacturer's specifications with the exception of the elution step, for which 50 µL of nuclease-free H_2O was used. This was then sent for sequencing to verify successful BAP tag integration (Figure 3.2.3). AVB101 cells were then utilised for protein production. AVB101 cells contain a *birA* gene coding for an IPTG-inducible biotin ligase enzyme, BirA that allows for the biotinylation of the BAP-tag *in vivo* in the presence of ATP [97]

2.2.1.4. Quantification of DNA Concentration

To measure DNA concentration a spectrophotometer was utilised (Nanodrop-lite spectrophotometer (ThermoScientific)). 2 µL of buffer in which the sample was eluted was used to "blank" the machine, and a fibreless cloth was used to clean the surface between each reading. For the reading, 2 µL of DNA sample was loaded onto the reading platform, and an A_{280} reading was taken to determine DNA concentration by utilising the Beer-Lambert Law.

2.2.1.5. Transformation of *E. coli* Through Heat Shock

A 10 µL aliquot of competent *E. coli* cells were incubated on ice for twenty minutes in a 1.5 mL microcentrifuge tube (Eppendorf). In a new 1.5 mL tube (Eppendorf), 1-5 µL of plasmid DNA (equal to 50-150 ng of DNA) was prechilled on ice for 10 minutes. To this DNA was added the cells, they were flicked to mix, and incubated on ice for 30 minutes. Following this, a 45 second heat shock occurred at 42°C, before placing back on ice for a further 2 minutes. To this was added 300 µL of 2TY, and the mixture was incubated at 230 rpm, 37°C for 1 hour. From this, a 100 µL aliquot was plated onto LB plates, containing appropriate antibiotic. This was then inverted and incubated overnight at 37°C.

Following the incubation step, individual colonies were picked and added to 5 mL of 2TY including appropriate antibiotic for overnight growth at 230 rpm, 37°C.

2.2.1.6. Sequencing of *E. coli* Plasmid DNA

Aliquots of DNA were prepared to the following specifications; 20-50 µL of sample in deionised H_2O, 50-100 ng/µL. Sequencing was performed by GeneWiz using the primers shown in Table 2.6. Results were analysed using ExPASy server (expasy.org)[98].

Plasmid	Name	Position	Sequence 5'-3'
pET11a	T7	Forward	TAATACGACTCACTATAGGG
pBSTG-Aff	M13R	Reverse	CAGGAAACAGCTATGAC

Table 2.6. Primers Used for DNA Sequencing

2.2.1.7. Plasmid Digests

To obtain sufficient plasmid DNA, pET11a plasmids were transformed into XL1 Blue Supercompetent cells (Agilent) and grown overnight in 5 mL 2TY with 100 µg/mL carbenicillin. This was then purified using QIAprep®Miniprep Kit (QIAGEN) before digestion overnight at 37°C using the specifications shown in Table 2.7.

Reagent	Volume
Plasmid DNA	Equal to 20 µg
Cutsmart™ Buffer	5 µL
NheI-HF™	1 µL (20 units)
NotI-HF™	1 µL (20 units)
Deionised H_2O	Up to total volume
Total Volume	50

Table 2.7. Plasmid Digestion Reagents

Following incubation, 2 µL of calf intestinal phosphatase (CIP) (New England Biolabs) was added to this mixture and incubated at 37°C for 30 minutes. Then, utilising a NucleoSpin® Gel and PCR clean-up kit (Macherey-Nagel) following the manufacturers guidance DNA was eluted in 50 µL of nuclease free H_2O. To this elution was added 2 µL CIP, 6 µL CutSmart™ Buffer (New England Biolabs) and nuclease free H_2O to a total volume of 60 µL, this was incubated at 37°C for 30 minutes. The digested products were then separated on an agarose gel (0.7% w/v) and extracted using a NucleoSpin® Gel and PCR clean-up kit (Macherey-Nagel) following the manufacturers guidance and eluted into 25 µL of nuclease free H_2O.

2.2.1.8. Plasmid Ligations

Ligation utilised 1 µL of T4 DNA ligase (NEB/Roche) added to 25 ng of insert DNA and 75 ng of digested vector DNA, to this was added 2 µL of 10x T4 DNA ligase buffer (NEB/Roche) and incubated overnight at room temperature. Products were then transformed using XL-1 Blue Supercompetent cells (Agilent) and plated onto LB agar plates with appropriate antibiotic and incubated at 37°C overnight.

2.2.1.9. Agarose Gel Electrophoresis

Samples of DNA were added to 10x Orange G loading dye at appropriate volumes. 10 µL of this was loaded into a 0.7% agarose gel made using 1x TAE buffer, with SYBRsafe DNA gel stain (Invitrogen) at 1x. As well as samples, 4 µL MassRuler DNA Ladder Mix (ThermoFisher) was loaded into at least one well. Gels were run on a RunOne Electrophoresis Cell tank (EmbiTec) for 40 minutes at 50V in 1x TAE running buffer. The gels were imaged utilising an Amersham Imager 600 (GE Healthcare).

2.2.2. Protein Production and Purification

2.2.2.1. UV Quantification of Protein Concentration

To quantify protein concentration, a Nanodrop-lite spectrophotometer was used (ThermoFisher). Initially the spectrophotometer was "blanked" using 2 µL of buffer the sample was in, followed by cleaning the reading surface between sample readings with lint free wipes. 2 µL of sample was used per reading, and an absorbance was taken at 280 nm. The Beer-Lambert Law was then utilised to determine the concentration of the protein. In the case of some of the Affimers that had not had their sequence verified, an average of their molar extinction coefficient was used from a previous sample of 24 Affimers that had been sequenced from the same phage display, then this was used as ε in the Beer-Lambert Law.

2.2.2.2. BL21 Star (DE3) Cell Production for VIM-1 and Affimers

For standard protein production, pET11a-Affimer or pET11a encoding a VIM-1 plasmid DNA was transformed into BL21 Star (DE3) cells. After plating up on LB agar plates with appropriate antibiotic, single colonies were picked and used to inoculate 5 mL of 2TY and incubated overnight at 37°C, 230 rpm. After overnight incubation, these were inoculated into 500 mL 2TY culture volumes, and grown to an OD_{600} of 0.7 at 37°C, 230 rpm. These were then induced with a final concentration of 0.5 mM IPTG and cultured overnight at 25°, 150 rpm. Cells were then harvested by centrifugation at 4000 xg for 20 minutes in a 5425 Eppendorf centrifuge (Eppendorf).

2.2.2.3. Biotinylated VIM-1 Protein Production in AVB101 cells

For biotinylated VIM-1 production, pET11a encoding a BAP-tagged VIM-1 plasmid DNA was transformed into AVB101 cells (Avidity). After plating up onto LB agar plates with appropriate antibiotic, single colonies were picked and used to inoculate 5 mL of 2TY and incubated overnight at 37°C, 230 rpm. After overnight incubation, these were inoculated into 500 mL Terrific Broth autoinduction media including trace elements (FisherScientific) culture volumes, containing appropriate antibiotic, which had been preheated to 25°C. To this culture was added stock biotin solution to a final concentration of 50 µM. This was then incubated for 24-48 hours, and cells were harvested by centrifugation for 20 minutes in a 5425 Eppendorf centrifuge.

2.2.2.4. Affimer Protein Production in JM83 cells

For small scale production of Affimers in phagemid vectors, protein was produced in JM83 cells. Phagemid DNA was transformed into JM83 chemically competent *E. coli* cells. After plating up onto LB agar plates with carbenicillin single colonies were picked and used to inoculate 200 µL of 2TY in a 2 mL tube (Eppendorf) and incubated for 6 hours at 37°C, 230 rpm.

100 µL of this was then used to inoculate 50 mL of Terrific Broth autoinduction media including trace elements (FisherScientific) containing appropriate antibiotic, this was incubated for 66 hours at 25°C, 230 rpm. After this, cells were harvested by centrifugation at 4,000 xg for 20 minutes in a 5425 Eppendorf centrifuge supernatant was discarded and cell pellets were lysed immediately or frozen at -20°C until required.

2.2.2.5. Nickel Affinity Chromatography Purification

Both Affimer and VIM-1 proteins were prepared for purification through nickel affinity chromatography.

Affimers were prepared by lysing cell pellets in 1/50 of the total culture volume in lysis buffer, to which was added 0.1 mg/mL lysozyme, 1% Triton X-100 (Sigma Aldrich), 1x Halt Protease Cocktail Inhibitor (ThermoFisher), 10 U/mL Benzonase® Nuclease (Millipore) to a total volume of 8 mL. These were then incubated at room temperature for 1 hour on a Stuart SB2 fixed speed rotator, followed by incubation in a water bath for 20 minutes set to 50°C. After which they were centrifuged for 20 minutes at 16,000 xg to pellet insoluble proteins and other cellular debris. The supernatant was collected separately for affinity chromatography.

VIM-1 proteins were prepared by lysing cell pellets in 40 mL of 4°C periplasmic lysis buffer. These were then incubated for 10 minutes at 4°C on a Stuart SB2 fixed speed rotator, followed by centrifugation for 20 minutes at 16,000 xg. The supernatant was removed, and the remaining pellet was resuspended in 20 mL of 4°C $MgSO_4$ and incubated on a rotator for 30 minutes. Following this, centrifugation for 20 minutes at 10,000 xg was done to pellet unwanted proteins and cellular debris. The supernatant was collected for affinity chromatography.

Both Affimers and VIM-1 contained a His-tag which allowed purification from either the soluble (Affimer) or periplasmic (VIM-1) fractions by using Amintra Ni-NTA resin (Expedeon) following the protocol. The amount of Ni-NTA resin used differed for each protein, but roughly 30 mg of protein per mL of resin was expected to have sufficient binding capacity. Ni-NTA affinity resin consists of nitriloacetic acid in a compound with Ni^{2+} suspended in agarose and 20% ethanol that allows for reversible binding of the His-tag present in these proteins for purification purposes, that can then be competed off through the use of PBS and Imidazole, allowing for an elution step in the process.

Depending on the volume of resin being used, it was resuspended in 7x wash buffer in a falcon tube. This was centrifuged for 1 minute at 1,000 xg to collect, and excess buffer was aspirated off. This occurred three times, the protein containing supernatant was then added to the washed resin after the third equilibration step and incubated for 2-4 hours at room temperature. After this, the resin was centrifuged for 1 minute at 1,000 xg and the supernatant was aspirated off and saved to run on an SDS-PAGE gel as an unbound fraction to check for remaining protein.

A 10 mL polystyrene column (ThermoFisher) had a filter placed at the exit point and was equilibrated by filling the column with wash buffer and allowed to empty via gravity flow. The resin was then

resuspended in the same wash buffer and transferred to the column. This was emptied via gravity flow, and the A_{280} reading via spectrophotometer was read until the absorbance was <0.09. After this step buffer was changed to elution buffer and 1 mL was added to the column and allowed to incubate for 5 minutes before emptying via gravity flow. Absorbance at A_{280} was checked until no protein remained in the resin. These fractions were saved in Protein LoBind Tubes (Eppendorf) and either dialysed immediately or snap frozen and stored at -80°C, an aliquot was saved to run on an SDS-PAGE gel for analysis.

2.2.2.6. **Size Exclusion Chromatography Purification**

Protein samples that were separated through size exclusion chromatography were filtered through a HiPrep™ 16/60 Sephacryl S100 HR column connected to an Akta Explorer system. This was first flushed with degassed water to remove the storage medium, 20% ethanol solution. Equilibration then occurred with filtered and degassed 1x PBS buffer. 200 µL of protein sample was loaded into the column using an injection loop. The columns absorbance was measured at 280 nm, with a flow rate of 0.5 mL/min while 0.5 mL fractions were collected. These collected fragments were subsequently analysed using SDS-PAGE electrophoresis.

2.2.2.7. **Dialysis of Purified Protein**

After purification, proteins were exchanged into 1x PBS through dialysis. Dialysis cassettes (Sartorius Vivaspin 500) were hydrated in deionised H_2O for 30 minutes before emptying, and protein samples were pipetted in. These cassettes were then placed in a float and floated in 5 L of 1x PBS for at 4°C, for 5 hours, with agitation. Dialysed proteins were then pipetted into Protein LoBind Tubes (Eppendorf) and either used immediately or snap frozen in either dry ice, or liquid nitrogen before storage at -80°C.

2.2.2.8. **SDS-PAGE Gel Electrophoresis**

Protein samples were run on a 15% SDS-PAGE gel to allow separation according to their mobility. Samples were mixed with 4x loading buffer and deionised water to a total volume of 20 µL and heated at 95°C for 5 minutes to allow protein denaturation in the sample. The 15% gel was made using a Bio-Rad mini-PROTEAN (bioRad) casting system, firstly with a separating section, then topped with a stacking gel with a 10 or 15 well comb depending on requirements. At least one well per run would contain 5 µL of PageRuler™ Prestained Protein Ladder (ThermoScientific) to allow size identification of protein bands. Gels were run at 140V in 1x SDS-PAGE running buffer for approximately 1 hour, or until the dye had reached the bottom of the casting plates.

2.2.2.9. **SDS-PAGE Gel Coomassie Blue staining**

SDS-PAGE gels were stained with a Coomassie Blue stain (2.1.2.2.) in order to facilitate visualisation of protein. Stain was applied to gel and left to incubate at room temperature for 1 hour, while gently rocking on a Stuart gyrorocker ssl3.

After this hour, excess stain was poured off, and gel destain (2.1.2.2.) was applied overnight. Where required a second application of destain was applied to the gel the next day to aid clarity of visualisation. Gels were imaged using an Amersham Imager 600 (GE Healthcare).

2.2.2.10. **Western Blot Analysis of SDS-PAGE gels**

To verify protein biotinylation, proteins were transferred from an SDS-PAGE gel onto a PVDF membrane with 0.2 µM pore size (bioRad) utilising transfer buffer and a Trans-Blot Turbo Transfer

system (bioRad) as per the manufacturers specifications. After transfer, membranes were incubated in 25 mL of TBS-T with 3% (w/v) BSA overnight at 4°C with gentle rocking. The following day membranes were washed 3 times in 25 mL TBS-T at room temperature, gently rocking for 10 minutes. Following this, membranes were incubated with TBS-T with 3% (w/v) BSA and primary antibody 1/5000 for 1 hour. The membranes were then washed 3 times in 25 mL TBS-T at room temperature, gently rocking for 10 minutes. Membranes were then incubated for 30-60 seconds with Immobilon® Forte Western HRP Substrate (Millipore) and visualised on an Amersham Imager 600 (GE Healthcare) using the chemiluminescence setting.

2.2.3. **Phage Display Techniques**

2.2.3.1. **Target Protein Biotinylation using EZ-Link® NH-SS-Biotin**

Initially, target proteins were biotinylated using EZ-Link® NH-SS-Biotin. This was accomplished by bringing it to room temperature and diluting to 5 mg/mL in DMSO. To 1 mg/mL of target protein was added EZ-Link biotin in a 20-fold molar excess, in a total volume of 100 µL using PBS as a medium. This was incubated at room temperature for 1 hour. This was then purified utilising Zebra™ Spin Desalting Columns 7K MWCO (ThermoScientific) to remove excess biotin, as per manufacturers specifications. Samples were then used immediately in phage display. Unless otherwise stated all protein samples used Protein LoBind Tubes (Eppendorf).

2.2.3.2. **Target Protein Biotinylation using integrated BAP-tag**

After initial screening described in 3.1. Targets used in phage display were those which had been biotinylated through the addition of the BAP-tag as described in 2.2.1.3.

2.2.3.2.1. **First Panning Round**

ER2738 cells were grown overnight on LB agar plates, a single colony was picked and used to inoculate 5 mL of 2TY tet (2TY media with 12 µL/mL tetracycline), and incubated at 230rpm, overnight at 37°C. Prepared at the same time was a Pierce™ Streptavidin Coated (HBC) 8-well strip (4 wells per target) (ThermoScientific) by aliquoting 300 µL per well of 2x blocking buffer, and incubating overnight with no agitation at 37°C.

The next day the wells were washed with 300 µL of PBST per well 3 times. 100 µL per well of 2x blocking buffer was then added to three of the four wells for pre-panning. The first 3 wells were used for pre-panning phage to do this, to the first well was added 5 µL of phage library followed by incubation at 500 rpm for 1 hour at room temperature. blocking buffer was then removed from the second well, and the contents of the first well was transferred to this one, incubation occurred again at 500 rpm for 1 hour at room temperature. After this, blocking buffer was removed from the third well, and the contents of the second were added to this one, followed by incubation at 500 rpm for 1 hour at room temperature. While the pre-panning steps occurred, biotinylated target was added to the fourth well, and incubated at 500 rpm for 2 hours at room temperature. The well with the biotinylated target was washed 3x with 200 µL PBST, and the contents of the third well was added to this, followed by incubation at 500 rpm for 2 hours at room temperature.

During this, 8 mL of fresh ER2738 cell cultures were prepared from the overnight culture per target. This involved diluting the overnight culture to give an A_{600} of 0.2 as shown in a Jenway Genova spectrophotometer (Jenway) and incubating for approximately 1 hour at 230rpm, 37°C to give a final A_{600} of approximately 0.6.

The panning well containing biotinylated target was washed 27x with 300 µL of PBST on a plate washed (TECAN HydroFlex) and phage was eluted in a stepwise manner. Firstly, 100 µL of a 0.2 M glycine pH 2.2 was added to the well and incubated for 10 minutes at room temperature. This was neutralised by adding 15 µL of 1 M Tris-HCl, pH 9.1, mixing, and adding to the previously prepared 8 mL of ER2738 cells in a 50 mL falcon tube (Sarstedt). Next 14 µL of Triethylamine (Sigma-Aldrich) was mixed with 986 µL of PBS and 100 µL of this was added to the panning well and allowed to incubate for 6 minutes at room temperature. This was neutralised with 50 µL of 1M Tris-HCl, pH 7. After this the contents of the well were added immediately to the same aliquot of ER2738 cells, followed by incubation at 90 rpm, 37°C for 1 hour. 1 µL of this was aliquoted onto an LB carb plate (LB agar plate containing carbenicillin), and the remaining cells were centrifugated for 5 minutes at 3,000 xg, and resuspended in 100 µL of 2TY, and aliquoted onto a separate LB carb plate. These were then inverted, and incubated overnight at 37°C.

The next day, the colonies presented on the 1 µL plate were counted and multiplied by 8,000 to estimate the total number of cells per 8 mL, an acceptable margin was considered to be between $0.5\text{-}2x10^6$. If this target was achieved, it was continued, if not, the first panning round was restarted. If continuing, the cells were scraped from the plates by adding 5 mL of 2TY carb to the plates and scraped using a disposable L-shaped spreader and transferred to a fresh 50 mL falcon tube, mixed. 2 mL 2TY carb was added to the plates and they were scraped again, to ensure collection of any cells. The absorbance of a 1:10 dilution was then measured at 600 nm to determine the dilution needed to bring the 8 mL to an absorbance of A_{600} = 0.2. The cells were then diluted with 2TY carb, and incubated for 1 hour at 230 rpm, 37°C. Following this, 0.32 µL of M13K07 helper phage (titre ca. 10^{14} mL) was added and incubation proceeded for 30 minutes at 90 rpm, 37°C. 16 µL of kanamycin was then added, and incubation occurred overnight at 170 rpm, 25°C.

The next day the cultures were centrifuged for 10 minutes at 3,500 xg, and the phage containing supernatant was transferred to fresh 50 mL falcon tubes. At this point, 125 µL of supernatant can be removed for the second panning round, the final steps of the first panning round are to preserve the remaining phage-containing supernatant. 2 mL of PEG-NaCl precipitation solution was added to the supernatant, and incubated overnight at 4°C. The next day this was centrifuged for 30 minutes at 4,816 xg to pellet the phage. The supernatant was poured off, and the pellet resuspended in 320 µL of TE. This was then transferred to a microcentrifuge tube and centrifuged for 10 minutes at 16,000 xg. The phage-containing supernatant was then transferred to a new microcentrifuge tube, and stored at either 4°C short-term, or diluted with 40-50% glycerol and stored at -80°C long-term.

2.2.3.2.2. Second Panning Round

ER2738 cells were grown overnight on LB agar plates, a single colony was picked and used to inoculate 5 mL of 2TY tet, and incubated at 230rpm, overnight at 37°C. 20 µL of Streptavidin beads (Dynabeads® MyOne™ Streptavidin T1, 10 mg/mL) per target were pre-blocked in 100 µL 2x blocking buffer (200 µL minimum volume) and incubated overnight at 20 rpm, room temperature on a Stuart SB2 fixed speed rotator (Stuart).

Two deep well 96 plates (ThermoScientific) were pre-blocked with 1 mL of 2x blocking buffer per well for panning. For elution, wells were pre-blocked with 300 µL of 2x blocking buffer, these were incubated for 2 hours at 37°C.Four deep well 96 plates (ThermoScientific) were prepared with 950 µL of 2x blocking buffer per well to be used for washing. The pre-blocked Streptavidin beads were centrifuged for 1 minute at 800 xg, the beads were immobilised on a magnet and the blocking buffer was removed and replaced by 100 µL of fresh 2x blocking buffer per 20 µL of beads, with a minimum of 200 µL.

To pre-pan the phage, 125 µL of fresh phage-containing supernatant was mixed with 125 µL of 2x blocking buffer (or 5 µL of the purified phage from 2.2.3.2.1 was combined with 245 µL of 2x blocking buffer) and 25 µL of the pre-blocked Streptavidin beads in Protein LoBind Tubes (Eppendorf). This was incubated at room temperature for 1 hour on the Stuart rotator. Following this, the beads were centrifuged for 1 minute at 800 xg and placed on a magnet. The phage-containing supernatant was transferred to a fresh Protein LoBind tube and another 25 µL of pre-blocked Streptavidin beads were added, this was then incubated at room temperature for 1 hour on the Stuart rotator. 15 µL of biotinylated target was added to 200 µL of 2x blocking buffer, to which was added 50 µL of pre-blocked Streptavidin beads, this was then incubated at room temperature for 1 hour on the Stuart rotator. Meanwhile buffer was removed from the pre-blocked deep well 96 plate, and pre-blocked elution plates. To the first elution plate was added 100 µL per well of 0.2 M glycine, pH 2.2, and to the second 100 µL per well of 14 µL of Triethylamine diluted in 986 µL of PBS was added.The tubes containing biotinylated target were centrifuged for 1 minute at 800 xg and placed on a magnet. The beads were then washed 3x in 500 µL of 2x blocking buffer. The tubes containing the pre-panned phage were centrifuged for 1 minute at 800 xg and placed on a magnet. The phage-containing supernatant was removed and transferred to the beads containing the biotinylated target and the mixture was resuspended before transfer to the pre-blocked deep well 96 plates. A KingFisher Flex was then set up to run the protocol outline in Table 2.8

Protocol Step	**Plate**	**Volume (ul)**	**Settings**
Tipcomb	96 DW tip comb		
Pick-Up: Tipcomb	KingFisher 96 KF plate		
Collect Beads	Plate: Binding Microtiter DW 96 plate		Collect count 1 Collect time (s) 1
Binding	Plate: Binding Microtiter DW 96 plate	300	**Beginning of Step** Release beads [hh:mm:ss]: 00:00:00 **Mixing/Heating Parameters** Mix time [hh:mm:ss]: 00:00:10 Speed: fast Mix time [hh:mm:ss]: 01:00:00 Speed: slow **End of step** Collect beads, count: 5 Collect time (s): 30
Wash 1	Plate: Wash 1 Microtiter DW 96 plate	950	**Beginning of Step** Release beads [hh:mm:ss]: 00:00:00 **Mixing/Heating Parameters** Mix time [hh:mm:ss]: 00:01:00

			Speed: slow **End of step** Collect beads, count: 5 Collect time (s): 30
Wash 2	Plate: Wash 2 Microtiter DW 96 plate	950	**Beginning of Step** Release beads [hh:mm:ss]: 00:00:00 **Mixing/Heating Parameters** Mix time [hh:mm:ss]: 00:01:00 Speed: slow **End of step** Collect beads, count: 5 Collect time (s): 30
Wash 3	Plate: Wash 3 Microtiter DW 96 plate	950	**Beginning of Step** Release beads [hh:mm:ss]: 00:00:00 **Mixing/Heating Parameters** Mix time [hh:mm:ss]: 00:01:00 Speed: slow **End of step** Collect beads, count: 5 Collect time (s): 30
Wash 4	Plate: Wash 4 Microtiter DW 96 plate	950	**Beginning of Step** Release beads [hh:mm:ss]: 00:00:00 **Mixing/Heating Parameters** Mix time [hh:mm:ss]: 00:01:00 Speed: slow **End of step** Collect beads, count: 5 Collect time (s): 30
pH Elution	Plate: pH elution KingFisher 96 KF plate	100	**Beginning of Step** Release beads [hh:mm:ss]: 00:00:00 **Mixing/Heating Parameters** Mix time [hh:mm:ss]: 00:07:30 Speed: slow Postmix[hh:mm:ss]: 00:00:05 Speed: Bottom mix **End of step** Collect beads, count: 5 Collect time (s): 30
Triethylamine Elution	Plate: Triethylamine KingFisher 96 KF plate	100	**Beginning of Step** Release beads [hh:mm:ss]: 00:00:00 **Mixing/Heating Parameters** Mix time [hh:mm:ss]: 00:03:30 Speed: slow Postmix[hh:mm:ss]: 00:00:05 Speed: Bottom mix **End of step** Collect beads, count: 5 Collect time (s): 30
Leave: Tipcomb	96 DW tip comb		

Table 2.8. Outline of Standard Panning steps for KingFisher Flex (Tiede, 2019[99]).

An hour before completion, 8 mL of fresh ER2738 cell cultures were prepared from the overnight culture per target. This involved diluting the overnight culture to give an A_{600} of 0.2 as shown in a Jenway Genova spectrophotometer and incubating for approximately 1 hour at 230rpm, 37°C to give a final A_{600} of approximately 0.6. The two elution steps required neutralising, with the first plate the glycine was neutralised by addition of 15 µL 1M Tris-HCl, pH 9.1, mixing and adding to the fresh ER2738 cell culture. The second plate was neutralised by addition of 50 µL of 1M Tris-HCl, pH 7, mixing and adding to the same culture. The cells were then incubated at 90 rpm, for 1 hour at 37°C, then centrifuged for 5 minutes at 3,000 xg before resuspending in 200 µL of 2TY carb, and aliquoting onto 2 LB carb plates, 100 µL each. These were then inverted and incubated overnight at 37°C.

The next day the cells were scraped from the plates by adding 5 mL of 2TY carb to the plates and scraped using a disposable L-shaped spreader and transferred to a fresh 50 mL falcon tube, mixed. 2 mL 2TY carb was added to the plates and they were scraped again, to ensure collection of any cells. The absorbance of a 1:10 dilution was then measured at 600 nm to determine the dilution needed to bring the 8 mL to an absorbance of A_{600} = 0.2. The cells were then diluted with 2TY carb, and incubated for 1 hour at 230 rpm, 37°C. Following this, 0.32 µL of M13K07 helper phage (titre ca. 10^{14} mL) was added and incubation proceeded for 30 minutes at 90 rpm, 37°C. 16 µL of kanamycin was then added, and incubation occurred overnight at 170 rpm, 25°C.

The next day the cultures were centrifuged for 10 minutes at 3,500 xg, and the phage containing supernatant was transferred to fresh 50 mL falcon tubes. At this point, 200 µL of supernatant can be removed for the third panning round, the final steps of the second panning round are to preserve the remaining phage-containing supernatant.

2 mL of PEG-NaCl precipitation solution was added to the supernatant, and incubated overnight at 4°C. The next day this was centrifuged for 30 minutes at 4,816 xg to pellet the phage. The supernatant was poured off, and the pellet resuspended in 320 µL of TE. This was then transferred to a microcentrifuge tube and centrifuged for 10 minutes at 16,000 xg. The phage-containing supernatant was then transferred to a new microcentrifuge tube, and stored at either 4°C short-term, or diluted with 40-50% glycerol and stored at -80°C long-term.

2.2.3.2.3. **Third Panning Round**

ER2738 cells were grown overnight on LB agar plates, a single colony was picked and used to inoculate 5 mL of 2TY tet, and incubated at 230rpm, overnight at 37°C. Prepared at the same time was a Streptavidin Coated (HBC) 8-well strip (ThermoScientific), 6 wells per target; four for pre-panning phage, one for panning against a target and one as a negative control, by aliquoting 300 µL per well of 2x blocking buffer and incubating overnight with no agitation at 37°C.

The next day the wells were washed 3x with 300 µL of PBST per well. 200 µL per well of 2x blocking buffer was then added to three of the four pre-panning wells. To the first pre-panning well was added 10 µL of 10x blocking buffer and 200 µL of the phage-containing supernatant saved from the second panning round (or 8 µL of purified phage combined with 212 µL of 2x blocking buffer) and incubated at 500 rpm for 1 hour at room temperature. The contents of the second well were removed, and the contents of the first well transferred to it, this was incubated at 500 rpm for another hour at room temperature. This was then repeated similarly for the third and fourth wells.

The contents of the panning well were removed and 100 µL of 2x blocking buffer was added to it along with 10 µL of the biotinylated target, this was incubated at 500 rpm for 1 hour at room

temperature. The target and negative control wells were washed 3x in PBST, and 100 µL of the pre-panning well phage was added to each of these, this was then incubated at 500 rpm, for 45 minutes at room temperature.

A fresh culture of ER2738 cells were prepared for both the biotinylated target and negative control as described in 2.2.3.2.2. and the panning wells were washed with 300 µL of PBST 27x. Phage was eluted by pH as described in 2.2.3.2.1. and the cultures of ER2738 cells from the biotinylated target and negative control wells were incubated at 90 rpm, for 1 hour at 37°C. A range of volumes were then aliquoted onto LB carb plates for the target culture; 0.01, 0.1, 1, 10, 25, 50, 100 µL, with the volumes being made up to 100 µL where necessary using 2TY. For the negative controls; 0.1, 1, 10, 100 µL LB carb plates were plated up, with the volumes being brought up to 100 µL again with 2TY. These were then inverted and incubated overnight at 37°C.

2.2.3.3. **Phage ELISA**

To confirm binding to VIM-1, phage ELISA was performed on randomly selected clones. Streptavidin (Molecular Probes) was diluted to 5 µg/mL in PBS, and 50 µL of this was added to every well of an F96 Maxisorp Nunc-Immuno Plate (ThermoScientific) and incubated at 4°C overnight, with storage at this temperature for up to 1 week.

Following this, 200 µL of 2TY carb was aliquoted into the necessary wells of a 96-well V-bottom deep well plate (Greiner) and individual colonies from the panning round were picked and placed into individual wells overnight at 1050 rpm, 37°C (Heidolf Incubator 1000). Following this, a new 96-well V-bottom deep well plate was prepared with 200 µL of 2TY carb per well and 25 µL of the prepared overnight culture was transferred into a new well, and incubated at 1050 rpm, 37°C for 1 hour. M13K07 helper phage (titre ca.10^{14}/mL) was diluted in 2TY carb 1/1000 with 10 µL of this added to each well, this was then incubated at 500 rpm, room temperature, for 30 minutes. Kanamycin was then diluted in 2TY carb 1/20 and 10 µL was added per well, this was then incubated at 750 rpm, room temperature overnight. The next day phage was harvested by centrifugation in the plate for 10 minutes at 3500 xg. The supernatant containing the phage was transferred to a previously prepared ELISA plate for binding against immobilised biotinylated target.

Streptavidin-coated plates were prepared by adding 200 µL 2x blocking buffer (diluted 10x blocking buffer (Sigma)) and incubating with no shaking at 37°C overnight. The next day plates were washed once with 300 µL of PBST on a plate washer (TECAN HydroSpeed). Biotinylated target was diluted 1/100 (using 2.5 – 5 µg of target) in 2x blocking buffer, and 50 µL of this was added to the top half (or left half) of the streptavidin coated 96-well plate. In the other half of the plate was aliquoted 50 µL of 2x blocking buffer as negative controls, the plate was incubated at 500 rpm, room temperature for 1 hour. Following this, all wells were washed once with 300 µL PBST, and 10 µL of 10x blocking buffer was added to each well. 40 µL of the supernatant containing the phage was aliquoted to a well containing VIM-1 target, and a well without as a negative control, this was then incubated at 500 rpm, room temperature for 1 hour. Following this incubation wells were washed once with 300 µL per well PBST, and Anti-Fd-Bacteriophage-HRP (Seramun Diagnostica) was diluted in 2x blocking buffer 1/1000, with 50 µL being aliquoted per well. This was then incubated at 500 rpm, room temperature for 1 hour. Following this all wells were washed 10x with 300 µL per well of PBST, after which 50 µL per well of TMB (SeramunBlau© fast TMB/substrate solution (Seramun Diagnostica)) and allowed to develop for approximately 3 minutes. Absorbance was measured at 620 nm using a ThermoScientific Multiskan FC (ThermoFisher).

2.2.4. Enzyme Assays

2.2.4.1. β-lactamase Activity Assay

VIM-1 hydrolyses nitrocefin (Merck) as it would a substrate due to its β-lactam ring, the rate of which can be measured through a colour change from yellow to red. B-lactamase assay buffer was used to dilute reagents to a final volume of 150 µL per well in a Nunc™ MicroWell™ 96-well microplate. In a standard well would be 50 µL VIM-1 protein, 50 µL nitrocefin (65 mM (Merck)), 50 µL β-lactamase assay buffer, control, or Affimer at 100x VIM-1 concentration if monitoring the Affimers effect on rate of hydrolysis. Controls used included an EDTA control, a no Affimer control, a no VIM-1 but Affimer control, and a no VIM-1 control.

Absorbance was measured approximately every 7 seconds at 482 nM and a constant temperature of 25°C using a Tecan Spark microplate reader (Tecan AG) to measure the rate of reaction, and the change in concentration of nitrocefin over time was calculated using the Beer-Lambert Law. Rates were measured using GraphPad Prism 9 (GraphPad Software Inc), using linear regression analysis.

3. Results

In previous work, Affimer reagents were found to bind to and inhibit NDM-1. Given the similarities between NDM-1 and VIM-1, it was proposed that Affimer inhibitors against VIM-1 could also be isolated. The aim of this project was to test this hypothesis.

3.1. Verona Integron-encoded Metallo β-lactamase (VIM-1) Verification and Production

The initial step of isolating Affimer reagents by phage display is to produce a high-quality protein of the target molecules. To do this, we used a pET11a vector containing the VIM-1 coding sequence previously cloned and provided by A. Herbert (University of Leeds) which featured a T7 promoter, a PelB signal sequence at the N-terminus, 6 his-tag and carbenicillin (*ampR*) resistance gene. The inclusion of the PelB sequence is required for export of VIM-1 through to the periplasm utilising the SecA/SecYEG system, where VIM-1 folding into an active enzyme containing Zn^{2+} takes place.

To verify the VIM-1 sequence, the vector DNA was transformed into XL1-Blue Supercompetent *E. coli* cells following the protocol 2.2.1.3 (see Materials and Methods). Briefly, 20 µL of 100 ng/µL plasmid DNA was sent for Sanger sequencing by Genewiz using a T7 forward promoter. The sequencing was translated using ExPASy server and verified against the VIM-1 coding sequence, shown in Figure 3.1.1 (a).

After successful verification, the pET11a-VIM-1 vector was transformed into BL21 Star (DE3) cells following the protocol in 2.2.2.2. (Materials and methods). Cells were then harvested by centrifugation and purified using size exclusion chromatography through a Superdex 200 increase resin in an ÄKTA column ((trade name, Cytiva) Figure 3.1.1 (b)). Size exclusion columns function by packing a column with beads which feature passages through them, the size of which can be selected depending on the protein being purified. As proteins pass through the column, smaller proteins can pass in and out of these beads, whereas larger proteins are excluded and therefore pass through the column faster and are therefore eluted sooner. Elutions were collected in 1 mL volumes, and those which appeared to be VIM-1 protein on the ÄKTA visual graph had 20 µL removed and analysed on a 15% SDS-PAGE gel to confirm the correct band size expected for VIM-1 protein, as shown in Figure 3.1.1 (c). Analysis showed good expression of the VIM-1 protein using 2TY broth and purification using an ÄKTA system.

Due to the importance of VIM-1 in the study it was necessary to ensure the protein concentration was accurate throughout each experiment. As such a BCA assay alongside spectrophotometer analysis was used to estimate VIM-1 concentration (Figure 3.1.1.). Bovine Serum Albumin (BSA) was used in a range of concentrations (20-2000 µg/mL) as a standard in the BCA assay to allow linear regression and assess the concentration of VIM-1 protein over a range of dilutions. It was found from the BCA assay to be approximately 2.21 g/L. Spectrophotometric analysis of the same samples gave a return of 2.11 g/mL (over an average of three 2 µL aliquots). As such there was a high degree of confidence the true protein concentration was being shown.

a

MKYLLPTAAAGLLLLAAQPAMASPLAHSGEPSGEYPTVNEIPVGEVRLYQIADGVWSHIATQSFDGAVY
PSNGLIVRDGDELLLIDTAWGAKNTAALLAEIEKQIGLPVTRAVSTHFHDDRVGGVDVLRAAGVATYAS
PSTRRLAEAEGNEIPTHSLEGLSSSGDAVRFGPVELFYPGAAHSTDNLVVYVPSANVLYGGCAVHELSSTS
AGNVADADLAEWPTSVERIQKHYPEAEVVIPGHGLPGGLDLLQHTANVVKAHKNRSVAEAAAHHHHH
HHH

PelB leader

His-tag

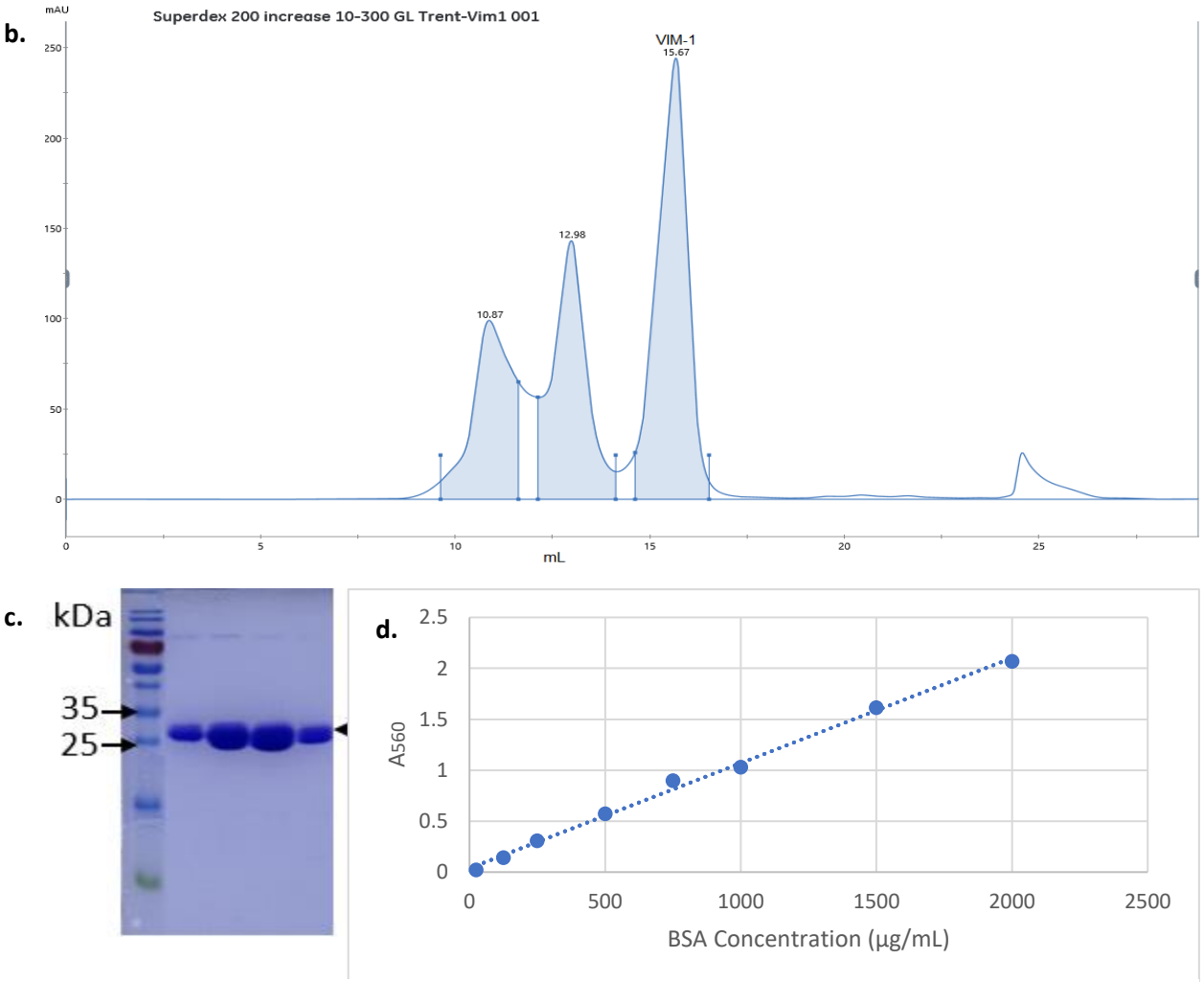

Figure 3.1.1. Sequence verification and production and purification of VIM-1. (a) Sequence of the verified VIM-1 construct. **(b)** The peak taken from ÄKTA purification of VIM-1 protein. **(c)** VIM-1 protein was purified from 400 mL bacterial cell lysate using ÄKTA Superdex 200. Protein elutions were analysed by 15% SDS-PAGE and stained with Coomassie blue to confirm elutions contained VIM-1 protein, expected at 29.44 kDa, as indicated by the black arrow. A PageRuler prestained protein ladder 10-180 kDa was loaded on the left to aid verification. (d) Standard curve of a BCA assay using BSA as standards. A concentration range of 20-2000 µg/mL BSA was used in the BCA assay as per manufacturers guidelines. Readings at A_{560} were taken and linear regression was calculated between this and the BSA, y = 0.001x + 0.0373. The A_{560} of diluted 10-fold, 100-fold and 1000-fold protein sample was taken, and interpolation of the calibration graph was used to estimate protein concentration (average 2219.333 µg/mL).

3.1.2. Phage ELISA

Next a phage display screen was carried out using the purified VIM-1 protein to isolate Affimer reagents. The purified VIM-1 protein was biotinylated using EZ-Link® NH-SS-Biotin which binds primarily to lysine residues. Three rounds of panning were performed against both VIM-1 and a positive control, Pyruvate dehydrogenase kinase (PDK) (provided by A. Tang, University of Leeds) which was biotinylated through an N-terminus biotin acceptor peptide (BAP)-tag. Following this, colonies were randomly selected from test plates and phage ELISA was carried out to verify binding to the biotinylated targets. Each selected clone was checked against a well containing immobilised biotinylated target, and a negative control where no target was present. Anti-Fd-Bacteriophage-HRP and 3,3'.5.5'-tetramethylbenzidine (TMB) were used as substrates. TMB was applied and allowed to

develop for 3 minutes. Absorbances were read at 620 nm on a ThermoScientific Multiskan FC plate reader, results of which are shown in Figure 3.1.2.

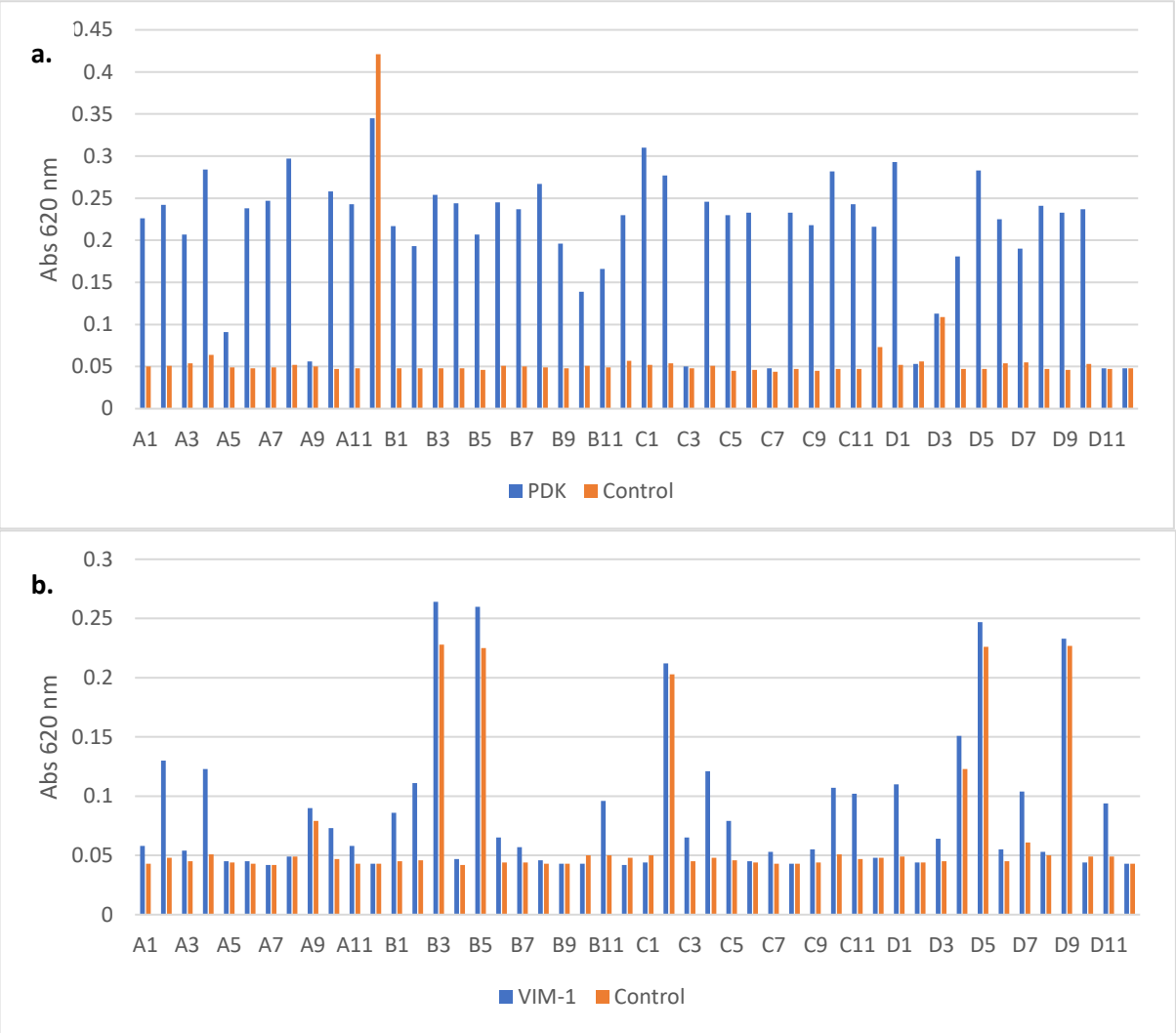

Figure 3.1.2. Phage ELISA results for EZ-link NHS-SS biotinylated VIM-1. Anti-Fd-Bacteriophage-HRP and SeramunBlau TMB were used to show visible colour change and allow for absorbances to be taken at 620 nm. **(a)** Phage ELISA results for biotinylated PDK used as a positive control. PDK was biotinylated through an integral BAP-tag located on the construct. Phage was exposed to control wells where no biotinylated target had been incubated to verify successful binding against target. **(b)** Phage ELISA results for VIM-1. VIM-1 was biotinylated through chemical biotinylation using EZ-link NHS-SS-Biotin. Phage was exposed to control wells where no biotinylated target had been incubated to verify successful binding.

The phage ELISA demonstrated the isolation of binding reagents for the positive control, with a high level of Affimer-target binding (bars in blue, figure 3.1.2.) and low levels of background in the negative control wells (bars in orange, figure 3.1.2.). This indicated that the phage display and ELISA was successful as due to the wash steps involved in performing phage ELISA, a higher absorbance should be seen where Affimer displaying phage is bound to immobilised target than to that of an "empty" well – in this case the control or "background signal". For example, when referring to the

PDK phage display (Figure 3.1.2.(a)) A4 has a high absorbance against PDK, and a low absorbance for the control, indicating the presence of more Affimer presenting phage. In contrast, A12 features a background higher than that of the binding to PDK, which would indicate either poor binding, or an error in those particular wells, regardless this would not be used. The results for the clones against VIM-1 however, showed little-to-no difference between the Affimer-target binding and the background absorbance in negative control wells. This indicated that instead of binding to the biotinylated target, it was merely background signal from the reagents, and that there would be a limited rationale for attempting to take any of these clones forward. The difference in target display between VIM-1 and PDK was the use of the BAP-tag on PDK to immobilise the target in the well. As such, it was decided to clone a BAP-tag onto the pET11a-VIM-1 construct and repeat phage display.

3.2. **Biotin Acceptor Peptide (BAP-tag) Cloning onto VIM-1**

The cloning of a BAP-tag onto the pET11a-VIM-1 construct was accomplished using protocol 2.2.1.3. (Materials and methods).

Using overlapping PCR mutagenesis, a biotin acceptor peptide sequence of G-L-N-D-I-F-E-A-Q-K-I-E-W-H-E was cloned into the pET11a-VIM-1 construct after the PelB leader sequence. The assay was optimised using a gradient of temperatures in a thermocycler, the results of which are shown in Figure 3.2.1.

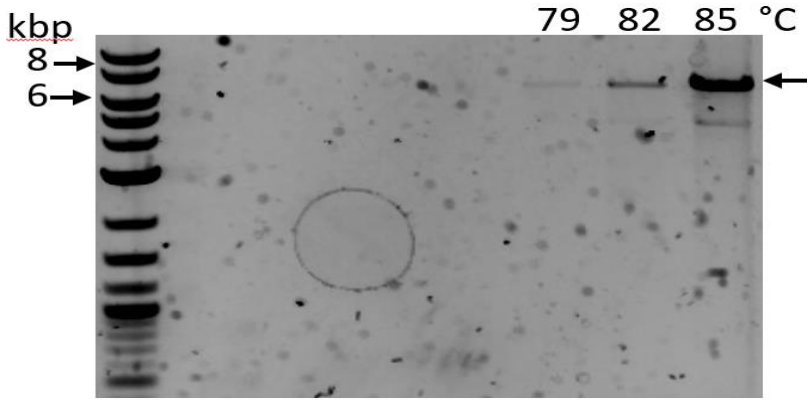

Figure 3.2.1. Agarose gel showing successful amplification of BAP-tagged VIM-1 sequence. PCR of the successful addition of a BAP-tag to VIM-1 construct directly after the PelB leader sequence. Products were run on a 0.7% agarose gel stained with orange loading dye against a 1 kb DNA ladder. The expected size of successful cloning should be 6700 bp, successful temperatures were labelled and indicated by the black arrow.

Following successful cloning, verification steps followed to ensure the BAP-tag was being successfully biotinylated. To verify the correct sequence, the pET11a-VIM-1-BAP vector was transformed into XL1-Blue Supercompetent *E. coli* cells following the protocol 2.2.1.3. (Materials and methods) 20 µL of 100 ng/µL plasmid DNA was sent for Sanger sequencing by Genewiz using a T7 forward promoter. The sequencing was translated using ExPASy server and verified against the VIM-1 coding sequence, shown in Figure 3.2.2.

Once verified, the pET11a-VIM-1-BAP vector was transformed via heat shock into AVB101 *E. coli* cells following the protocol 2.2.2.3. (materials and methods) which contain a *birA* gene coding for an IPTG-inducible biotin ligase enzyme, BirA that allows for the biotinylation of the BAP-tag *in vivo* in

MKYLLPTAAAGLLLLAAQPAMAGLNDIFEAQKIEWHESPLAHSGEPSGEYPTVNEIPVGEVRLYQIADGVWSH
IATQSFDGAVYPSNGLIVRDGDELLLIDTAWGAKNTAALLAEIEKQIGLPVTRAVSTHFHDDRVGGVDVLRAA
GVATYASPSTRRLAEAEGNEIPTHSLEGLSSSGDAVRFGPVELFYPGAAHSTDNLVVYVPSANVLYGGCAVHEL
SSTSAGNVADADLAEWPTSVERIQKHYPEAEVVIPGHGLPGGLDLLQHIANVVKAHKNRSVAEAAAHHHHH
HHH

PelB leader

BAP-tag

Figure 3.2.2. Sequence verification of successful integration of BAP-tag onto pET11a-VIM-1 construct. The sequence showed no interruption to the PelB leader or start of the VIM-1 protein sequence. His-tag still present to allow for nickel affinity chromatography purification.

the presence of ATP [97]. Once lysed, VIM-1 protein was purified through nickel affinity chromatography, elution's were collected in 500 µL aliquots, and analysed on a 15% SDS-PAGE gel to confirm bands at the new expected weight of 31.25 kDa (Figure 3.2.3 (a)).

Following verification of cloning the BAP-tag in frame with VIM-1, the biotinylation of the BAP sequence was confirmed by Western blotting (Figure 3.2.3 (b)). Protein concentration was measured by spectrophotometer, and dilutions were made to obtain samples of 50 and 100 ng of VIM-1 protein. These were transferred from an SDS-PAGE gel onto PVDF membranes and probed for the presence of biotin using streptavidin conjugated to HRP, shown in Figure 3.2.3 (b). This was compared to a protein that had previously been confirmed to be biotinylated at its BAP-tag. Following verification of successful biotinylation, VIM-1 proteins were snap-frozen and stored at –80°C prior to use in phage display.

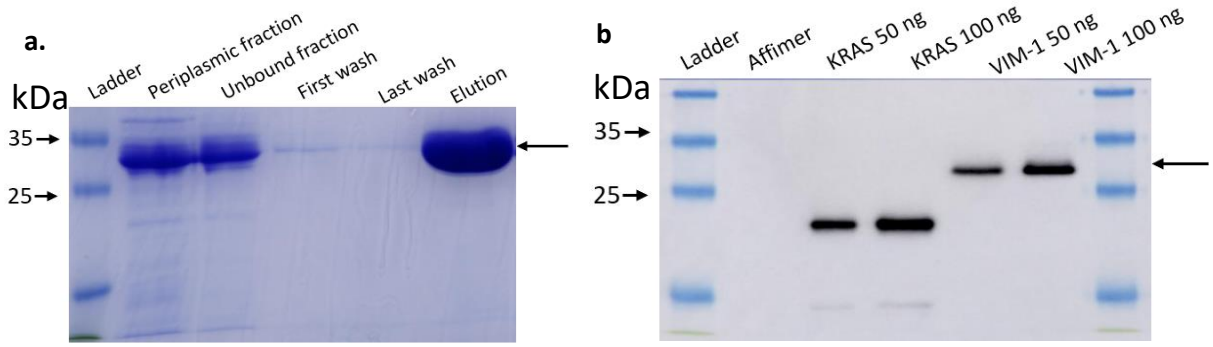

Figure 3.2.3. SDS-PAGE and western blot verification of successful BAP-tag insertion to VIM-1 sequence. (a) Purified BAP-tagged VIM-1 protein from pET11a vector. The protein was purified from 500 mL BL21 Star bacterial cell lysate using nickel affinity chromatography. Protein elutions were analysed by 15% SDS-PAGE gel and stained with Coomassie blue to confirm successful integration of the BAP-tag. Integration of the BAP-tag was expected to result in a protein size of approximately 31.25 kDa, indicated by the black arrow. **(b)** Western blot analysis to confirm presence of BAP-tag on the VIM-1 construct. A negative control of unbiotinylated Affimer, and positive control of previously successful biotinylated KRAS were used to confirm successful probing VIM-1 is indicated by the black arrow at the expected size.

3.2.1. Phage Display and Phage ELISA with BAP-tagged VIM-1

After confirmation of biotinylation and purity of the VIM1 protein, phage display screen was performed in an attempt to isolation Affimer reagents. Three rounds of panning were performed against both VIM-1 and the previous positive control, biotinylated PDK. Following this, colonies were randomly selected from test plates and phage ELISA was carried out to verify binding to the biotinylated targets. Each clone was checked against a well containing immobilised biotinylated target, and a negative control where no target was present. Absorbances were read at 620 nm on a ThermoScientific Multiskan FC plate reader, results of which for VIM-1 are shown in Figure 3.2.4.

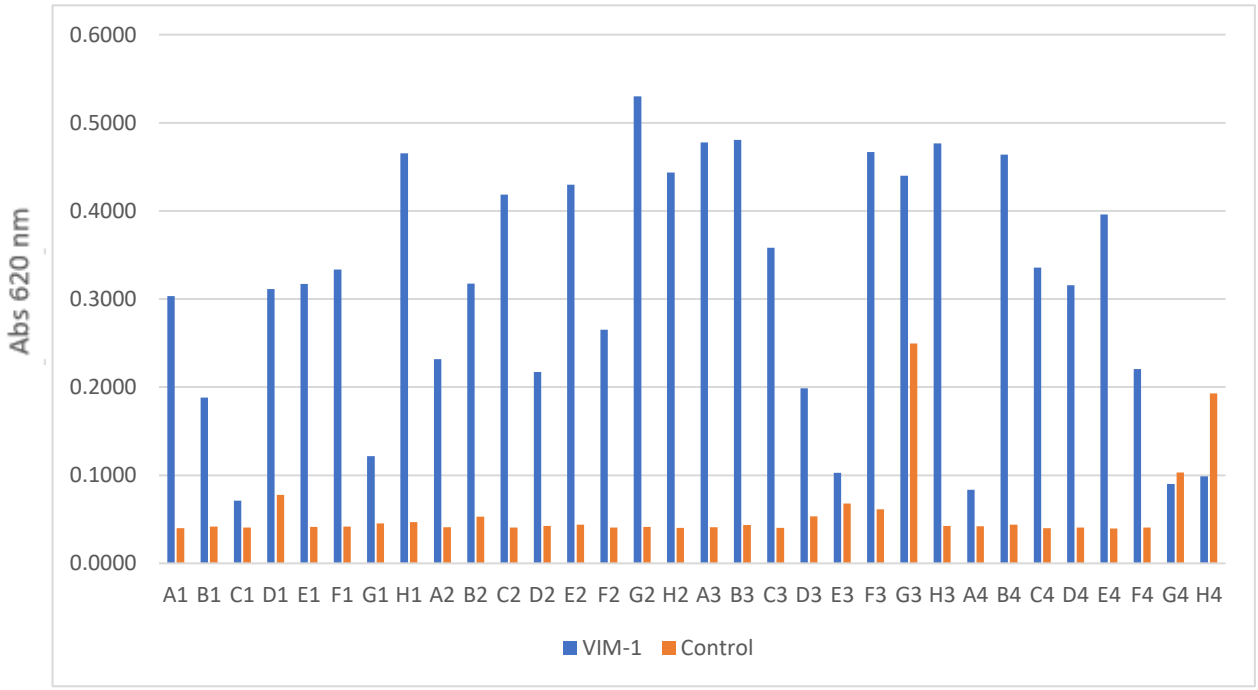

Figure 3.2.4. Phage ELISA results for VIM-1 biotinylated through BAP-tag. Phage ELISA was completed with BAP-tagged VIM-1. Phage was exposed to control wells where no biotinylated target had been incubated to verify successful binding. The positive control was also used which had been proven to be successful before (results for this not shown here). Anti-Fd-Bacteriophage-HRP and SeramunBlau TMB were used and allowed to develop for 3 minutes to show visible colour change and allow for absorbances to be taken at 620 nm.

Of the thirty-two clones randomly chosen, twenty-seven showed high levels of Affimer-target binding in contrast to the negative control wells. These were taken forward for sequencing from the phagemid vector to assess the variable regions and the variability between the reagents, shown in figure 3.2.5.

Well	VR1	VR2	Unique?
A1	MAAPRFWPE	AAE------	Yes
B1	FESPYFWPV	AAE------	Yes
C1	WWPMAHGYE	KEAMGHKHK	No (x4)
D1	HASMNRWQE	QSHWWFGIF	Yes
E1	QWYIWTSWW	AAE------	Yes
G1	TAGTQYNQE	LLRYPKQSF	Yes
H1	YHETTVQHN	RREIYQLKW	Yes
A2	NTFWFTYFA	KPTREFQLI	Yes
B2	FRRENYTTE	KRNWGWWSH	No (x3)
C2	WRDMIYASY	AYYHNSDNT	Yes
D2	VIQANKELD	RKMIWKFHV	Yes
E2	FMAPHFWPG	AAE------	Yes
G2	REQQDWTVE	HYNYPWAAG	Yes
H2	THAPFFWPE	AAE------	Yes
A3	WWPMAHGYE	KEAMGHKHK	No (x4)
B3	EMEVQHGYH	WRRIWNYHW	Yes
C3	VIYYRDDYY	WKFLTILEI	Yes
D3	VKESQMVRS	LTWFMRGIY	Yes
E3	FRRENYTTE	KRNWGWWSH	No (x3)
F3	FRRENYTTE	KRNWGWWSH	No (x3)
G3	HNGRFRYHT	AHRWWWNWD	Yes
H3	MRAPIYWPE	AAE------	Yes
A4	LRAPVFWPV	AAE------	Yes
B4	WWPMAHGYE	KEAMGHKHK	No (x4)
C4	WWPMAHGYE	KEAMGHKHK	No (x4)
D4	IQLTQNGNS	AWWIKMQNI	Yes
F4	ILYWKQEYY	WNTYDTVEI	Yes

Figure 3.2.5. Results of Affimers picked from phage ELISA results for BAP-tagged VIM-1. Affimers were produced utilising method found in 2.2.2.2, and Sanger sequenced by GeneWiz. The variation between variable regions was compared to establish unique binders or repetition. 22 unique Affimers were discovered, with 2 replicated, 5 of which contained a single variable region, and 17 with two variable regions.

3.2.2. Autoinduction Expression of Affimer

The phagemids contain an amber codon between the Affimer and pIII, allowing production of Affimer in certain cell strains without the need to subclone into a different expression vector. The phagemids were transformed in to JM83 cells and grown in 50 mL of autoinduction media. Although this yields a small amount of protein enough is produced to measure activity in a nitrocefin assay.

After autoinduction cells were harvested by centrifugation, lysed, and purified using nickel affinity chromatography, elution's were collected in 500 µL aliquots, and analysed on a 15% SDS-PAGE gel to confirm bands at the new expected weight of ~12 kDa (Figure 3.2.6).

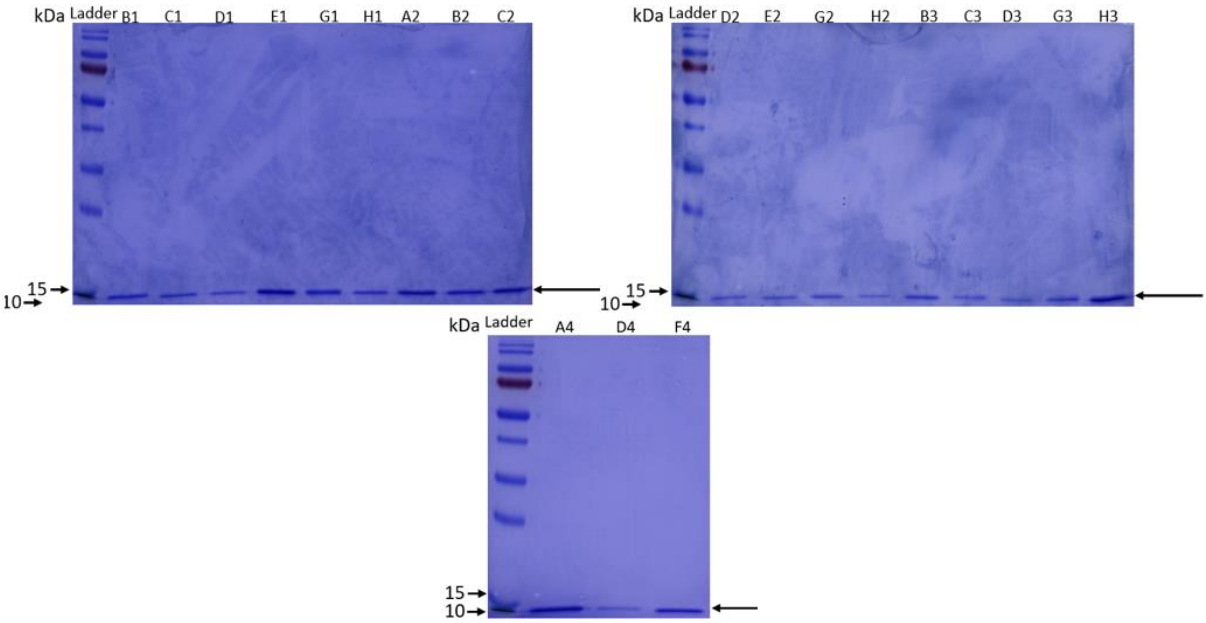

Figure 3.2.6. SDS-PAGE of Affimers to verify production and purification. Affimers were produced in 50 mL of JM83 cell culture and purified by nickel affinity chromatography. 2 µL samples were used from the elution step. Samples were denatured in 1x sample buffer and denatured by boiling for 5 minutes before loading. 5 µL of PageRuler molecular weight ladder was added into the first well. Gels were stained with Coomassie blue dye. Expected bands of ~12 kDa are indicated by the black arrows.

Successfully purified Affimers were cassette dialysed in 1x PBS to remove imidazole from solution, and snap frozen at -80°C until ready for use in nitrocefin assays.

3.2.3. Alanine Affimer Production

As well as the Affimer reagents from phage display, it was required to make a stock of alanine Affimer for use as a control in the nitrocefin assays. Alanine Affimers contain stunted variable regions; VR1 contains 4 alanines only, VR2 contains 2 alanines and a glutamic acid. These are used as a control to verify that the basic Affimer structure will not interfere with an assay, by independently binding, as it cannot feature any other amino acid residues in these positions or others in the variable regions.

Alanine Affimer was produced using protocol 2.2.2.2 (materials and methods). Cells were harvested by centrifugation, lysed, and purified using nickel affinity chromatography. Elution's were collected in 500 µL aliquots and analysed on a 15% SDS-PAGE gel to confirm bands at the new expected weight of ~12 kDa (Figure 3.2.7).

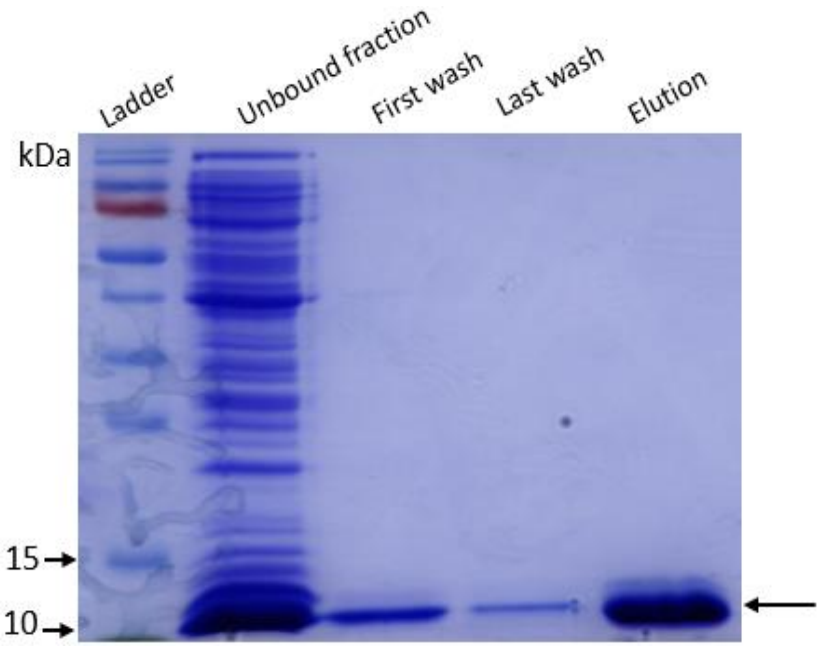

Figure 3.2.7. SDS-PAGE to verify Alanine Affimer production and purification in BL21 Star (DE3) cells. Purified alanine Affimer from pET11a vector used for negative control. The protein was eluted from 500 mL bacterial cell lysate using nickel affinity chromatography. 2 µL samples were taken from the elution step and denatured in 1x sample buffer and denatured by boiling for 5 minutes before loading. 5 µL of PageRuler molecular weight ladder was added into the first well. Protein elution fractions were analysed on a 15% SDS-PAGE gel and stained with Coomassie blue to confirm expected protein size, indicated by the black arrow.

Alanine Affimer was successfully produced and purified and dialysed in 1x PBS to ensure removal of imidazole from solution, and snap frozen at -80°C until ready for use in nitrocefin assays.

3.3. Nitrocefin assay results

3.3.1. Affimer Concentration at 10-fold VIM-1 Concentration

Nitrocefin is hydrolysed by β-lactamases due to the presence of a β-lactam ring in its structure. The rate of hydrolysis by metallo-β-lactamases such as VIM-1 can be measured through observing a colour change from yellow to red (482 nm) when using nitrocefin as a substrate. As such, any inhibitory effect that Affimer reagents might cause through binding to VIM-1 could be traced through observing the activity of VIM-1 with nitrocefin only, and in the presence of Affimer reagents.

Previously unpublished work on NDM-1 has demonstrated that Affimers can successfully inhibit nitrocefin hydrolysis by NDM-1 by up to 85% at five-fold the enzyme concentration (500 nM Affimer to 100 nM NDM-1)[87], [88]. As such initial tests were done with 10-fold Affimer concentration to VIM-1 concentration, in an attempt to visualise any inhibition that may occur. Once that was established, IC_{50} testing would follow. The Affimer reagents expressed in JM83 were diluted to 3 µM, and VIM-1 was diluted to 300 nM, as observed by the A_{280} on a spectrophotometer (three separate aliquots of 2 µL tested, with an average taken between the three). The actual concentrations in the 96-well plate were 1/3rd of these concentrations, as 50 µL of each was put in, for a final volume per well of 150 µL. Results are shown in Figure 3.3.1.

Controls included; an EDTA control to which graphs are normalised (5 mM EDTA, 100 nM VIM-1, 65 µM nitrocefin), to chelate the Zn^{2+} in the VIM-1 active site and nullify its capacity for hydrolysis, a no VIM-1 control (65 µM nitrocefin, 50 µL assay buffer, 1 µM random Affimer) to ensure no hydrolysis occurs either spontaneously or through interaction with the Affimer structure, a no Affimer control (100 nM VIM-1, 65 µM nitrocefin, 50 µL assay buffer) to establish an expected level of hydrolysis uninterrupted, and an alanine Affimer control (1 µM alanine Affimer, 100 nM VIM-1, 65 µM nitrocefin) to ensure no inhibition or excess activation of VIM-1 occurred with a basic Affimer structure. All reactions and controls were set up in triplicate on each plate.

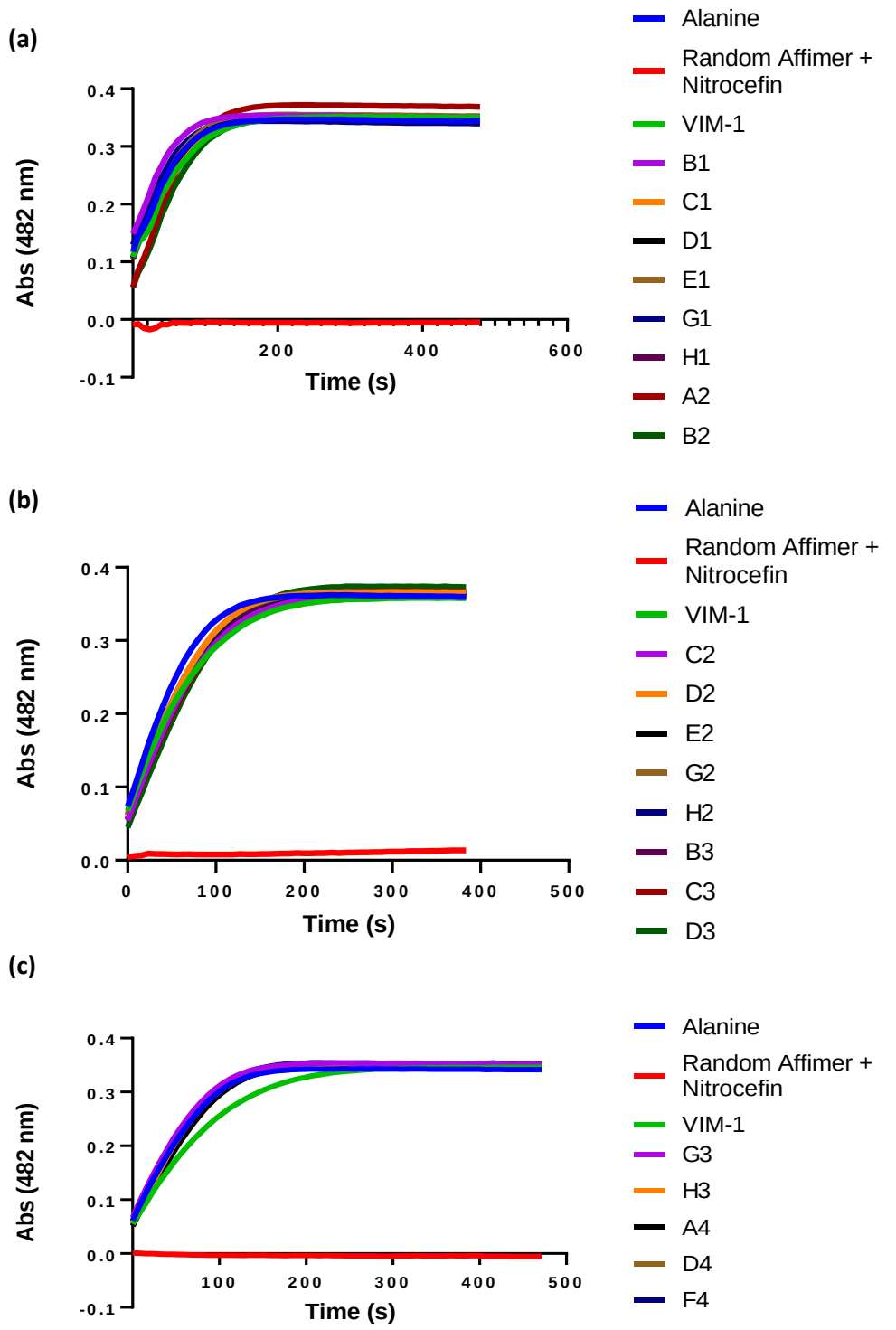

Figure 3.3.1. Effects of Affimer reagents on rate of nitrocefin hydrolysis by VIM-1. Graphs were calculated using data collected at approximately 7 second intervals with absorbance readings at 482 nm. All data points were normalised against EDTA control. **(a)** and **(b)** show no appreciable difference in Affimer activity on hydrolysis rate. **(c)** shows a slight anomalous result in the VIM-1 rate, but observing the alanine Affimer control, it appears to be likely that there was an issue with the loading of the plate or reagents, in that particular set of wells. *n*=3.

Linear regression analysis (y = mx + c where Y is concentration, m is the gradient of the slope and indicates rate, x is time, and c is the intercept) for the first 100 seconds of the assay were used to determine initial rate (A_{482}/s). The extinction coefficient ε=20,500 $M^{-1}cm^{-1}$ was then used in the Beer-Lambert Law to calculate change in hydrolysed nitrocefin concentration over time (rate μM^{-1}) and each rate was normalised against the EDTA control.

This allowed for a quantification of the effect various Affimer reagents had against the activity of VIM-1 alone, the results are shown in Figure 3.3.2.

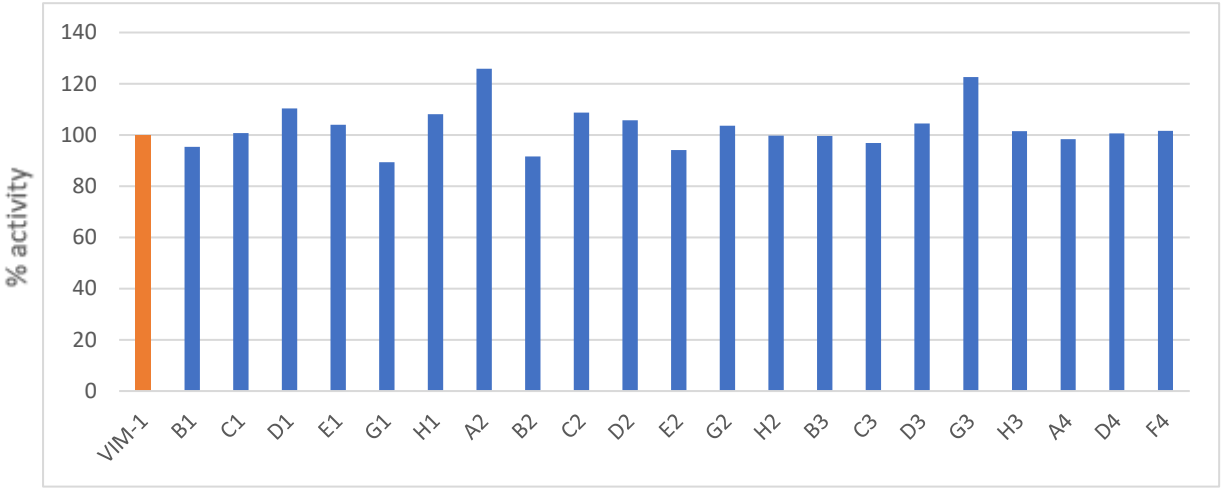

Figure 3.3.2. Activity of VIM-1 under different conditions as a percentage of unimpeded activity. Using VIM-1 only control as a standard, initial rates were calculated under different Affimer conditions, and established as a percentage against the rate of VIM-1 only. At 10-fold Affimer concentration to VIM-1, there did not appear to be any significant change in rate.

3.3.2. Affimer Concentration at 100-fold VIM-1 Concentration

In order to test whether the Affimer reagents selected from the phage ELISA had any inhibitory effect, a further set of nitrocefin assays was completed with a 100-fold Affimer concentration to VIM-1 (300 nM VIM-1, 30 µM Affimer). Affimer reagents were diluted to a suitable concentration, and assays were run using the same conditions as those for the 10-fold Affimer to VIM-1 tests.

(a)

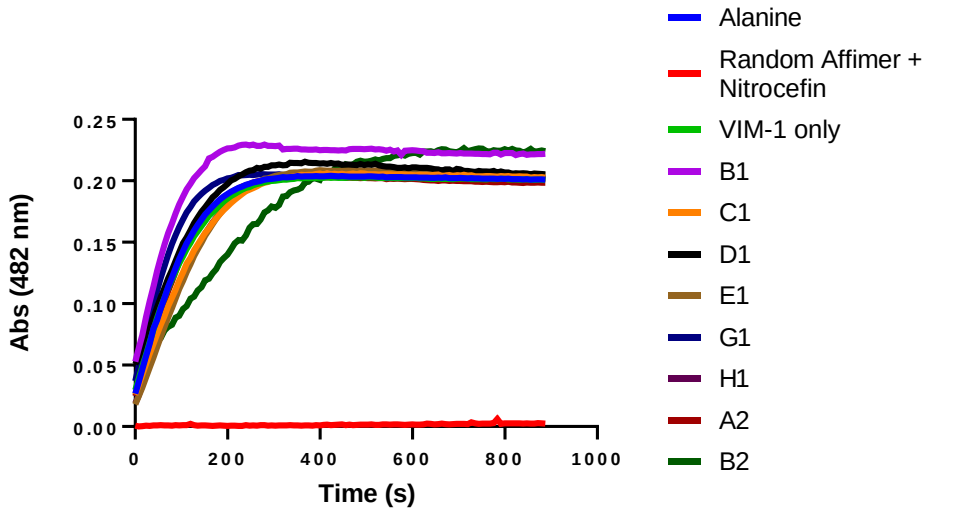

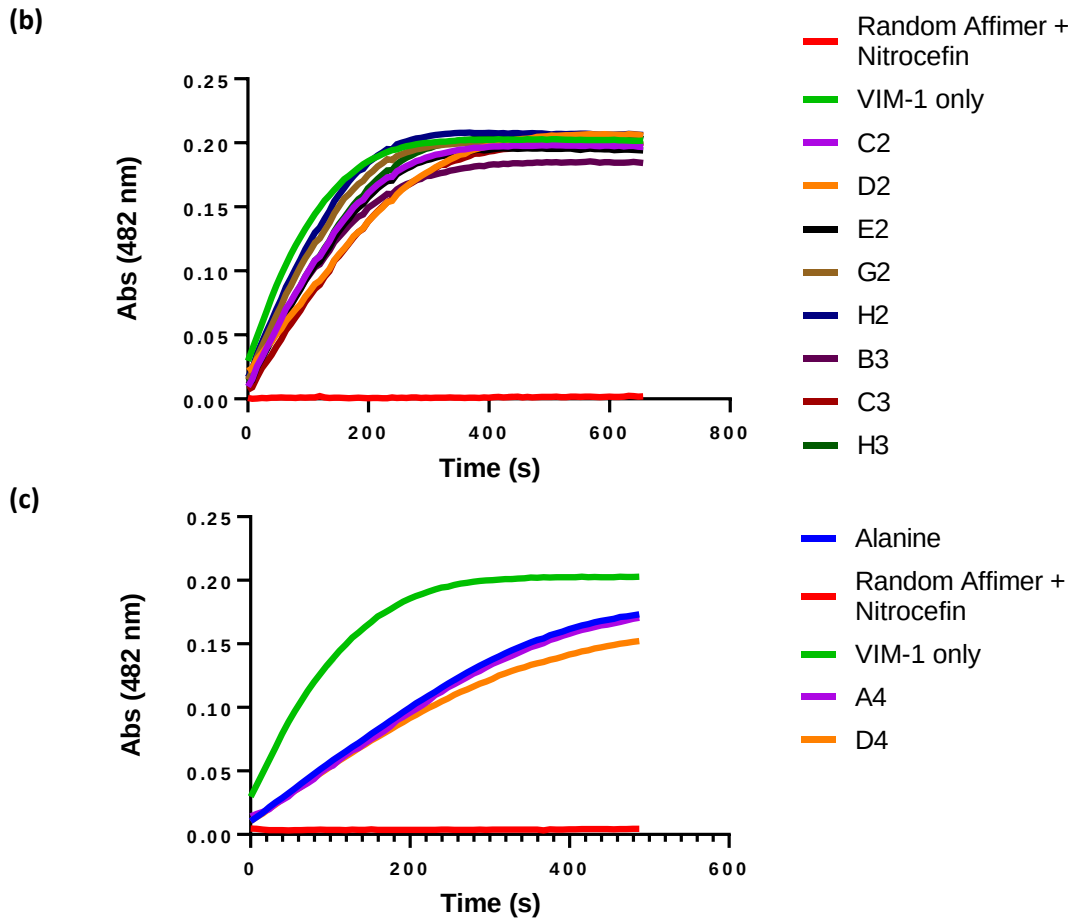

Figure 3.3.3. Effects of Affimer reagents on rate of nitrocefin hydrolysis by VIM-1. Graphs were calculated using data collected at approximately 7 second intervals with absorbance readings at 482 nm. All data points were normalised against EDTA control. **(a)** Shows fairly uniform progression between variables with a marked difference in B2 **(b)** Shows fairly uniform results between variables with slight fluctuation in D2 and B3 **(c)** Showed some marked errors in either loading of VIM-1 only wells, or all other wells. *n*=3.

From observing the effects the variable Affimer reagents had on the rate of nitrocefin hydrolysis by VIM-1, there appeared to be only a few Affimers that may have some inhibitory effect at this molar excess. To further visualise this, the initial rates were calculated from the first 100 seconds during which all rates were constant. The results were observed against VIM-1 only, shown in Figure 3.3.4. The exception to this were the results from Figure 3.3.3 (c), these results were run once more and found to have no inhibitory effect.

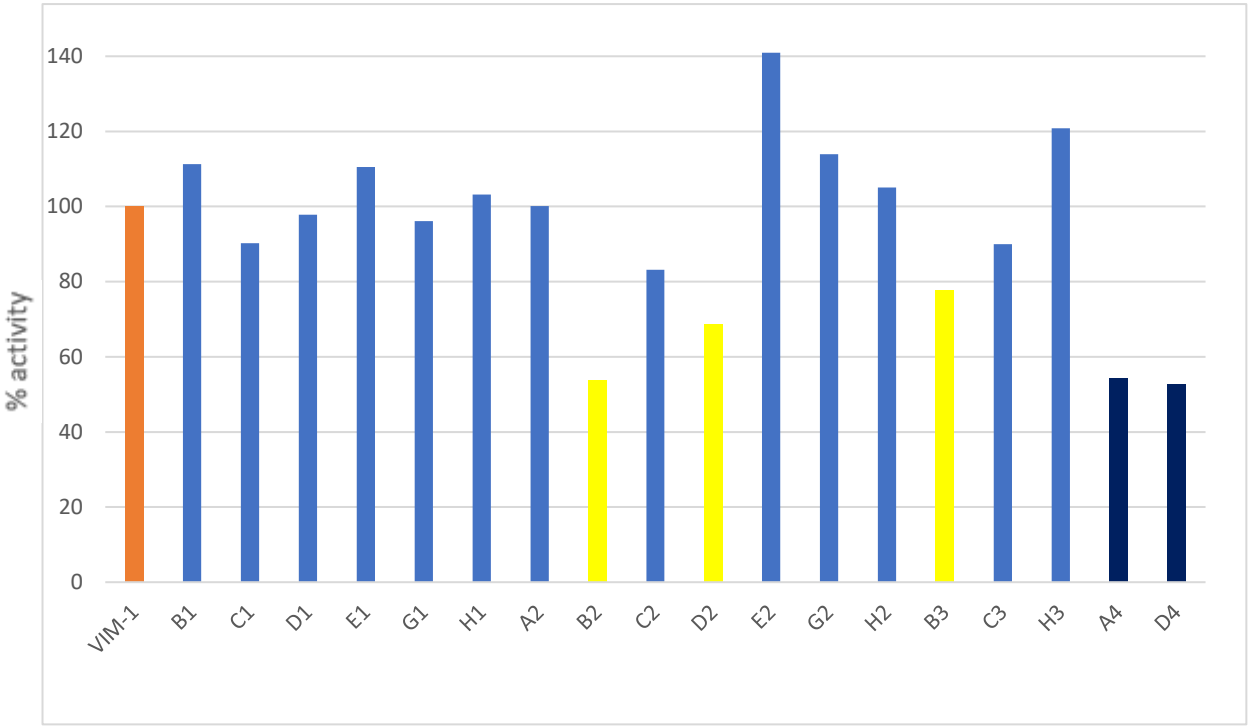

Figure 3.3.4. Activity of VIM-1 under different conditions as a percentage of unimpeded activity. The activity of VIM-1 was calculated using gradient of the initial rates and compared against different Affimer conditions as a percentage. Affimers that showed the greatest inhibition are highlighted in yellow.

From figure 3.3.4 three Affimers were chosen to take forward to produce in greater quantities, and further characterise their inhibition of VIM-1's hydrolysis of nitrocefin. A4 and D4 appeared to show the greatest inhibition in Figure 3.3.4, but the results from their assay were not conclusive. Subcloning was performed in tandem with another round of phage display, to select for more target-binding Affimer clones.

3.4. Subcloning Affimers B2, D2, B3 into pET11a Vector

To allow for greater protein expression of the chosen Affimers, they were subcloned into pET11a vectors. This was done by amplifying the Affimer DNA sequence from the phagemid (Figure 3.4.1.), *DpnI* digested, purified, and digested with *NheI* and *NotI* restriction enzymes. This was then combined with pET11a digest with the same restriction enzymes, in a ratio of 6:1 vector DNA to insert DNA and incubated overnight at 4°C. These ligations were then transformed into XL1-Blue Supercompetent cells via heat shock, plated onto LB Agar plates and carbenicillin to check for successful ligation, and single colonies were used to inoculate 5 mL of 2TY, and incubated overnight at 37°C, 230 rpm. Plasmid DNA was then purified using a QIAprep spin Miniprep Kit. Specific details can be found in materials and methods, 2.2.1.8. Successful integration was verified by Sanger sequencing by Genewiz, and the ligated pET11a-Aff-(B2/D2/B3) plasmids were transformed into BL21 Star (DE3), following protocol 2.2.2.2. (Materials and methods). Elutions were collected in 500 µL aliquots and analysed on a 15% SDS-PAGE gel to confirm bands at the new expected weight of ~12 kDa (Figure 3.4.2).

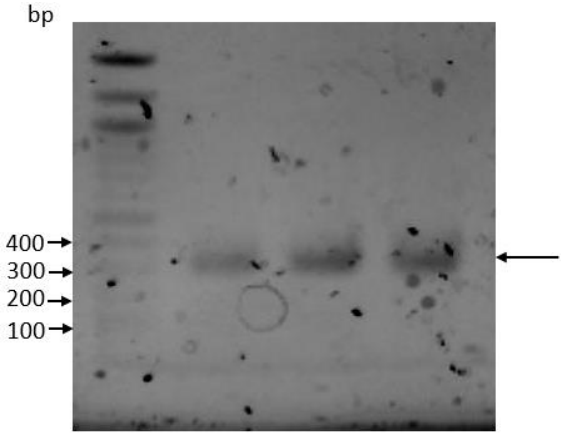

Figure 3.4.1. Agarose gel to verify successful amplification of Affimer DNA from phagemid vector. Affimer sequence was amplified from the phagemid vector using stock primers supplied by A. Herbert (University of Leeds) and loaded into a 0.7% agarose gel. 5 µL of FastGene 100 bp DNA marker was loaded into the first well. Expected bands of ~300 bp are indicated by a black arrow.

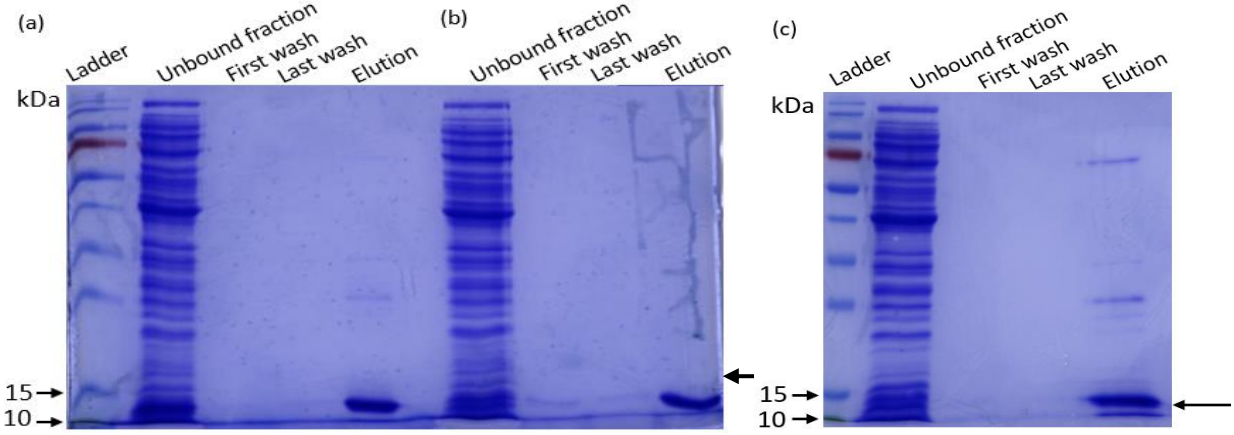

Figure 3.4.2. SDS-PAGE gel to verify successful subcloning of Affimers into pET11a vectors. Affimers were produced from 500 mL of BL21 Star (DE3) cells culture and purified by nickel affinity chromatography. 2 µL samples of the elution were denatured in 1x sample buffer in a 15 µl volume and denatured by boiling for 5 minutes before loading. 5 µL of PageRuler molecular weight ladder was added into the first well. Gels were stained with Coomassie blue dye. Expected bands of ~12 kDa are indicated by the black arrows. **(a)** Shows a clear band of Affimer B2 **(b)** Shows a clear band of Affimer D2 **(c)** Shows a clear band of Affimer B3 with slight shadowing in the well.

3.4.2. Nitrocefin Assay Results

Linear regression was performed as previously explained from these results, this allowed for a quantification of the effect various Affimer reagents had against the activity of VIM-1 alone, the results are shown in Figure 3.4.4.

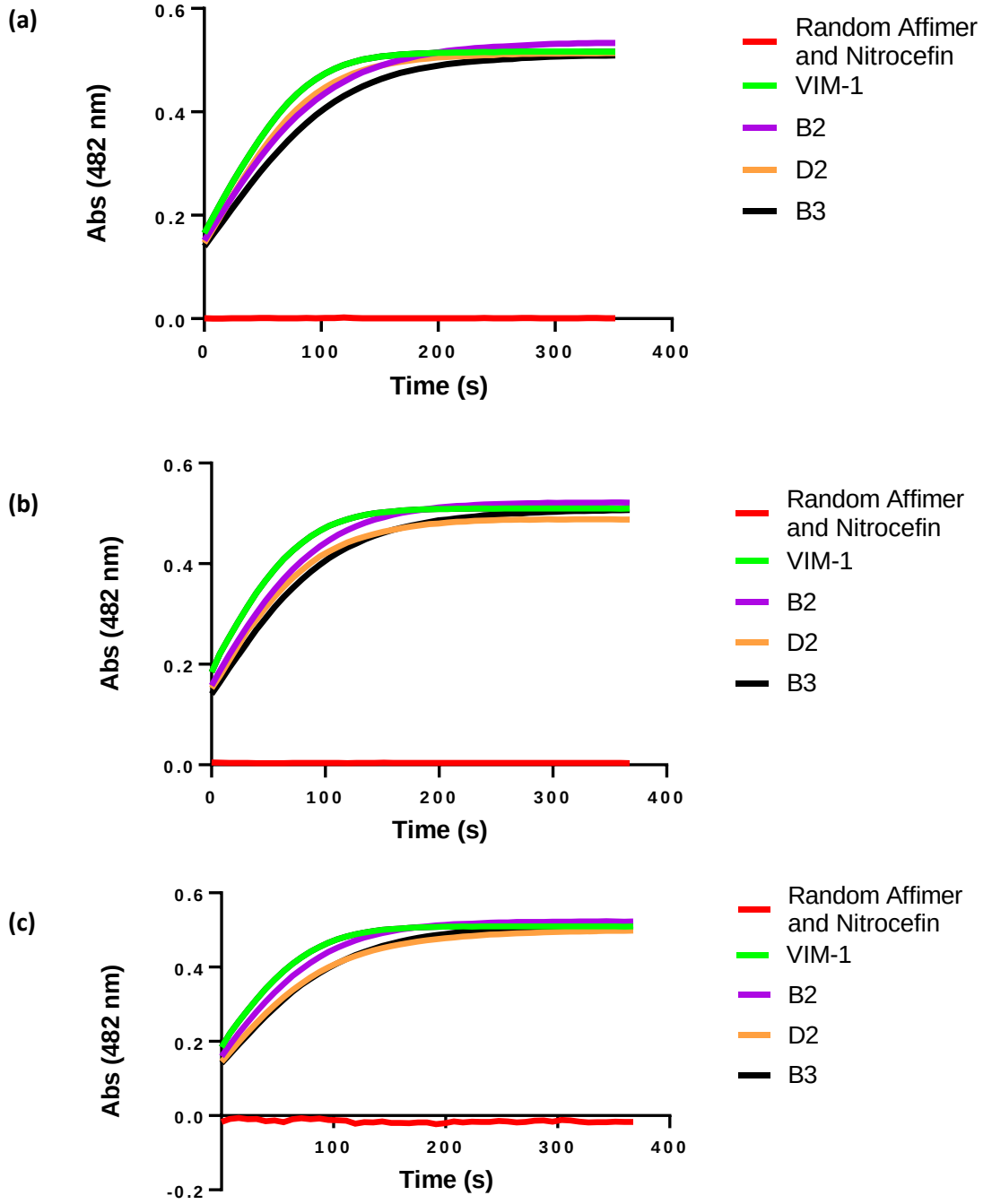

Figure 3.4.3 Effects of Affimer reagents on rate of nitrocefin hydrolysis by VIM-1. Graphs were calculated using data collected at approximately 7 second intervals with absorbance readings at 482 nm. All data points were normalised against EDTA control. **(a)** Appears to show some slight inhibition of VIM-1 with D2 and B3 **(b)** Appears to show slight inhibition of VIM-1 with B3 **(c)** Appears to show slight inhibition of VIM-1 with D2 and B3. n=3.

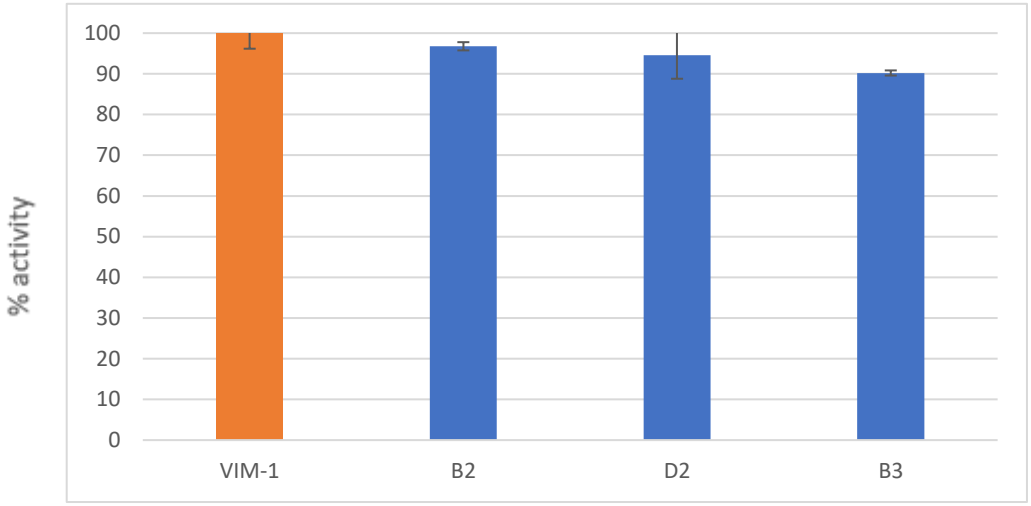

Figure 3.4.4. Activity of VIM-1 under different conditions against unimpeded activity. The activity of VIM-1 was calculated using gradient of the initial rates and compared against different Affimer conditions as a percentage. *n*=3, error bars represent standard error from 3 replicate experiments.

Following the results of the β-lactamase activity assays using the subcloned Affimers it did not appear that a significant inhibitor of VIM-1 had been found. Unfortunately, the initial rates were hard to calculate given the start of the readings occurred when absorbance at 482 nm had almost reached 0.2 and so the start of the reaction had been missed.

3.5. Isolation of 500 New Clones for Testing by Phage ELISA

Given the results from the preliminary set of Affimer clones that were selected by phage ELISA, it was thought that by testing a larger number of Affimer clones it would be possible to find an Affimer that significantly inhibits VIM-1.

Purified phage from the second panning round of the initial screen against BAP-tagged VIM-1 was used to repeat the third panning round in order to create a new pool of Affimer clones from which to choose. In total, 500 clones were picked following phage display. Anti-Fd-Bacteriophage-HRP and TMB were used once again and given 3 minutes to develop before absorbances were taken at 620 nm on a ThermoScientific Multiskan FC plate reader.

3.5.1. Phage ELISA Results

(1a)

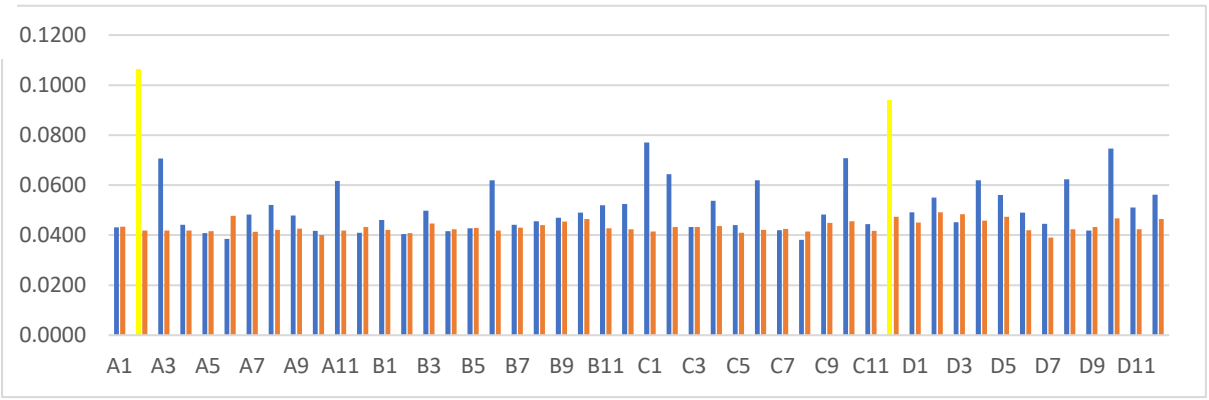

(1b)

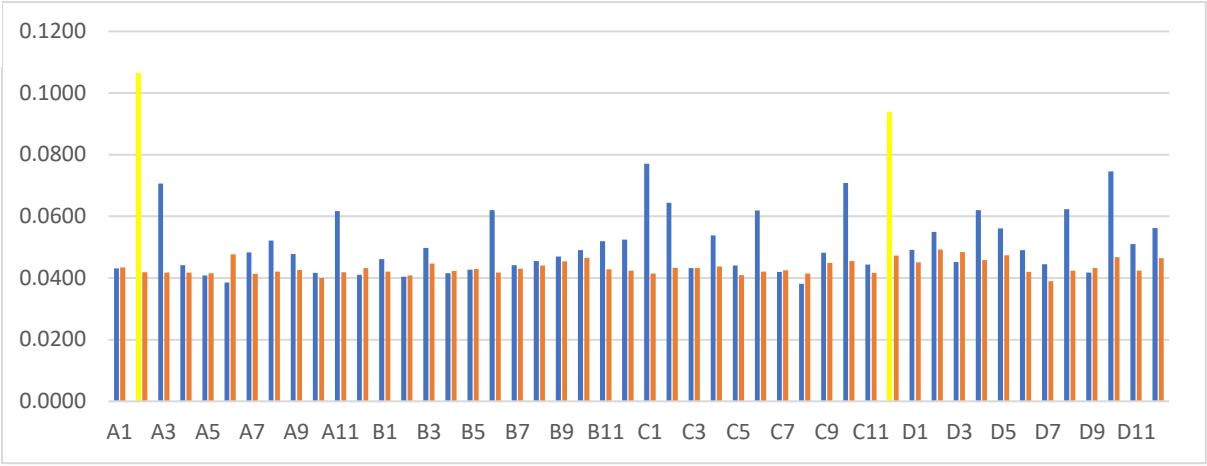
0.1200
0.1000
0.0800
0.0600
0.0400
0.0200
0.0000
A1 A3 A5 A7 A9 A11 B1 B3 B5 B7 B9 B11 C1 C3 C5 C7 C9 C11 D1 D3 D5 D7 D9 D11

(2a)

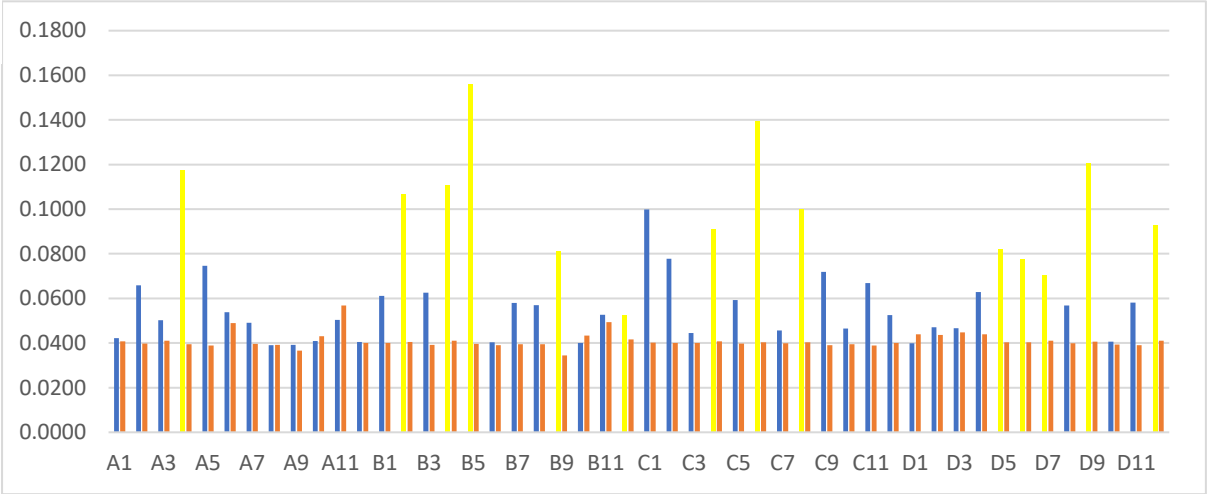
0.1800
0.1600
0.1400
0.1200
0.1000
0.0800
0.0600
0.0400
0.0200
0.0000
A1 A3 A5 A7 A9 A11 B1 B3 B5 B7 B9 B11 C1 C3 C5 C7 C9 C11 D1 D3 D5 D7 D9 D11

(2b)

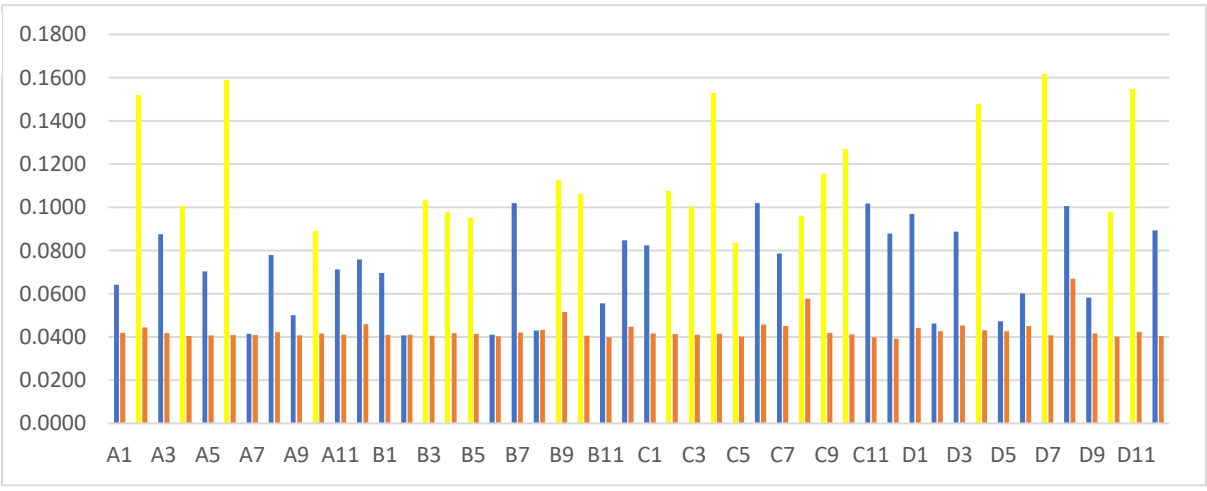
0.1800
0.1600
0.1400
0.1200
0.1000
0.0800
0.0600
0.0400
0.0200
0.0000
A1 A3 A5 A7 A9 A11 B1 B3 B5 B7 B9 B11 C1 C3 C5 C7 C9 C11 D1 D3 D5 D7 D9 D11

(3a)

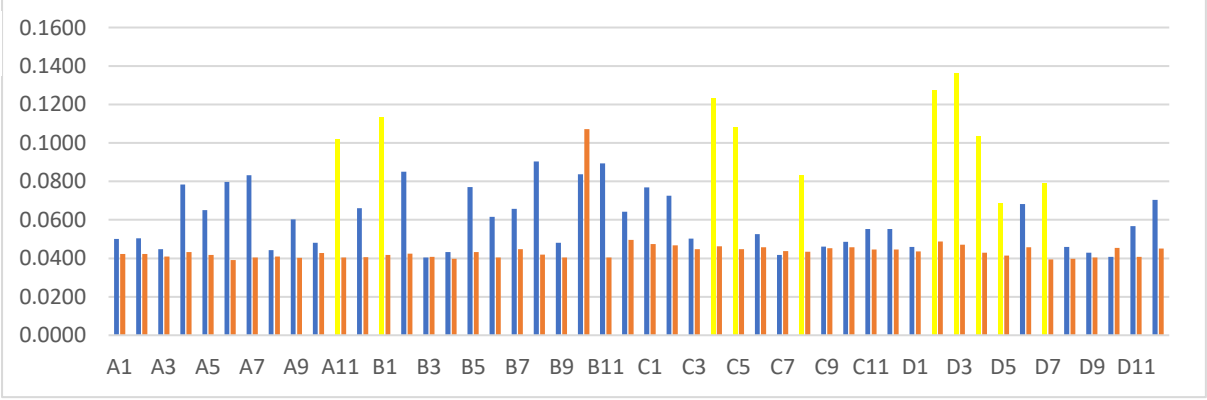
0.1600
0.1400
0.1200
0.1000
0.0800
0.0600
0.0400
0.0200
0.0000
A1 A3 A5 A7 A9 A11 B1 B3 B5 B7 B9 B11 C1 C3 C5 C7 C9 C11 D1 D3 D5 D7 D9 D11

(3b)

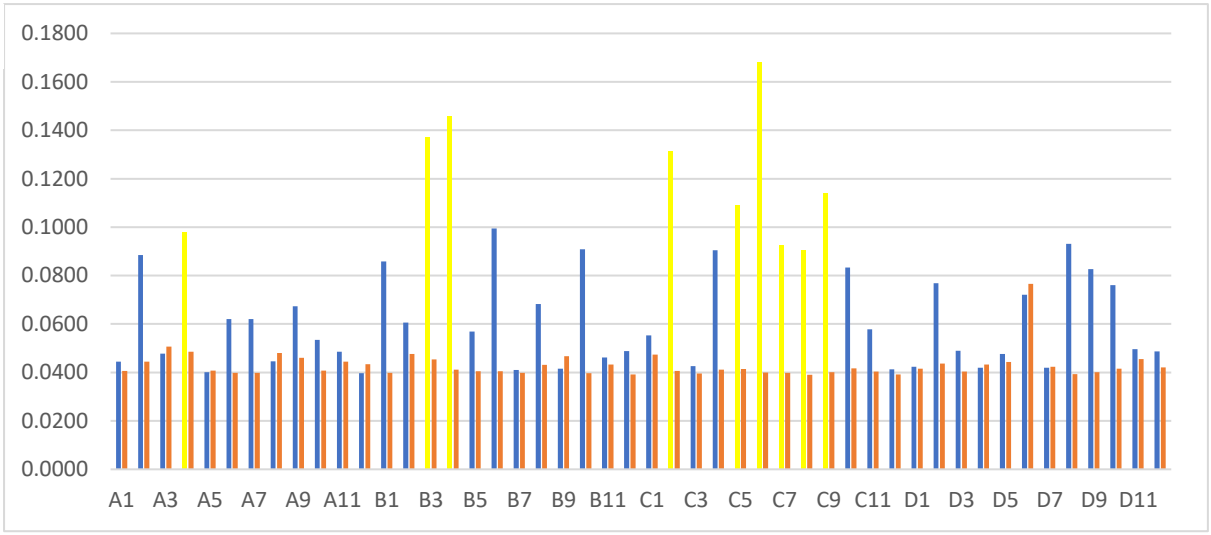
0.1800
0.1600
0.1400
0.1200
0.1000
0.0800
0.0600
0.0400
0.0200
0.0000
A1 A3 A5 A7 A9 A11 B1 B3 B5 B7 B9 B11 C1 C3 C5 C7 C9 C11 D1 D3 D5 D7 D9 D11

(4a)

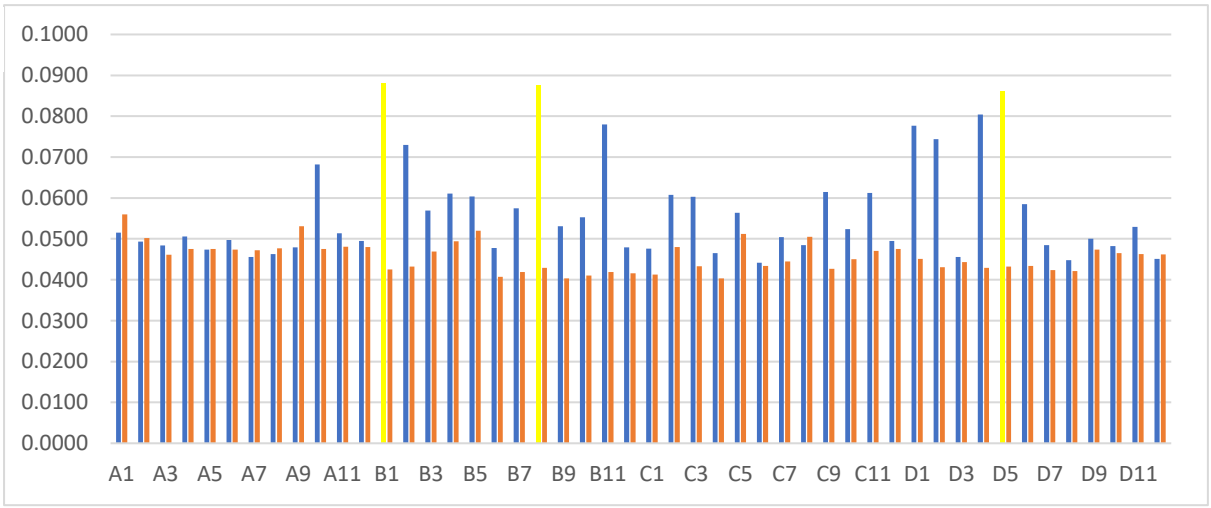
0.1000
0.0900
0.0800
0.0700
0.0600
0.0500
0.0400
0.0300
0.0200
0.0100
0.0000
A1 A3 A5 A7 A9 A11 B1 B3 B5 B7 B9 B11 C1 C3 C5 C7 C9 C11 D1 D3 D5 D7 D9 D11

(4b)

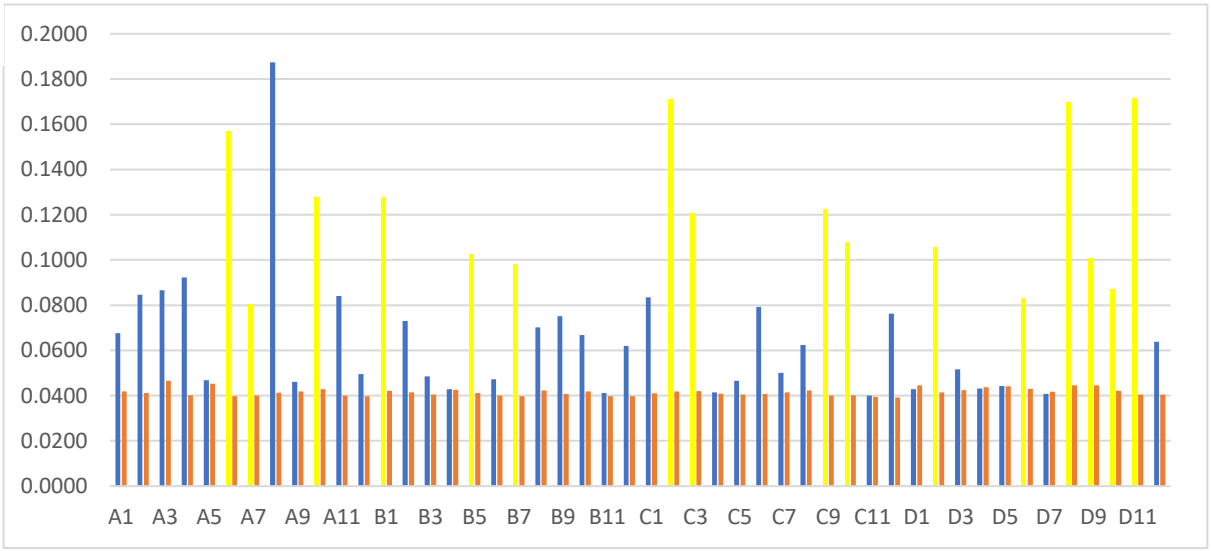
0.2000
0.1800
0.1600
0.1400
0.1200
0.1000
0.0800
0.0600
0.0400
0.0200
0.0000
A1 A3 A5 A7 A9 A11 B1 B3 B5 B7 B9 B11 C1 C3 C5 C7 C9 C11 D1 D3 D5 D7 D9 D11

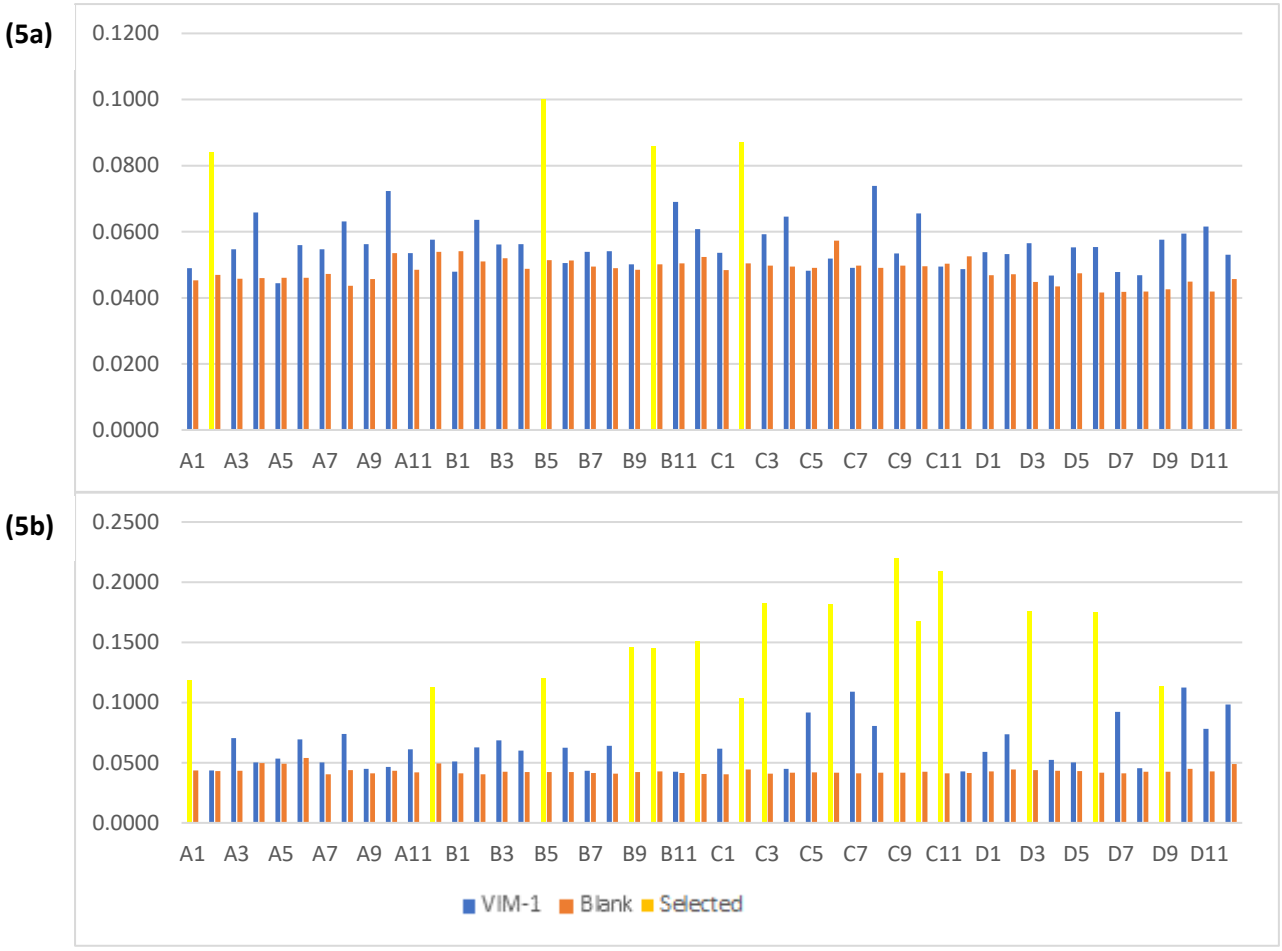

Figure 3.5.1. Phage ELISA results for BAP-tagged, biotinylated VIM-1. Phage ELISA was completed with BAP-tagged VIM-1. Phage was exposed to control wells where no biotinylated target had been incubated to verify successful binding. A positive control was also used which had been proven to be successful before (results not shown here). Anti-Fd-Bacteriophage-HRP and SeramunBlau TMB were used to show visible colour change and allow for absorbances to be taken at 620 nm. Each graph represents an individual plate. Colonies chosen to take forward are shown in yellow rather than blue, and are given a new identifying number in Fig 3.5.2.

The absorbance disparity between wells (shown in Figure 3.5.1.) containing immobilised VIM-1 and negative control was not as large as it was in the initial phage ELISA, TMB could have been allowed longer to develop, and this may have improved the absorbances shown as well. Despite this a mixture of colonies were selected, from different absorbances, in an effort to try and locate an efficient inhibitor.

Of the 500 colonies picked, 96 were chosen to take forward. These were given new identifiers for ease of use, shown in Figure 3.5.2.

Plate	Well	New Well	ID number
1a	A2	A1	1
	C12	A2	2
1b	B11	A3	3
	D2	A4	4
2a	A4	A5	5
	B2	A6	6
	B4	A7	7
	B5	A8	8
	B9	A9	9
	B12	A10	10
	C4	A11	11
	C6	A12	12
	C8	B1	13
	D5	B2	14
	D6	B3	15
	D7	B4	16
	D9	B5	17
	D12	B6	18
2b	A2	B7	19
	A4	B8	20
	A6	B9	21
	A10	B10	22
	B3	B11	23
	B4	B12	24
	B5	C1	25
	B9	C2	26
	B10	C3	27
	C2	C4	28
	C3	C5	29
	C4	C6	30
	C5	C7	31
	C8	C8	32
	C9	C9	33
	c10	C10	34
	D4	C11	35
	D7	C12	36
	D10	D1	37
	D11	D2	38
3a	a11	D3	39
	b1	D4	40
	c4	D5	41
	c5	D6	42
	c8	D7	43
	d2	D8	44
	d3	D9	45
	d4	D10	46
	d5	D11	47
	d7	D12	48

Plate	Well	New Well	ID number
3b	A4	E1	49
	B3	E2	50
	B4	E3	51
	C2	E4	52
	C4	E5	53
	c5	E6	54
	c6	E7	55
	c7	E8	56
	c8	E9	57
	c9	E10	58
4a	B1	E11	59
	B8	E12	60
	D5	F1	61
4b	A6	F2	62
	a7	F3	63
	a10	F4	64
	b1	F5	65
	b5	F6	66
	b7	F7	67
	c2	F8	68
	c3	F9	69
	c9	F10	70
	c10	F11	71
	d2	F12	72
	d6	G1	73
	d8	G2	74
	d9	G3	75
	d10	G4	76
	d11	G5	77
5a	a2	G6	78
	b5	G7	79
	b10	G8	80
	c2	G9	81
5b	a1	G10	82
	a12	G11	83
	b5	G12	84
	b9	H1	85
	b10	H2	86
	b12	H3	87
	C2	H4	88
	c3	H5	89
	c6	H6	90
	c9	H7	91
	c10	H8	92
	c11	H9	93
	d3	H10	94
	d6	H11	95
	d9	H12	96

Figure 3.5.2. New Affimer identification. For ease of identification from the 500 colony ELISA, chosen Affimers were given a new identification number from 1-96.

3.5.2. Affimer Production and Purification in JM83 cells

These Affimers were produced in JM83 as previously described, lysed and purified by nickel affinity chromatography and assessed on 15% SDS-PAGE gels, shown in Figures 3.5.3 and 3.5.4.

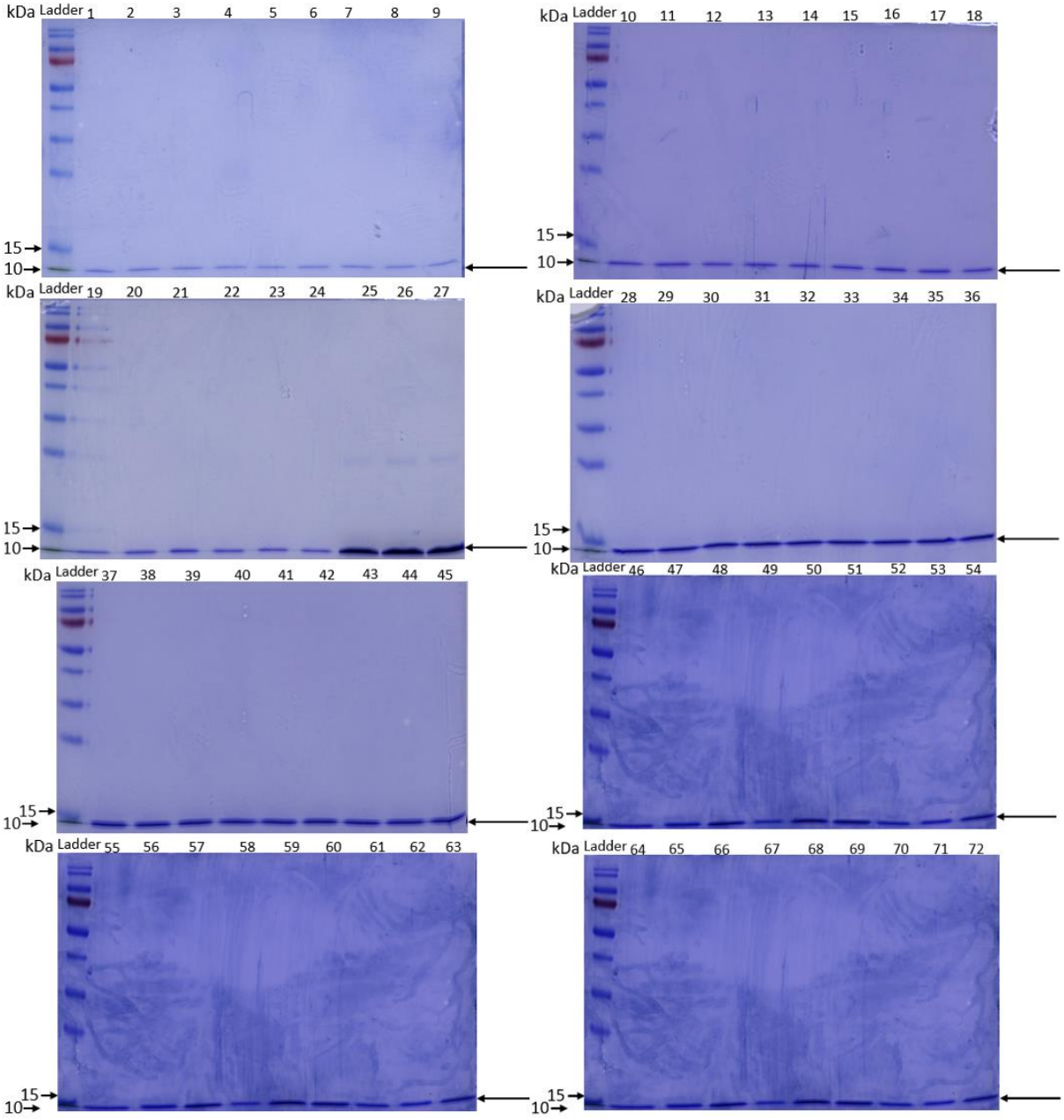

Figure 3.5.3. SDS-PAGE gel to verify production and purification of Affimers 1-72 in JM83 cells. Affimers were produced in 50 mL of JM83 cell culture and purified by nickel affinity chromatography. 2 µL samples were denatured in 1x sample buffer by boiling for 5 minutes before loading. 5 µL of PageRuler molecular weight ladder was added into the first well. Gels were stained with Coomassie blue dye. Expected bands of ~12 kDa are indicated by the black arrows.

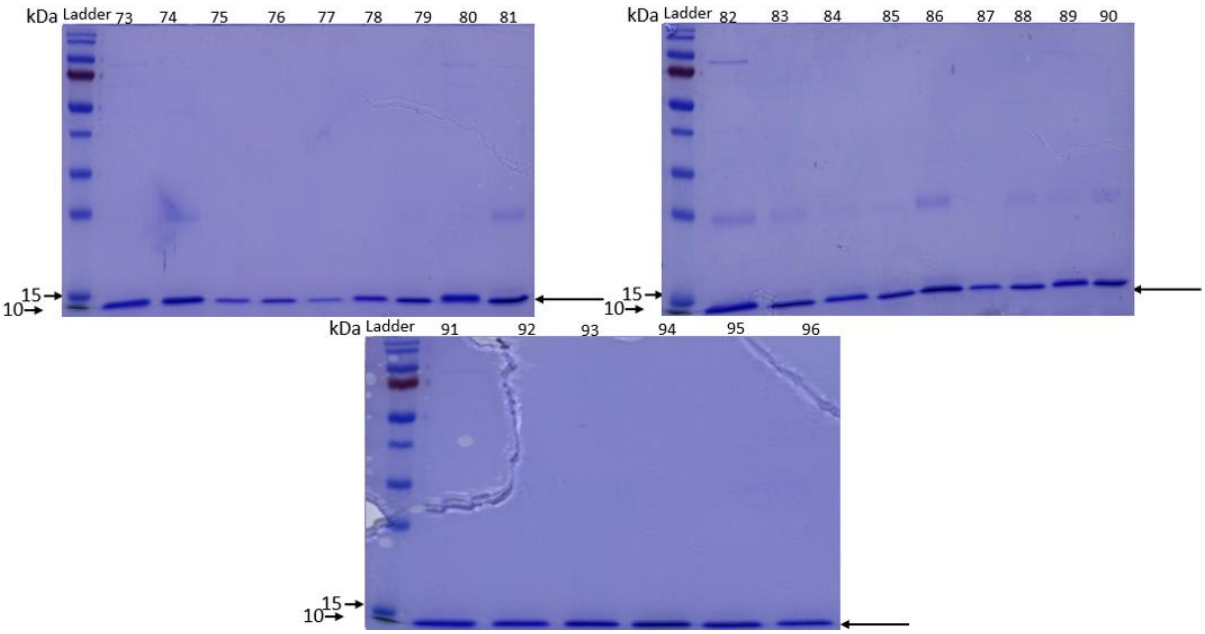

Figure 3.5.4. SDS-PAGE gel to verify production and purification of Affimers 73-96 in JM83 cells. Affimers were produced in 50 mL of JM83 cells culture and purified by nickel affinity chromatography. 2 µL samples were denatured in 1x sample buffer by boiling for 5 minutes before loading. 5 µL of PageRuler molecular weight ladder was added into the first well. Gels were stained with Coomassie blue dye. Expected bands of ~12 kDa are indicated by the black arrows.

Affimer reagents were dialysed into 1x PBS and diluted to a concentration of 30 µM, and assays were run in triplicate using the same conditions as those for the previous nitrocefin hydrolysis tests, results shown in Figure 3.5.5.

3.5.3. Nitrocefin Assay Results for JM83 Produced Affimers

There were some issues in this set of nitrocefin hydrolysis runs. It is likely human error in the loading occurred and there are some anomalous results for the VIM-1 only controls. Given these apparent loading issues, as well as the difficulty to evaluate the initial rate is hard given the absorbance at 482 nm is incongruous, a second set of tests were run. This required re-producing the Affimers in JM83 cells. While this occurred, Affimers that appeared to warrant further characterisation were chosen from this set of data and processed for subcloning into pET11a vectors.

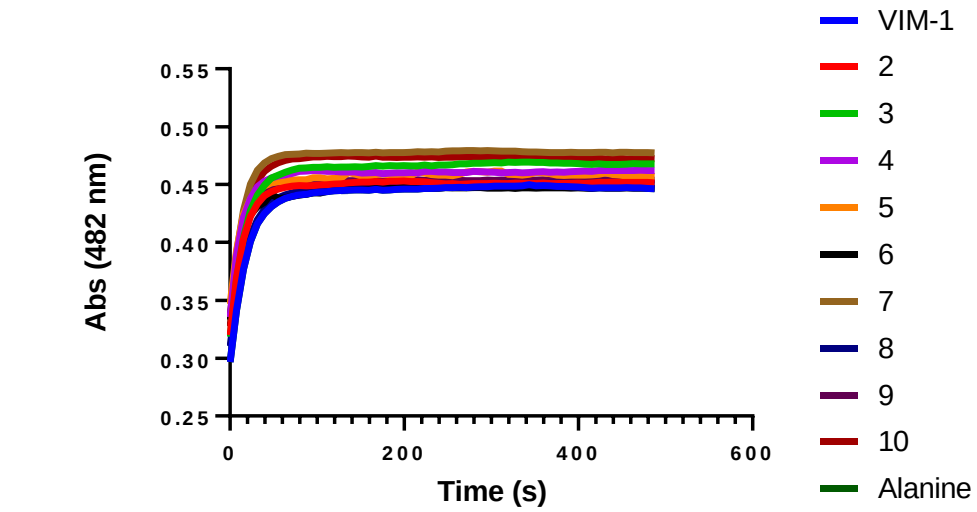
Abs (482 nm)
0.55
0.50
0.45
0.40
0.35
0.30
0.25
0
200
400
600
Time (s)
VIM-1
2
3
4
5
6
7
8
9
10
Alanine

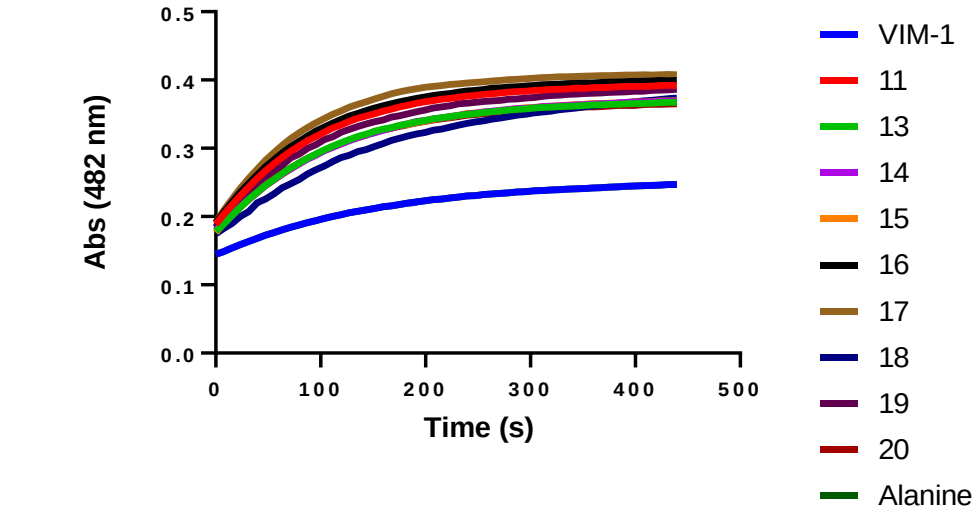
Abs (482 nm)
0.5
0.4
0.3
0.2
0.1
0.0
0
100
200
300
400
500
Time (s)
VIM-1
11
13
14
15
16
17
18
19
20
Alanine

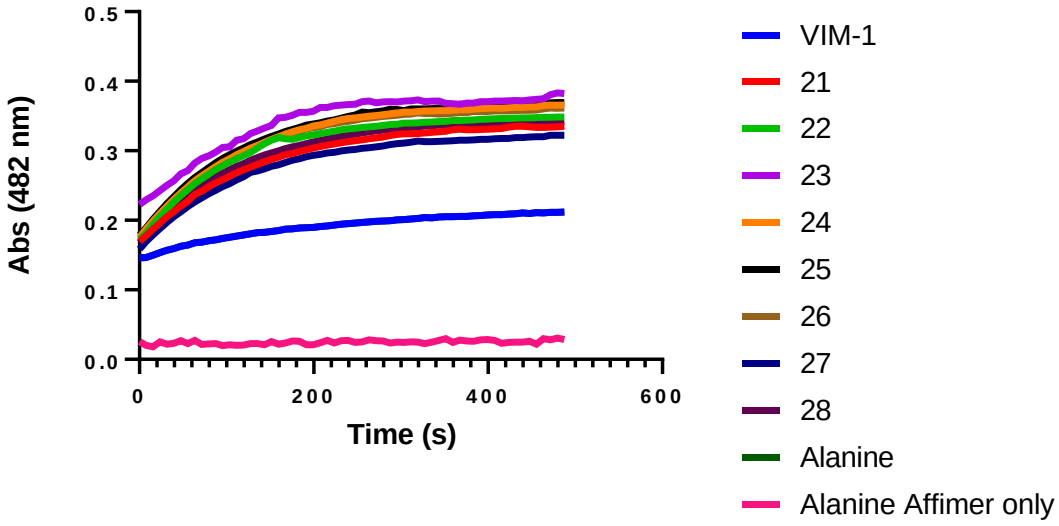
Abs (482 nm)
0.5
0.4
0.3
0.2
0.1
0.0
0
200
400
600
Time (s)
VIM-1
21
22
23
24
25
26
27
28
Alanine
Alanine Affimer only

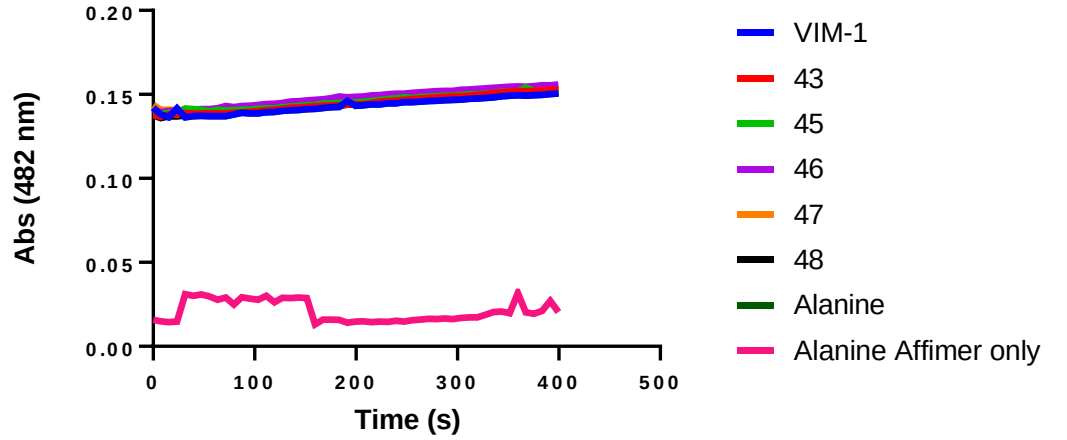
Abs (482 nm)
0.20
0.15
0.10
0.05
0.00
0
100
200
300
400
500
Time (s)
VIM-1
43
45
46
47
48
Alanine
Alanine Affimer only

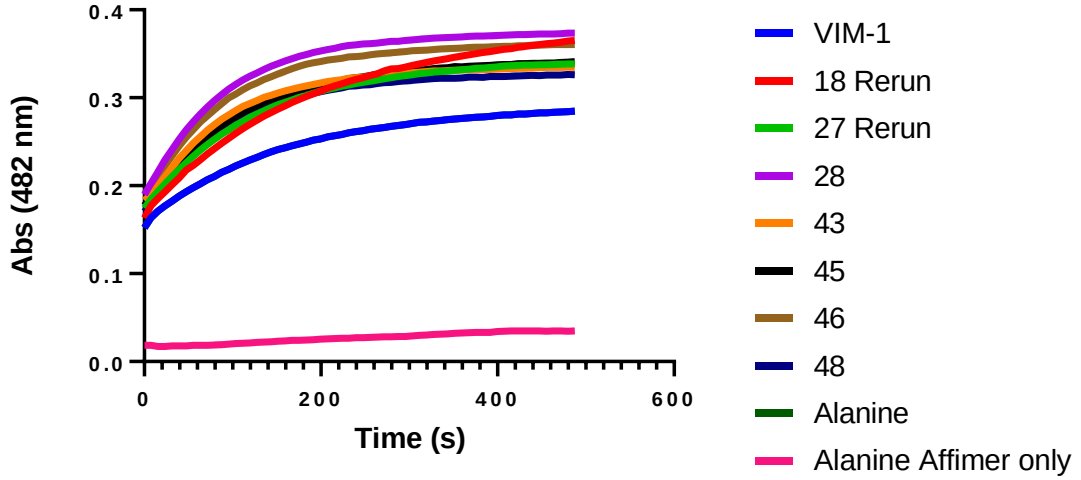
Abs (482 nm)
0.4
0.3
0.2
0.1
0.0
0
200
400
600
Time (s)
VIM-1
18 Rerun
27 Rerun
28
43
45
46
48
Alanine
Alanine Affimer only

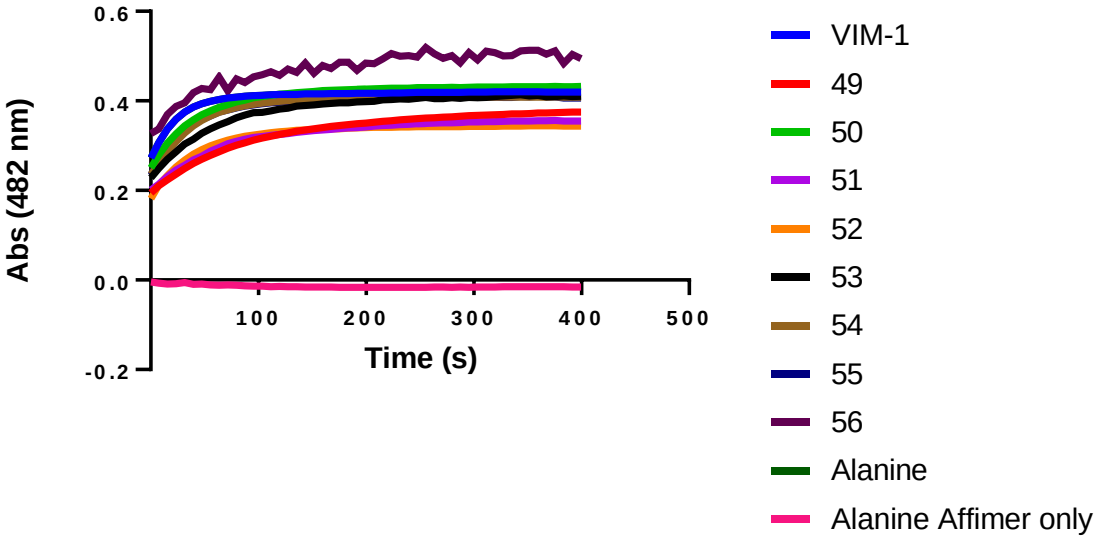
Abs (482 nm)
0.6
0.4
0.2
0.0
-0.2
100
200
300
400
500
Time (s)
VIM-1
49
50
51
52
53
54
55
56
Alanine
Alanine Affimer only

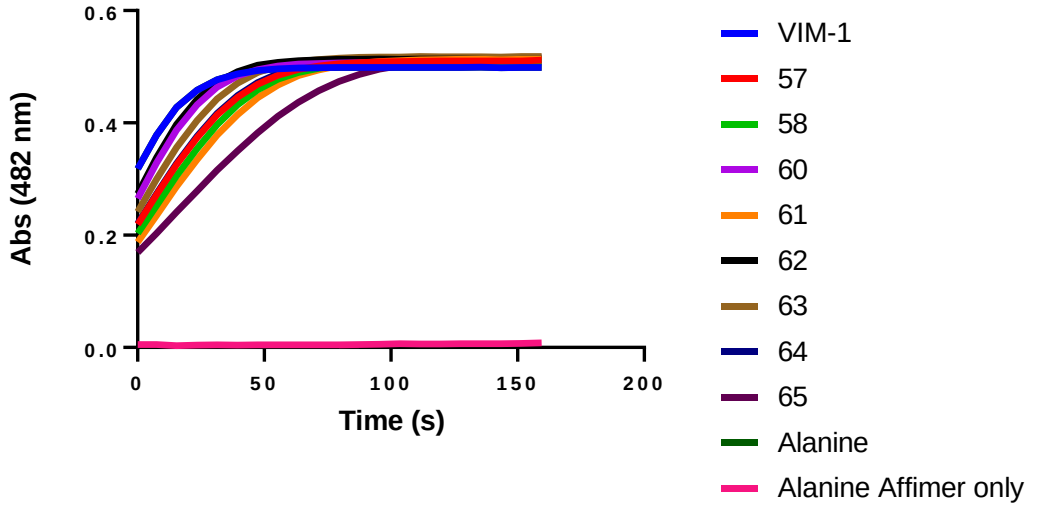
Abs (482 nm)
0.6
0.4
0.2
0.0
0
50
100
150
200
Time (s)
VIM-1
57
58
60
61
62
63
64
65
Alanine
Alanine Affimer only

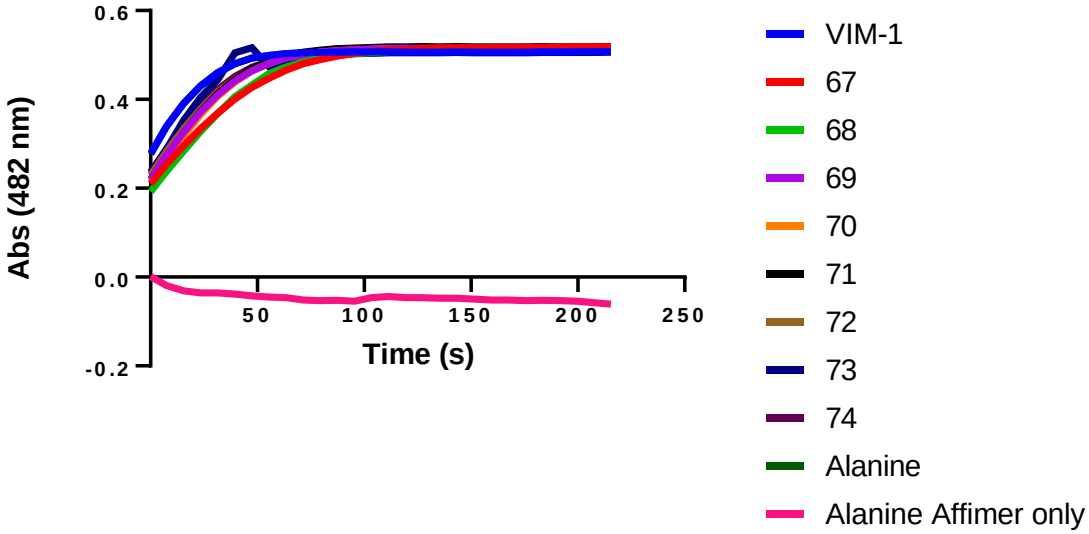
Abs (482 nm)
0.6
0.4
0.2
0.0
-0.2
50
100
150
200
250
Time (s)
VIM-1
67
68
69
70
71
72
73
74
Alanine
Alanine Affimer only

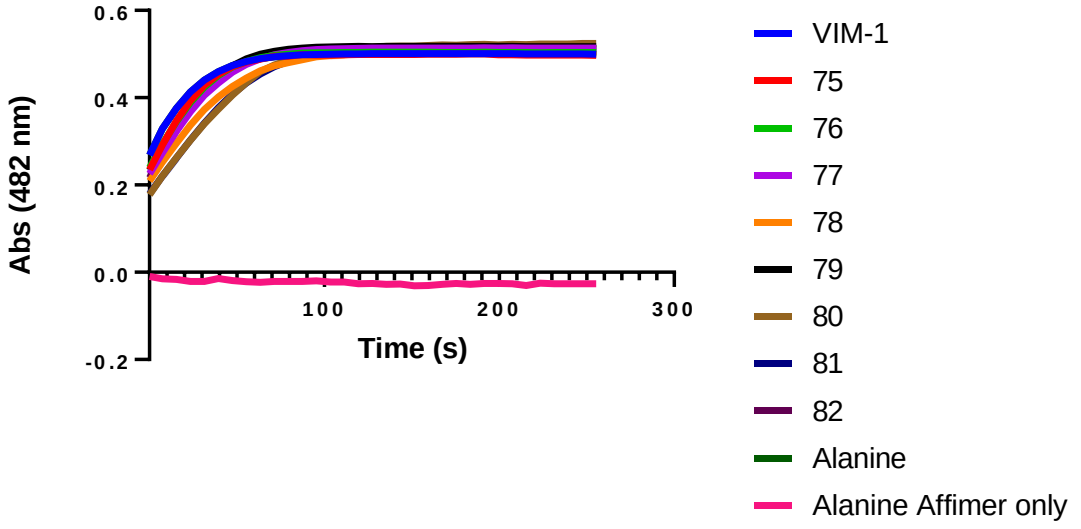
Abs (482 nm)
0.6
0.4
0.2
0.0
-0.2
100
200
300
Time (s)
VIM-1
75
76
77
78
79
80
81
82
Alanine
Alanine Affimer only

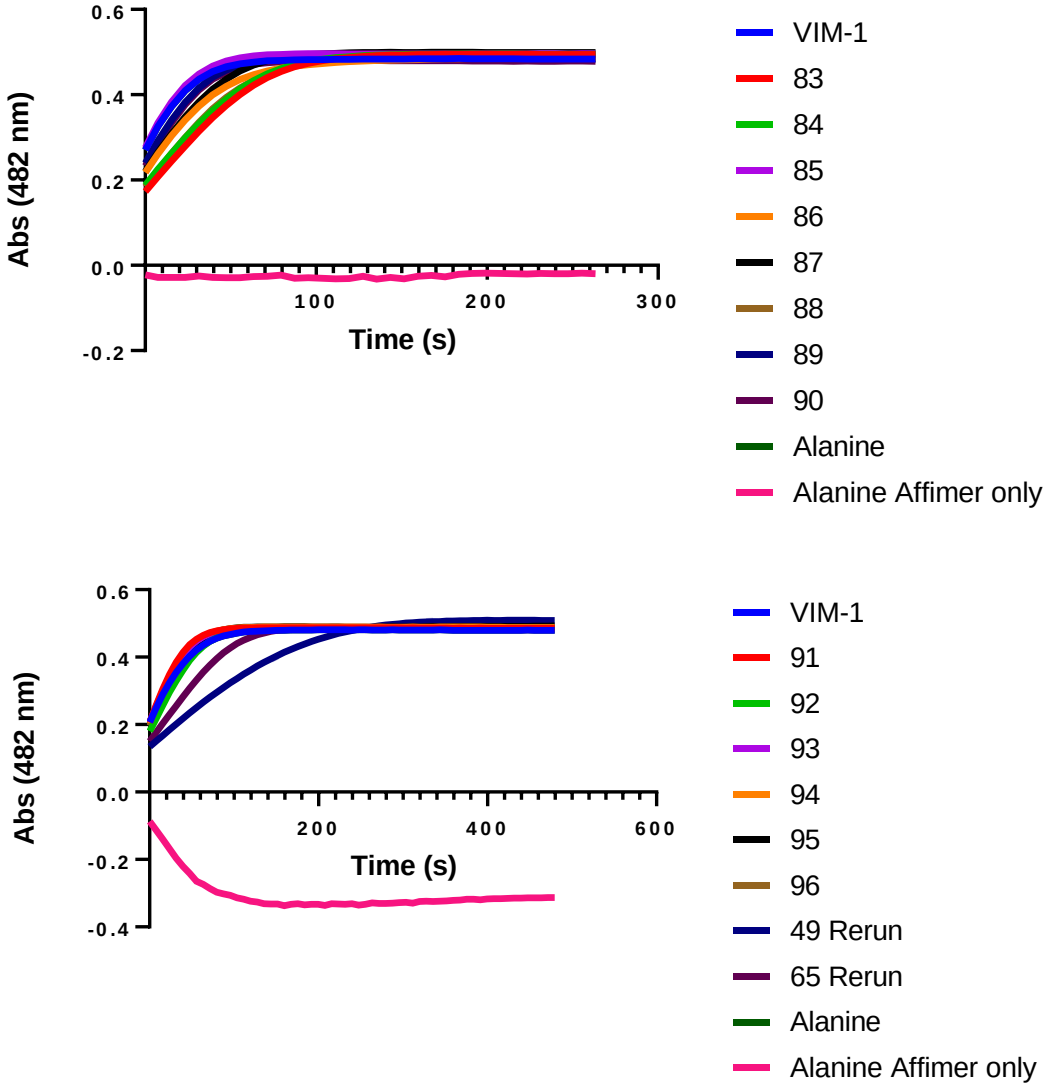

Figure 3.5.5. Effects of Affimer reagents on rate of nitrocefin hydrolysis by VIM-1. Graphs were calculated using data collected at approximately 7 second intervals with absorbance readings at 482 nm. All data points were normalised against EDTA control.

3.6. Subcloning selected Affimer reagents into pET11a

Phagemid DNA of selected Affimers for subcloning was sent for Sanger sequencing to verify the sequence of the Affimers variable regions, shown in Figure 3.6.1. Those that had their sequence returned were amplified and subcloned into pET11a vectors as previously described.

Name	VR1	VR2	Unique?
18	LPRKWDRAE	HIIYVNQKL	Yes
49	FMAPHFWPG	AAE------	No (x2)
53	MSAPFWFPE	AAE------	Yes
57	LRAPVFWPV	AAE------	Yes
58	VMDLMWAYW	AAE------	Yes
61	KRAPVFWPE	AAE------	Yes
65	MFSPVFWPE	AAE------	Yes
68	FMAPHFWPG	AAE------	No (x2)
76	No Priming		-
83	No Priming		-
84	No Priming		-

Figure 3.6.1. Sequence data for Affimer reagents. pBSTG-Aff DNA containing Affimer sequences were produced utilising method found in 2.2.2.2, and Sanger sequenced by GeneWiz. The variation between variable regions was compared to establish unique binders or repetition. 7 unique Affimers were found, 1 with two variable regions, and 6 with a single variable region. Affimers 76, 83, and 84 were sent for sequencing again but found no priming once more.

Name	VR1	VR2
18	LPRKWDRAE	HIIYVNQKL
49	FMAPHFWPG	AAE------
53	MSAPFWFPE	AAE------
61	KRAPVFWPE	AAE------
65	MFSPVFWPE	AAE------
57	LRAPVFWPV	AAE------
58	VMDLMWAYW	AAE------

Figure 3.6.2. Sequence validation of subcloned Affimer reagents in pET11a constructs. pET11a-Aff DNA was produced utilising method found in 2.2.2.2, and Sanger sequenced by GeneWiz. Of the original Affimers selected, those that had successfully primed and been sequenced were successfully subcloned into pET11a vectors.

3.6.1. Verification of purification of subcloned Affimer reagents in pET11a vectors

Once their sequence had been validated, the subcloned Affimer constructs were transformed into BL21 Star (DE3) *E. coli* cells as per protocol 2.2.2.2. (Materials and methods).

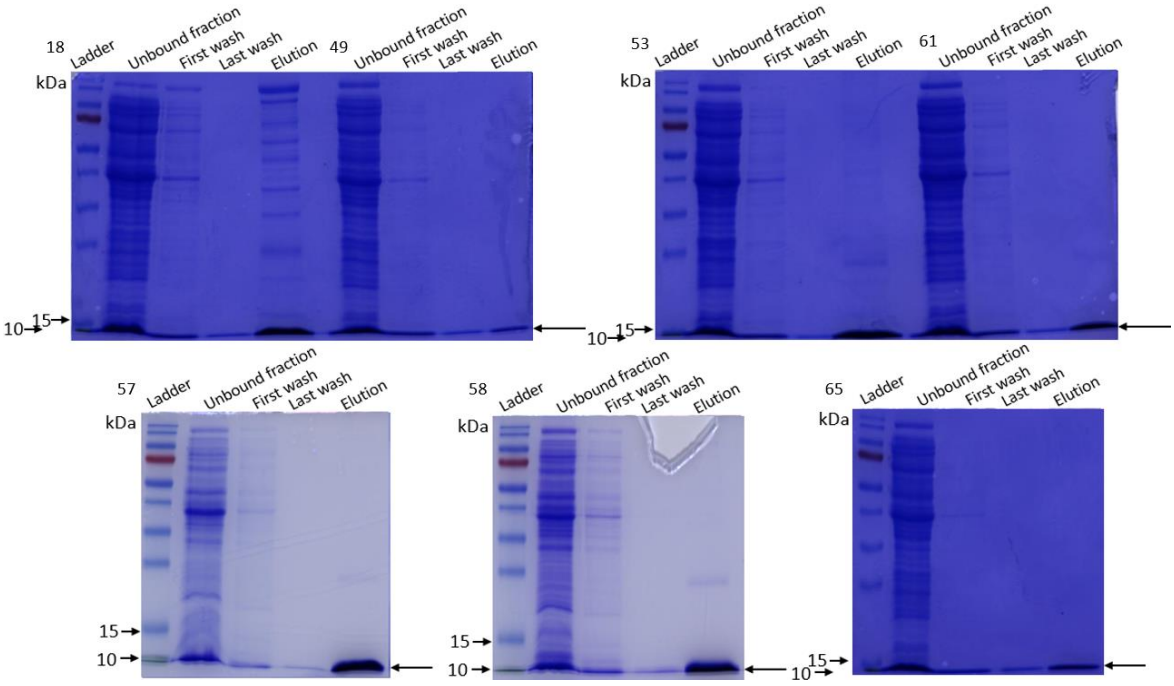

Figure 3.6.3. SDS-PAGE gel to verify production and purification of subcloned Affimers in BL21 Star cells. Affimers were produced from 500 mL of BL21 Star (DE3) cells culture and purified by nickel affinity chromatography. 2 µL samples were gathered from the elution step. Samples were denatured in 1x sample buffer and denatured by boiling for 5 minutes before loading. 5 µL of PageRuler molecular weight ladder was added into the first well. Gels were stained with Coomassie blue dye. Expected bands of ~12 kDa are indicated by the black arrows.

The expected bands appeared on the SDS-PAGE gels to verify the presence of Affimer. This suggestion is further supported by the method of protein purification, nickel affinity chromatography that is used to bind proteins with a His-tag, such as these Affimers. However, the 15% SDS-PAGE gels made did not appear to allow for sufficient separation to confirm this against a protein ladder. As such, a pre-cast gradient gel was used, and 10 µL aliquots of each elution step were analysed against a PageRuler molecular weight ladder and stained with Coomassie blue to aid verification.

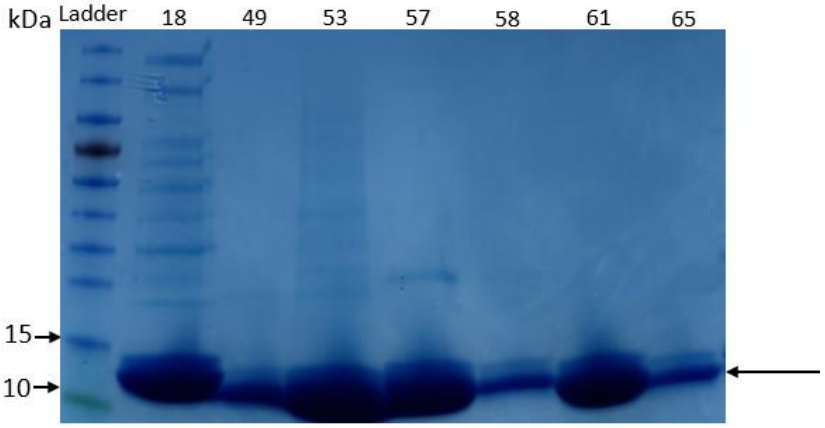

Figure 3.6.4. Pre-cast SDS-PAGE gel to verify correct size of subcloned Affimers in BL21 Star (DE3). Affimers were produced from 500 mL of BL21 Star (DE3) cells culture and purified by nickel affinity chromatography. 2 µL samples were denatured in 1x sample buffer by boiling for 5 minutes before loading. 5 µL of PageRuler molecular weight ladder was added into the first well. Gels were stained with Coomassie blue dye. Expected bands of ~12 kDa are indicated by the black arrow. A pre-cast, gradient gel was used in an effort to better show the correct migration through the gel to show the size of Affimer proteins expected in comparison to a 15% SDS-PAGE gel.

3.6.2. Nitrocefin Assay Results

In order to gather more data regarding the initial rate of VIM-1 in the presence of various Affimer reagents, this second test, results seen in Figure 3.6.5 used a 100-fold Affimer concentration but had the overall concentration of the VIM-1 and Affimer reagents reduced to 75 nM and 7.5 µM respectively. Successfully subcloned Affimers are shown in Figure 3.6.6.

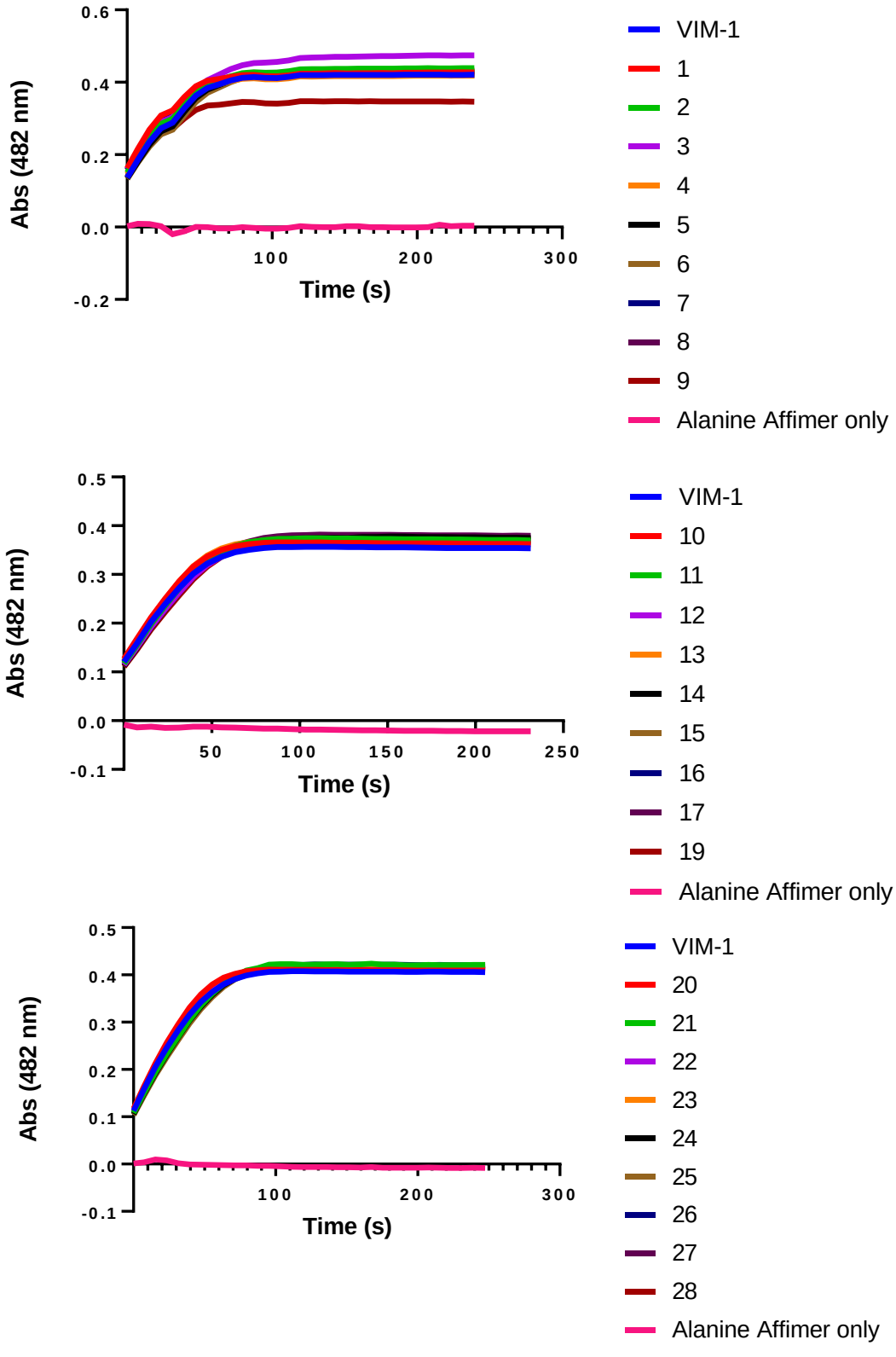

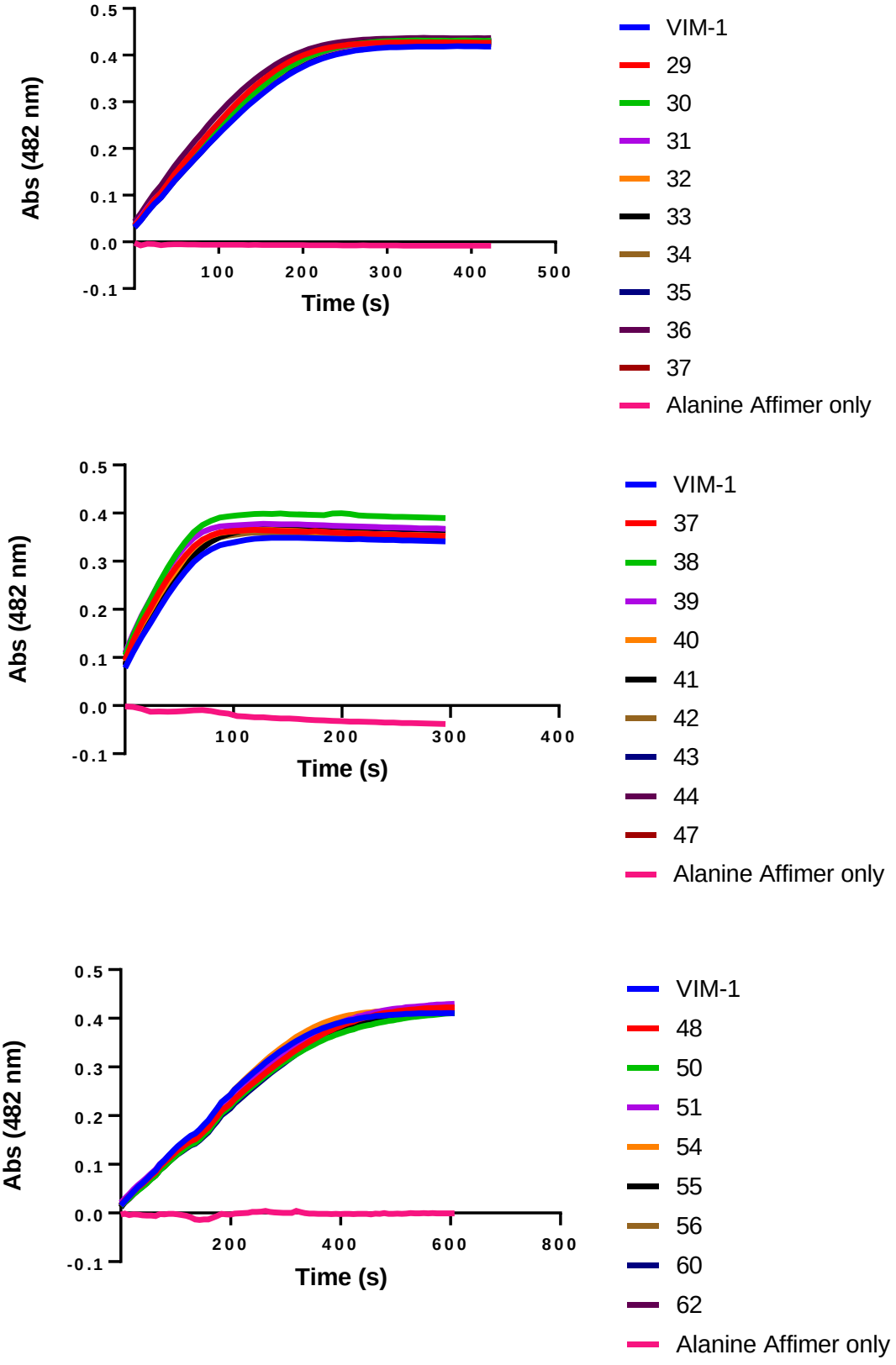
Abs (482 nm)
0.5
0.4
0.3
0.2
0.1
0.0
-0.1
100
200
300
400
500
Time (s)
VIM-1
29
30
31
32
33
34
35
36
37
Alanine Affimer only
Abs (482 nm)
0.5
0.4
0.3
0.2
0.1
0.0
-0.1
100
200
300
400
Time (s)
VIM-1
37
38
39
40
41
42
43
44
47
Alanine Affimer only
Abs (482 nm)
0.5
0.4
0.3
0.2
0.1
0.0
-0.1
200
400
600
800
Time (s)
VIM-1
48
50
51
54
55
56
60
62
Alanine Affimer only

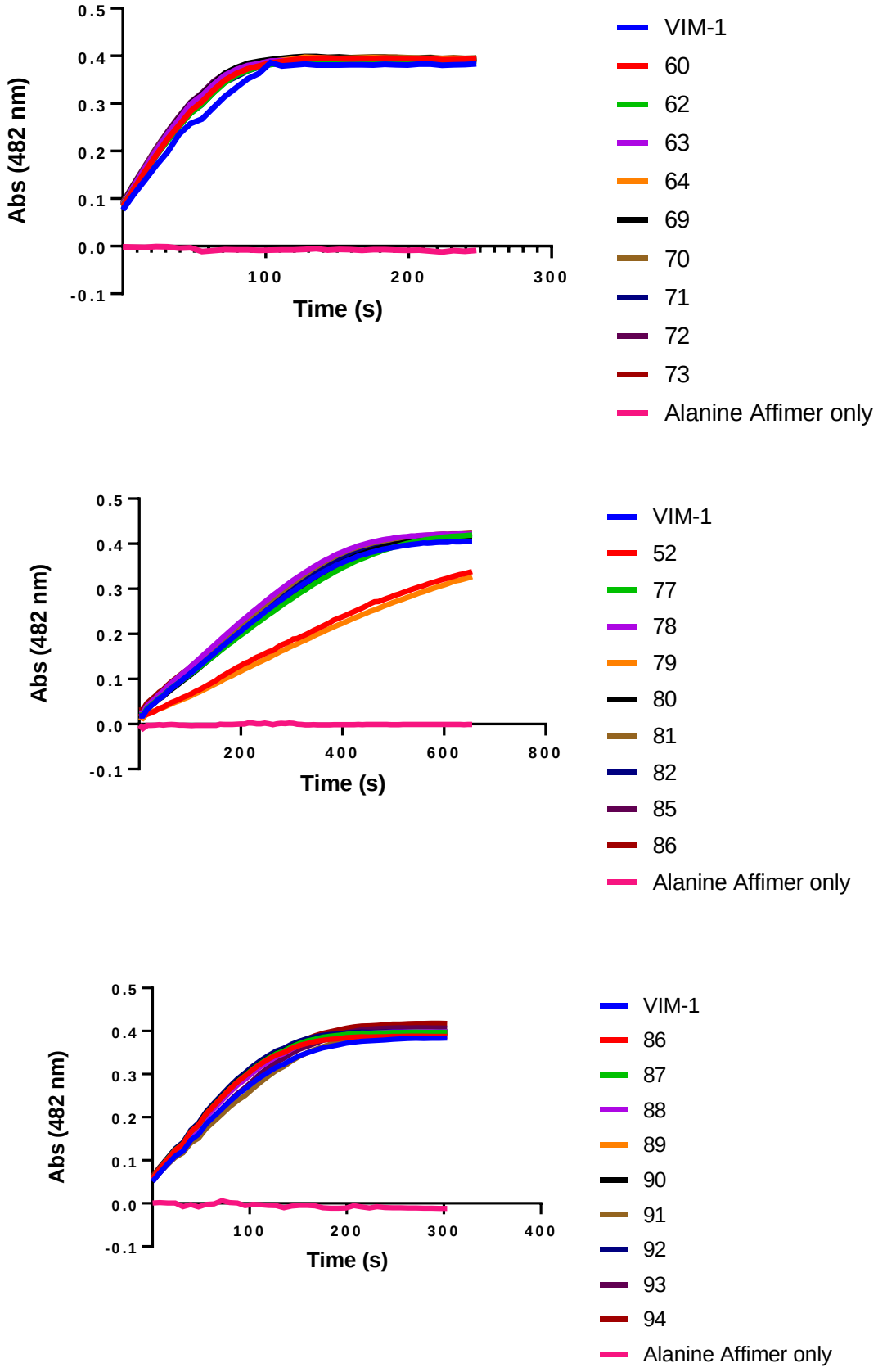

Figure 3.6.5. Effects of Affimer reagents on rate of nitrocefin hydrolysis by VIM-1. Graphs were calculated using data collected at approximately 7 second intervals with absorbance readings at 482 nm. All data points were normalised against EDTA control. *n*=3.

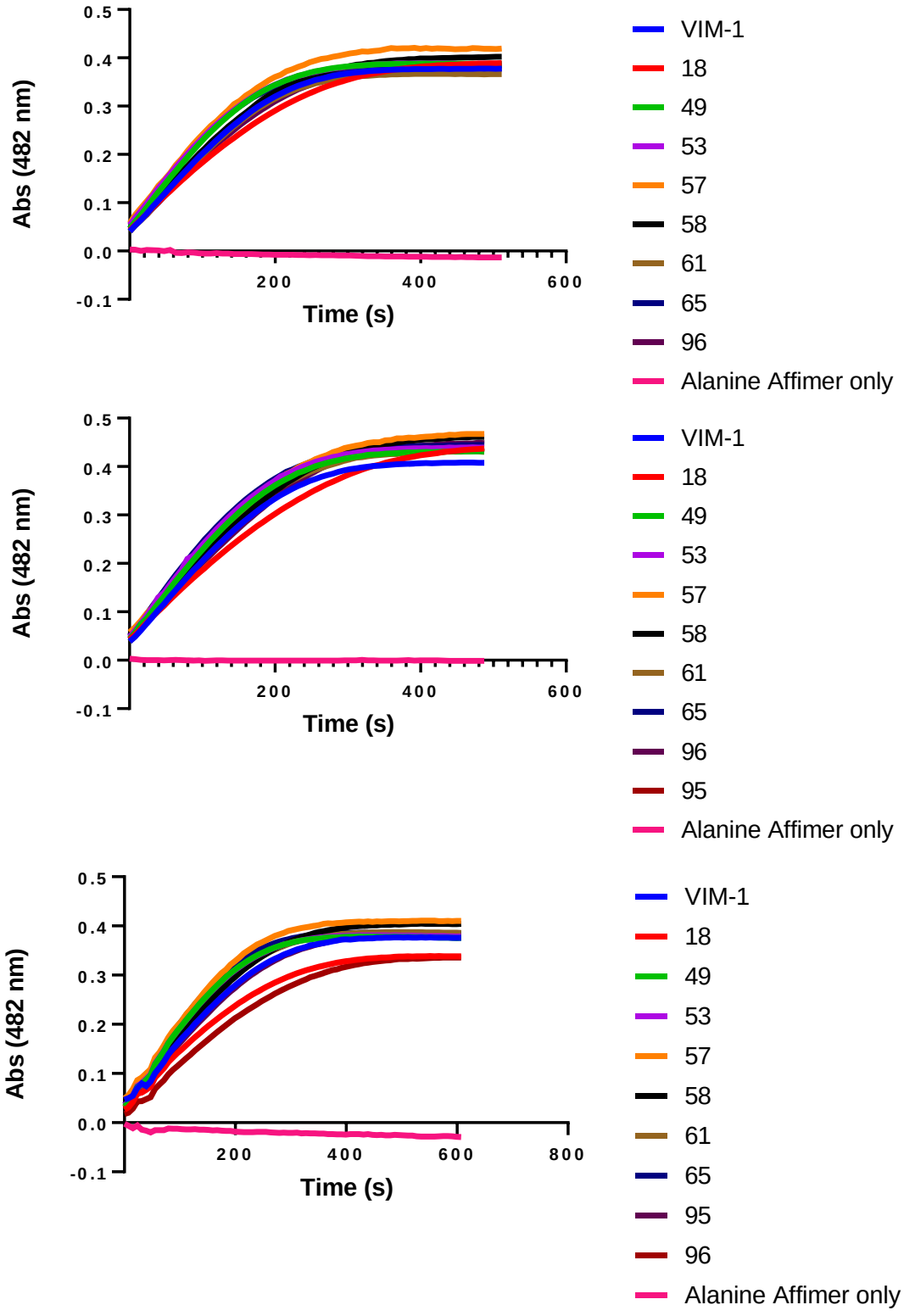

Figure 3.6.6 Effects of Affimer reagents on rate of nitrocefin hydrolysis by VIM-1. Graphs were calculated using data collected at approximately 7 second intervals with absorbance readings at 482 nm. All data points were normalised against EDTA control. *n*=3.

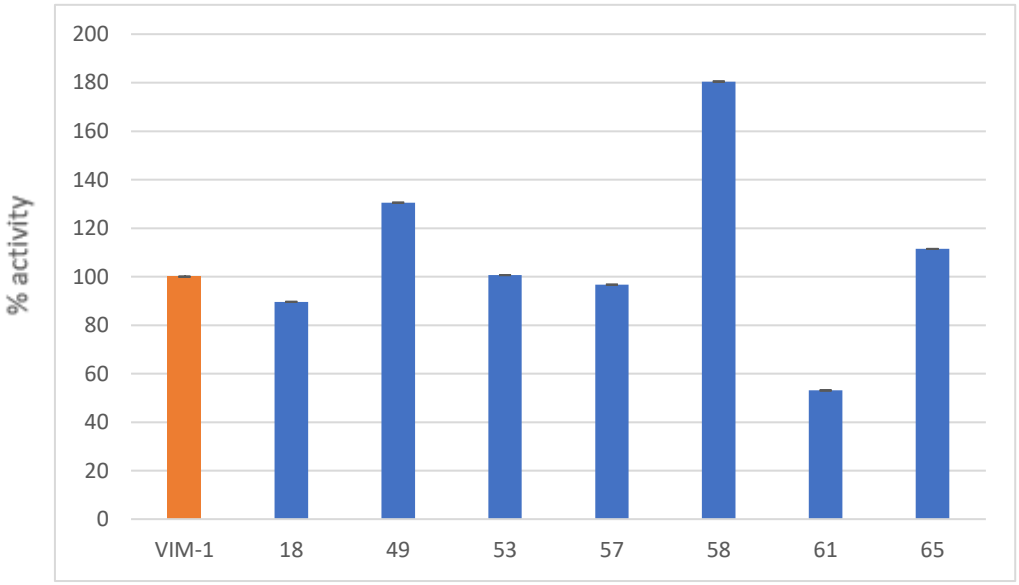

Figure 3.6.7. Activity of VIM-1 under different conditions as a percentage of unimpeded activity. Using VIM-1 only control as a standard, initial rates were calculated from the first 103 seconds of the assay and showed nitrocefin hydrolysis under different Affimer conditions and established as a percentage. *n*=3

The final set of nitrocefin assays suggested that of the Affimers tested during this project, Affimer61 had the best inhibition. At 100-fold Affimer concentration, nitrocefin hydrolysis by VIM-1 was reduced by 47%. Further characterisation of this Affimer could elucidate its method of inhibition, and a spectrum of assays at various concentrations would be able to establish its IC_{50}. Due to time constraints however, this will rely on future experimentation. Interestingly, Affimer58 appeared to increase the rate of nitrocefin hydrolysis by VIM-1 by 80%. It is single loop as is Affimer61 and shares a similar overall hydrophobicity in its sequence, though appears to lack any basic residues that Affimer61 has at positions 1 and 2.

3.7. **Sequence Similarity between Sequenced Affimers**

All of the Affimers sequenced during this thesis were analysed for themes that might indicate their binding to VIM-1. Affimers that bind to VIM-1 appear to have a propensity towards hydrophobic residues, as seen in Table 3.7.1. Figure 3.7.2. shows a weighted Kullback-Leibler logo that of these, tryptophan is the most likely amino acid at all but 3 points.

Affimer clone	Variable Region 1								
Ala Aff	A	A	A	A	*	*	*	*	*
A1	M	A	A	P	R	F	W	P	E
B1	F	E	S	P	Y	F	W	P	V
C1	W	W	P	M	A	H	G	Y	E
D1	H	A	S	M	N	R	W	Q	E
E1	Q	W	Y	I	W	T	S	W	W
G1	T	A	G	T	Q	Y	N	Q	E
H1	Y	H	E	T	T	V	Q	H	N
A2	N	T	F	W	F	T	Y	F	A
B2	F	R	R	E	N	Y	T	T	E
C2	W	R	D	M	I	Y	A	S	Y
D2	V	I	Q	A	N	K	E	L	D
E2	F	M	A	P	H	F	W	P	G
G2	R	E	Q	Q	D	W	T	V	E
H2	T	H	A	P	F	F	W	P	E
A3	W	W	P	M	A	H	G	Y	E
B3	E	M	E	V	Q	H	G	Y	H
C3	V	I	Y	Y	R	D	D	Y	Y
D3	V	K	E	S	Q	M	V	R	S
E3	F	R	R	E	N	Y	T	T	E
F3	F	R	R	E	N	Y	T	T	E
G3	H	N	G	R	F	R	Y	H	T
H3	M	R	A	P	I	Y	W	P	E
A4	L	R	A	P	V	F	W	P	V
B4	W	W	P	M	A	H	G	Y	E
C4	W	W	P	M	A	H	G	Y	E
D4	I	Q	L	T	Q	N	G	N	S
F4	I	L	Y	W	K	Q	E	Y	Y
18	L	P	R	K	W	D	R	A	E
49	F	M	A	P	H	F	W	P	G
53	M	S	A	P	F	W	F	P	E
57	L	R	A	P	V	F	W	P	V
58	V	M	D	L	M	W	A	Y	W
61	K	R	A	P	V	F	W	P	E
65	M	F	S	P	V	F	W	P	E

	Variable Region 2								
Ala Aff	A	A	E	*	*	*	*	*	*
A1	A	A	E	*	*	*	*	*	*
B1	A	A	E	*	*	*	*	*	*
C1	K	E	A	M	G	H	K	H	K
D1	Q	S	H	W	W	F	G	I	F
E1	A	A	E	*	*	*	*	*	*
G1	L	L	R	Y	P	K	Q	S	F
H1	R	R	E	I	Y	Q	L	K	W
A2	K	P	T	R	E	F	Q	L	I
B2	K	R	N	W	G	W	W	S	H
C2	A	Y	Y	H	N	S	D	N	T
D2	R	K	M	I	W	K	F	H	V
E2	A	A	E	*	*	*	*	*	*
G2	H	Y	N	Y	P	W	A	A	G
H2	A	A	E	*	*	*	*	*	*
A3	K	E	A	M	G	H	K	H	K
B3	W	R	R	I	W	N	Y	H	W
C3	W	K	F	L	T	I	L	E	I
D3	L	T	W	F	M	R	G	I	Y
E3	K	R	N	W	G	W	W	S	H
F3	K	R	N	W	G	W	W	S	H
G3	A	H	R	W	W	W	N	W	D
H3	A	A	E	*	*	*	*	*	*
A4	A	A	E	*	*	*	*	*	*
B4	A	A	E	*	*	*	*	*	*
C4	A	A	E	*	*	*	*	*	*
D4	A	W	W	I	K	M	Q	N	I
F4	W	N	T	Y	D	T	V	E	I
18	H	I	I	Y	V	N	Q	K	L
49	A	A	E	*	*	*	*	*	*
53	A	A	E	*	*	*	*	*	*
57	A	A	E	*	*	*	*	*	*
58	A	A	E	*	*	*	*	*	*
61	A	A	E	*	*	*	*	*	*
65	A	A	E	*	*	*	*	*	*

Key
HYDROPHOBIC
ACIDIC
BASIC
NEUTRAL

Table 3.7.1. Comparison of variable regions of Affimers sequenced during this thesis. Of the 34 Affimers sequenced, 19 had a full variable region 2. Hydrophobic amino acids were favoured in Affimers that bound within their sequence.

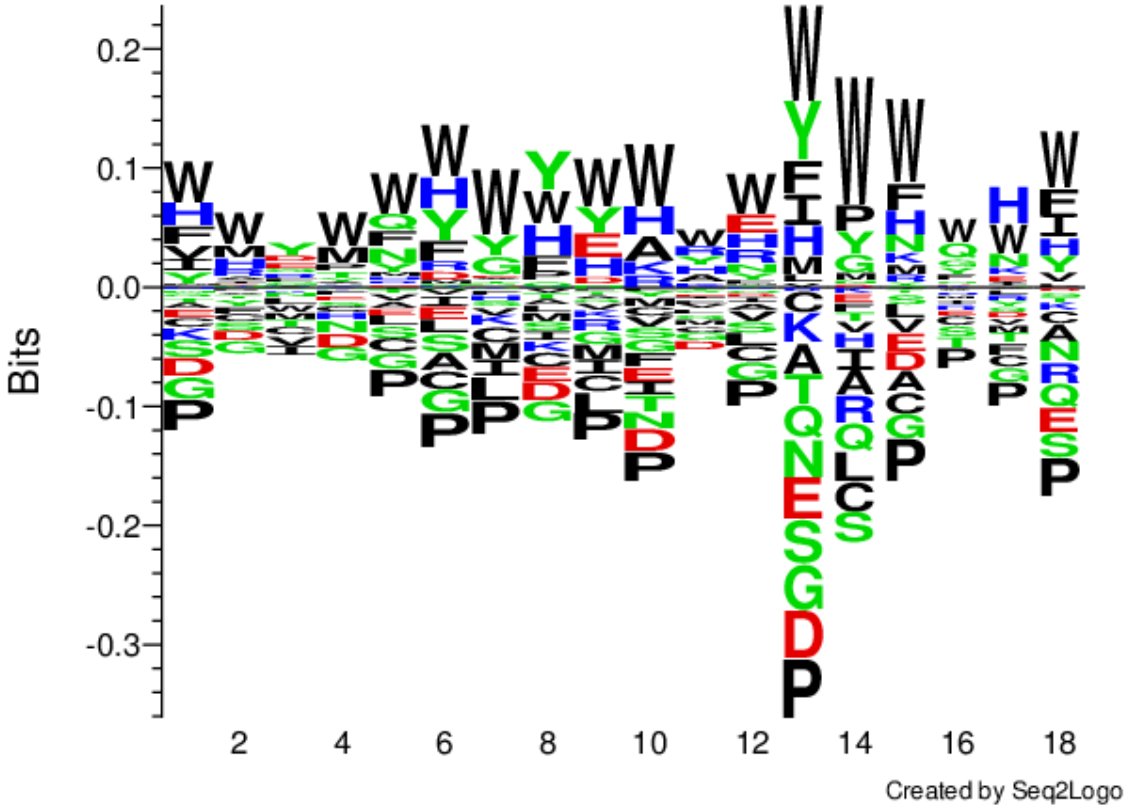

Figure 3.7.2. Weighted Kullback-Leibler divergence of Affimers sequenced during this thesis. Tryptophan is favoured in all positions except 3, 8, and 16 Image created using Seq2Logo [100].

Without protein structure to validate Affimer interactions with VIM-1, it is purely speculative, but it indicates that hydrophobicity is important within variable region 1 – and 2 where present – in binding interactions between Affimers found in this study and VIM-1.

4. Discussion

As the global spread of antimicrobial resistance continues to increase, so too does the need for novel reagents that are able to detect, bind, and modulate resistance mechanisms. Inhibitors that target metallo-β-lactamases are highly sought-after as their function allows them to threaten the efficacy of our current clinical arsenal of antibiotics.

Affimer reagents have previously been found to inhibit the activity of NDM-1, a metallo-β-lactamase (MBL) with a functional similarity to VIM-1. In prior studies at the University of Leeds inhibition of NDM-1 was found to be up to 85% at five-fold the Affimer. A. Herbert and Dr L. Faveri identified Affimer 21 which inhibits NDM-1 by a non-competitive mechanism[88][87]. This work investigates the proposal that Affimer reagents could be found to have a similar inhibitory effect on VIM-1.

4.1. VIM-1 Protein Expression and Purification

Initially VIM-1 proteins were expressed in BL21 Star (DE3) cells, which yielded a good quantity of protein, around 3 mg per 500 mL culture. Initially VIM-1 was chemically biotinylated through the use of EZ-link NHS-SS-Biotin, which binds primarily to lysine residues, of which there are six in VIM-1. Chemical biotinylation is a common method of biotinylating proteins prior to immobilisation on streptavidin coated surfaces in preparation for phage panning in phage display and phage ELISA[81]. In this study chemical biotinylation was found not to be successful (see Results 3.1.2.) An alternate method of protein biotinylation is to add a biotin acceptor peptide (BAP) tag to the terminus of a protein sequence. In strains containing the *BirA* plasmid, an expression plasmid for BirA ligase, the BAP tag is biotinylated. For this reason, AVB101 cells were used for the expression of biotinylated protein. Expression in AVB101 cells showed a protein yield of 2.8 mg per 500mL culture. The extent of biotinylation of the resulting protein was analysed via Western blot and ELISA assays.

It should be noted for future work on preparing biotinylated protein for the purpose of protein immobilisation, is that the genetic BAP-tag approach results in a lower diversity of orientations of the immobilised protein compared to that of chemical biotinylation. As such, it may be that though the results of the phage display were better than when using chemical biotinylation (such as through NHS-SS-Biotin) it may represent in other cases a reduced ability to find a suitable Affimer or other binder that would instead have bound to a -now secluded- section of the protein. This should also be a consideration when proteins such as metallo-β-lactamases are being used, as covering the active site of an enzyme could reduce the potential of finding a broad-spectrum Affimer reagent that acts as an inhibitor.

4.2. Affimer Protein Expression and Purification

As described in section 3.2.2, for initial screening purposes Affimers were produced in 50 mL of autoinduction media and purified by nickel affinity chromatography. This provided a sufficient protein yield to perform nitrocefin assays in triplicate on a single plate. Once selected and subcloned into pET11a vectors, Affimers were produced in 500 mL culture volumes and purified by nickel affinity chromatography. This yielded greater protein expression, commonly greater than 10 mg of protein per culture which was enough for several assays in both biological and technical triplicate repeats. One advantage of Affimers is their high yield from *E. coli* cells, which is advantageous over other technologies such as the production of antibodies and was evident in this study.

Coupled with these findings, the nickel affinity chromatography as a purification method appeared to be efficacious, yielding high amounts of protein in pure samples. Bands on SDS-PAGE gels were clear signifying their expression, with little - to no - protein contamination.

4.3. Affimers as inhibitors of Metallo-β-lactamases

In this thesis, inhibition of the rate of nitrocefin hydrolysis by VIM-1 was accomplished with Affimer61, reducing the rate by 47%, which suggests that Affimer reagents can modulate the activity of VIM-1. Further characterisation must be performed on this and other Affimers, to establish an IC_{50} and determine the method of inhibition. An IC_{50} denotes in this case the amount of Affimer required to inhibit the hydrolysis of nitrocefin by VIM-1 by 50%. This would be established by performing a series of nitrocefin assays utilising a constant VIM-1 concentration, with an initially high (in order to establish maximal inhibition, close to 100%) but decreasing concentration of Affimer reagent. Technical and biological repeats would be necessary as within this study, to establish at what concentration of Affimer is VIM-1 inhibited by 50%. The lower this value, the better the Affimer would be since less of the reagent would be required to reach this inhibitory level.

Structural characterisation of the Affimer-target complex would shed light on the binding interactions and the method of inhibition of Affimer 61. Identification of the binding site of Affimer61 could also be referenced against known sequences of VIM-variants to establish the likelihood of whether it could be used as an inhibitor against these also.

The use of alanine Affimers in this project is consistent with other controls used in Affimer projects. The truncated variable regions, consisting primarily of alanine to allow structure and flexibility without complex sidechain interactions, allows for establishing during assays that the basic structure of the Affimer itself is not responsible for perceived effects. In the case of this project, it was to ensure that the Affimer structure was not able to either hydrolyse the nitrocefin reagent independently or inhibit VIM-1 activity.

4.3.1. Affimers as Therapeutics and Diagnostics

As discussed in the introduction (see 1.5.2) there are currently no clinically approved metallo-β-lactamase inhibitors currently in use, though some are in late-stage clinical trials. This goes to demonstrate the potential impact a successful inhibitory Affimer could have clinically. If it could be shown that inhibition is possible through the use of an Affimer reagent against a single MBL, tests could be performed to identify any potential inhibition of related MBLs. If it was not applicable due to the binding location varying between tangentially related MBLs, the high variability in binding potential for the rest of the phage library could be screened in a similar way against a new target or ranges of targets, in order to try and identify a specific binder – and potential inhibitor – for each.

4.3.2 Intracellular Delivery

One challenge to overcome for the use of Affimers as therapeutics is the use of a reliable system for intracellular delivery. Due to their size and polarity, proteins are more challenging to diffuse across a cell membrane than small molecules. A protein such as an Affimer is around 12 kDa, and is therefore unlikely to passively diffuse across a membrane in great enough numbers to elicit an efficacious response [101]. The added complexity of a double-membrane cell envelope in the case of Gram-negative bacteria means it is increasingly difficult. There is evidence to suggest though that MBL's like NDM-1 and VIM-1 are localised to the periplasm, such that an inhibitor need only permeate

through the outer membrane of a Gram-negative bacterium to be effective thereby indicating a higher level of target accessibility compared to cytoplasmic targets [101], [102].

Cell-penetrating peptides (CPP's) are water soluble, partly hydrophobic peptides that have the ability to penetrate a cell membrane without causing significant damage, and have the capacity to deliver an internalised covalently bound biologically active cargo with low toxicity [103]. In 2004 TP10 CPPs were shown to deliver SYTOX Green - a nucleic acid stain – preferentially to *S. aureus* cells when incubated with both HeLa and non-invasive *S. aureus,* fluorescence increased in *S. aureus* without increasing at the same rate in HeLa cells [104]. In 2015, CPPs were covalently conjugated to peptide nucleic acids (PNAs) to target intracellular RNA polymerase α subunit (*rpo*A) expression, and found a 50% reduction in gene expression at 1 μM[105].

Polymersomes are lipid based delivery systems that can release their encapsulated molecule under a variety of conditions such as change in pH, redox potential, ionic strength or instability within the design of the system[106]. Polymersomes have the ability to encapsulate amphiphilic, hydrophobic, and hydrophilic molecules making them well suited to carrying proteins [107]. They have been shown to have the capacity to deliver drug mixtures of doxorubicin (DOX) and paclitaxel (TAX) into tumour tissues in hours at a low pH and 37°C [108].

4.3.3. Development of resistance

Bacteria have the ability to acquire resistance to new methods of inhibition, in ways previously described in 1.1.2. It is important to consider how the use of Affimer proteins as VIM-1 inhibitors could exert a selective pressure which may lead to the evolution of resistance, it is possible bacteria could develop such mechanisms of resistance to any Affimer reagents.

The evolution of resistance can only be tested in longitudinal studies of Gram-negative bacteria by treating VIM-1 expressing cells with various concentrations of Affimer61 and antibiotics then passaging over a number of weeks to assess whether any strains were capable of evading Affimer inhibition by acquiring resistance. An adaptive library evolution, similar to those used in 2014 by Jahn et al. could be utilised, whereby increasing antibiotic drug concentration in set stages over a period of two weeks resulted in cells expressing increased resistance to the antibiotics used [109].

4.3.4. Immunogenicity

The ability of a substance to provoke an immune response in a host is referred to as immunogenicity, and this is another important consideration when developing novel reagents such as the Affimer [110]. Anti-drug antibodies (ADAs) can be expressed in response to a therapeutic, and bind in a tiered response that can cause immune complexes to be formed, and can result in erroneous activation of the complement cascade [111].

With regards to the immunogenicity of the Affimer structure, Avacta Life Sciences Ltd published observations using human *ex vivo* samples. Three different structures of Affimer scaffold were tested at five-fold the concentration of Avastin after a period of seven days in T-cell cultures, and analysed by flow cytometry [110]. It was found that all three structures elicited low levels of immune response, among these the type 2 Affimer structure that was used in this thesis[110]. These results give hope to the future use of Affimer technology in therapeutics.

4.4. Continuation of the Project and Future Applications

Affimer61 was shown to bind to VIM-1 and successfully modulate its activity in an *n=3* series of experiments. Further work is required to establish an IC_{50} of this Affimer as well as its effectiveness against VIM-1 expressing bacteria *in vivo*, and a crystal structure of VIM-1 with Affimer bound would help to elucidate its method of inhibition, and possible application to other VIM-variants.

Work to express VIM-1 variants and test Affimer cross reactivity is also necessary, as there is a great need for cross-reactive metallo beta lactamase inhibitors. Further phage display screening could also be used to select cross-reactive Affimer binders in the hope of isolating a broad range inhibitor.

4.4.1. Ongoing work using reagents created in this project

Since the conclusion of research on this project, L. Medinger (University of Leeds) has continued testing for Affimer reagent inhibitors of VIM-1. Using the purified phage from the second round of phage display and stocks of BAP-tagged VIM-1 created during this project he has performed the third pan of phage display and phage ELISA to try and identify unique Affimers that target VIM-1.

In early tests, one such Affimer appears to have an inhibitory effect on VIM-1 at 33-fold concentration (50 nM VIM-1, 1.5 µM Affimer14), results are shown Figure 4.1.

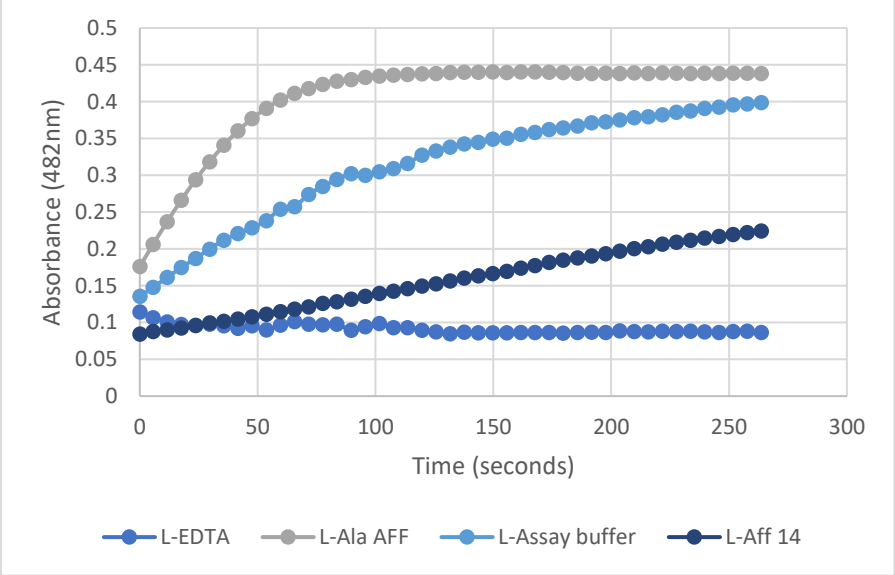

Figure 4.1. Effects of Affimer reagents on rate of nitrocefin hydrolysis by VIM-1. Rates shown were calculated using data collected at approximately 7 second intervals with absorbance readings at 482 nm. All rates were normalised against EDTA control. (Unpublished data, L. Medinger, 2022).

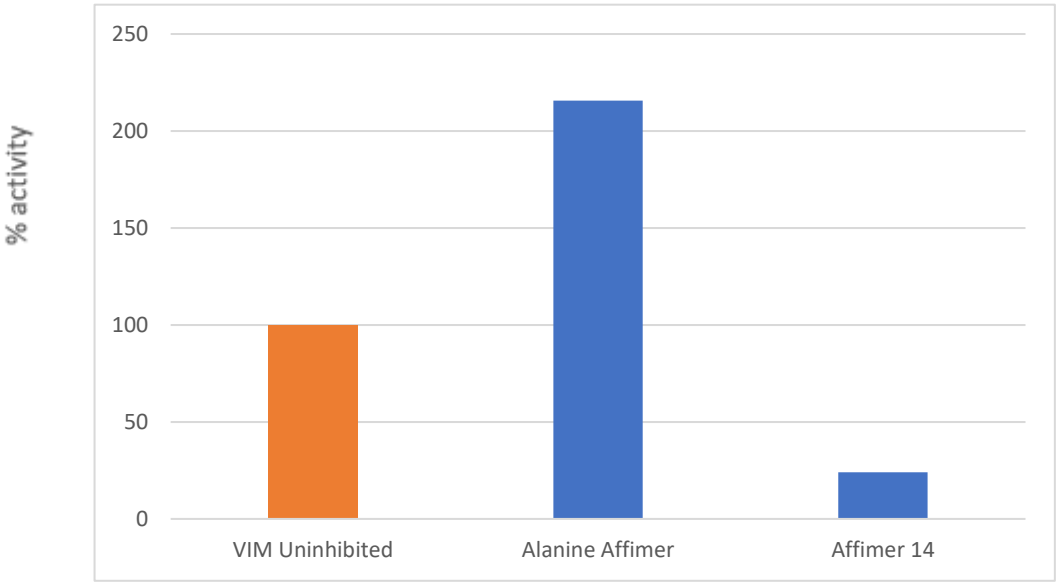

Figure 4.2. Activity of VIM-1 under different conditions as a percentage of unimpeded activity. Using VIM-1 only control as a standard, initial rates were calculated under different Affimer conditions, and established as a percentage against the rate of VIM-1 only. Affimer14 concentration at 33-fold VIM-1 concentration. (Unpublished data, L. Medinger, 2022).

Given the disparity between VIM-1 and VIM-1 with alanine Affimer control, user error may account for some loading errors involved in setting up the plate, however these initial results show a reduction in VIM-1 activity by 76%. These results, coupled with those found during this project, go some way to supporting the initial hypothesis.

Affimer61, which showed the greatest inhibition in the initial project, as well as Affimer 14 from this latest work both have a single variable region, compared in Figure 4.3.

61	K	R	A	P	V	F	W	P	E
14	R	F	N	N	S	F	F	K	A

Figure 4.3. Sequence comparison of variable region 1 of Affimer61 and Affimer14. Both Affimers have a propensity towards hydrophobic residues (green), and feature two basic residues (blue). Affimer14 contains 3 neutral (grey) residues towards the start of the variable loop however, whereas the Affimer from this study has an acidic residue at the end of the loop.

If further experimentation shows good inhibition of VIM-1, sub-libraries based on the variable loop sequences of Affimer61 or Affimer14 could also be useful for investigating the potential improvement of the inhibitory effects.

5. Conclusions

Affimer reagents have been shown during this project to be able to bind to VIM-1, and in preliminary experiments show inhibitory effects on its rate of hydrolysis of nitrocefin. The modification of a target protein by inclusion of a biotin acceptor peptide tag has also been demonstrated to be a useful technique to assist in screening, though further investigation may be needed on resultant orientation of a BAP-tagged protein when bound to streptavidin.

Future work needs to be done to characterise the type of inhibition witnessed during these results, as well as a given Affimers ability to inhibit VIM-1 *in vivo*. When coupled with prior work on NDM-1, these are good steps towards verifying Affimers as desperately needed inhibitors of metallo-β-lactamases in the ongoing struggle against antibiotic resistant pathogens. The rapid screening of Affimer libraries against a target alongside their low cost and ease of manufacturing make Affimers useful tools for the future.

References

[1] R. S. Schwartz, “Paul Ehrlich’s Magic Bullets,” *N. Engl. J. Med.*, vol. 350, no. 11, pp. 1079–1080, Mar. 2004, doi: 10.1056/NEJMp048021.

[2] P. Ehrlich and S. Hata, *Die experimentelle Chemotherapie der Spirillosen*, vol. VIII. Berlin, Heidelberg: Springer Berlin Heidelberg, 1910.

[3] T. N. F. 1939, “Gerhard Domagk,” *NobelPrize.org*, 2022. https://www.nobelprize.org/prizes/medicine/1939/domagk/facts/ (accessed May 05, 2022).

[4] A. Fleming, “On the Antibacterial Action of Cultures of a Penicillium, with Special Reference to their Use in the Isolation of B. influenzæ.,” *British journal of experimental pathology*, vol. 10, no. 3. pp. 226–236, Jun. 1929.

[5] E. Chain *et al.*, “THE CLASSIC: penicillin as a chemotherapeutic agent. 1940.,” *Clin. Orthop. Relat. Res.*, vol. 439, pp. 23–26, Oct. 2005, doi: 10.1097/01.blo.0000183429.83168.07.

[6] S. A. Waksman and H. B. Woodruff, “Streptothricin, a New Selective Bacteriostatic and Bactericidal Agent, Particularly Active Against Gram-Negative Bacteria.,” *Exp. Biol. Med.*, vol. 49, no. 2, pp. 207–210, Feb. 1942, doi: 10.3181/00379727-49-13515.

[7] A. Schatz, E. Bugle, and S. A. Waksman, “Streptomycin, a Substance Exhibiting Antibiotic Activity Against Gram-Positive and Gram-Negative Bacteria.*,” *Exp. Biol. Med.*, vol. 55, no. 1, pp. 66–69, Jan. 1944, doi: 10.3181/00379727-55-14461.

[8] S. A. Waksman, “Microbial Antagonisms and Antibiotic Substances | Ovid,” *Soil Sci.*, vol. 59, no. 6, p. 482, 1945, Accessed: Apr. 28, 2021. [Online]. Available: https://oce.ovid.com/article/00010694-194506000-00012/HTML.

[9] R. Emmerich and O. Löw, “Bakteriolytische Enzyme als Ursache der erworbenen Immunität und die Heilung von Infectionskrankheiten durch dieselben,” *Zeitschrift für Hyg. und Infekt.*, vol. 31, no. 1, pp. 1–65, 1899.

[10] M. Hutchings, A. Truman, and B. Wilkinson, “Antibiotics: past, present and future,” *Current Opinion in Microbiology*, vol. 51. Elsevier Ltd, pp. 72–80, Oct. 01, 2019, doi: 10.1016/j.mib.2019.10.008.

[11] W. C. Reygaert, “An overview of the antimicrobial resistance mechanisms of bacteria,” *AIMS Microbiol.*, vol. 4, no. 3, pp. 482–501, Jun. 2018, doi: 10.3934/microbiol.2018.3.482.

[12] A. Jayol, L. Poirel, A. Brink, M.-V. Villegas, M. Yilmaz, and P. Nordmann, “Resistance to Colistin Associated with a Single Amino Acid Change in Protein PmrB among Klebsiella pneumoniae Isolates of Worldwide Origin,” 2014, doi: 10.1128/AAC.00084-14.

[13] P. Lassaux *et al.*, “Biochemical and structural characterization of the subclass B1 metallo-β-lactamase VIM-4,” *Antimicrob. Agents Chemother.*, vol. 55, no. 3, pp. 1248–1255, Mar. 2011, doi: 10.1128/AAC.01486-09.

[14] P. S. Borra *et al.*, “Structural and Computational Investigations of VIM-7: Insights into the Substrate Specificity of VIM Metallo-β-Lactamases,” *J. Mol. Biol.*, vol. 411, no. 1,

pp. 174–189, Aug. 2011, doi: 10.1016/j.jmb.2011.05.035.

[15] J. Fishovitz, J. A. Hermoso, M. Chang, and S. Mobashery, “Penicillin-binding protein 2a of methicillin-resistant Staphylococcus aureus,” *IUBMB Life*, vol. 66, no. 8, pp. 572–577, Aug. 2014, doi: 10.1002/iub.1289.

[16] U. Choi and C.-R. Lee, “Distinct Roles of Outer Membrane Porins in Antibiotic Resistance and Membrane Integrity in Escherichia coli,” *Front. Microbiol*, vol. 10, p. 953, 2019, doi: 10.3389/fmicb.2019.00953.

[17] M. Putman, H. W. Van Veen, and W. N. Konings, “Molecular Properties of Bacterial Multidrug Transporters,” 2000. [Online]. Available: https://journals.asm.org/journal/mmbr.

[18] J.-M. Pages *et al.*, “Efflux Pump, the Masked Side of ß-Lactam Resistance in Klebsiella pneumoniae Clinical Isolates,” *PLoS One*, vol. 4, no. 3, p. e4817, Mar. 2009, doi: 10.1371/journal.pone.0004817.

[19] Q. Chi Truong-Bolduc *et al.*, “Implication of the NorB Efflux Pump in the Adaptation of Staphylococcus aureus to Growth at Acid pH and in Resistance to Moxifloxacin,” *Antimicrob. Agents Chemother.*, vol. 55, no. 7, pp. 3214–3219, 2011, doi: 10.1128/AAC.00289-11.

[20] F. Akrami, M. Rajabnia, and A. Pournajaf, “Review Article Resistance integrons; A mini review,” *Casp. J Intern Med*, vol. 10, no. 4, pp. 370–376, 2019, doi: 10.22088/cjim.10.4.370.

[21] L. Cré Met *et al.*, “Nosocomial outbreak of carbapenem-resistant Enterobacter cloacae highlighting the interspecies transferability of the bla OXA-48 gene in the gut flora,” *J Antimicrob Chemother*, 2012, doi: 10.1093/jac/dkr547.

[22] J. M. Musser, “Antimicrobial agent resistance in mycobacteria: molecular genetic insights.,” *Clin. Microbiol. Rev.*, vol. 8, no. 4, pp. 496–514, Oct. 1995, doi: 10.1128/CMR.8.4.496.

[23] “TACKLING DRUG-RESISTANT INFECTIONS GLOBALLY: FINAL REPORT AND RECOMMENDATIONS THE REVIEW ON ANTIMICROBIAL RESISTANCE CHAIRED BY JIM O’NEILL,” 2016.

[24] V. A. Ogawa, T. A. Tran, and C. M. Shah, Eds., *Understanding the Economics of Microbial Threats*. Washington, D.C.: National Academies Press, 2018.

[25] R. C. (Wellcome), “Why is it so hard to develop new antibiotics?,” *Wellcome*, 2020. https://wellcome.org/news/why-is-it-so-hard-develop-new-antibiotics (accessed Jan. 30, 2022).

[26] J. Davies, “Where have All the Antibiotics Gone?,” *Can. J. Infect. Dis. Med. Microbiol. = J. Can. des Mal. Infect. la Microbiol. medicale*, vol. 17, no. 5, pp. 287–90, Sep. 2006, doi: 10.1155/2006/707296.

[27] J. W. BARTHOLOMEW and T. MITTWER, “The Gram stain.,” *Bacteriol. Rev.*, vol. 16, no. 1, pp. 1–29, Mar. 1952, [Online]. Available: http://www.ncbi.nlm.nih.gov/pubmed/14925025.

[28] F. C. Neuhaus, “The Enzymatic Synthesis of D-Alanyl-D-alanine II.,” 1962. doi: 10.1016/S0021-9258(18)50132-0.

[29] A. Bouhss *et al.*, “Role of the Ortholog and Paralog Amino Acid Invariants in the Active Site of the UDP-MurNAc-l-alanine:d-glutamate Ligase (MurD),” *Biochemistry*, vol. 38, no. 38, pp. 12240–12247, Sep. 1999, doi: 10.1021/bi990517r.

[30] J. M. Ghuysen, “Serine beta-lactamases and penicillin-binding proteins.,” *Annu. Rev. Microbiol.*, vol. 45, pp. 37–67, 1991, doi: 10.1146/annurev.mi.45.100191.000345.

[31] L. E. Hancock, B. E. Murray, and J. Sillanpää, *Enterococcal Cell Wall Components and Structures*. Massachusetts Eye and Ear Infirmary, 2014.

[32] J. van Heijenoort and L. Gutmann, “Correlation between the structure of the bacterial peptidoglycan monomer unit, the specificity of transpeptidation, and susceptibility to beta -lactams,” *Proc. Natl. Acad. Sci.*, vol. 97, no. 10, pp. 5028–5030, May 2000, doi: 10.1073/pnas.97.10.5028.

[33] E. Y. Klein *et al.*, “Supporting Information Appendix for Global increase and geographic convergence in antibiotic consumption between 2000 and 2015.”

[34] L. Borgianni *et al.*, “Mutational Analysis of VIM-2 Reveals an Essential Determinant for Metallo-Lactamase Stability and Folding,” *Antimicrob. Agents Chemother.*, vol. 54, no. 8, pp. 3197–3204, 2010, doi: 10.1128/AAC.01336-09.

[35] A. J. Fratoni, D. P. Nicolau, and J. L. Kuti, “A guide to therapeutic drug monitoring of β-lactam antibiotics,” *Pharmacother. J. Hum. Pharmacol. Drug Ther.*, vol. 41, no. 2, pp. 220–233, Feb. 2021, doi: https://doi.org/10.1002/phar.2505.

[36] D. Lee, S. Das, N. L. Dawson, D. Dobrijevic, J. Ward, and C. Orengo, “Novel Computational Protocols for Functionally Classifying and Characterising Serine Beta-Lactamases,” *PLoS Comput. Biol.*, vol. 12, no. 6, Jun. 2016, doi: 10.1371/journal.pcbi.1004926.

[37] T. Sawa, K. Kooguchi, and K. Moriyama, “Molecular diversity of extended-spectrum β-lactamases and carbapenemases, and antimicrobial resistance,” *J. Intensive Care*, vol. 8, no. 1, p. 13, Dec. 2020, doi: 10.1186/s40560-020-0429-6.

[38] K. Bush, G. A. Jacoby, and A. A. Medeiros, “A functional classification scheme for beta-lactamases and its correlation with molecular structure,” *Antimicrob. Agents Chemother.*, vol. 39, no. 6, pp. 1211–1233, Jun. 1995, doi: 10.1128/AAC.39.6.1211.

[39] R. P. Ambler, “The structure of β-lactamases,” *Philos. Trans. R. Soc. London. B, Biol. Sci.*, vol. 289, no. 1036, pp. 321–331, May 1980, doi: 10.1098/rstb.1980.0049.

[40] C. L. Tooke *et al.*, “β-Lactamases and β-Lactamase Inhibitors in the 21st Century,” *J. Mol. Biol.*, vol. 431, no. 18, pp. 3472–3500, Aug. 2019, doi: 10.1016/j.jmb.2019.04.002.

[41] P. Yang, Y. Chen, S. Jiang, P. Shen, X. Lu, and Y. Xiao, “Association between antibiotic consumption and the rate of carbapenem-resistant Gram-negative bacteria from China based on 153 tertiary hospitals data in 2014,” *Antimicrob. Resist. Infect. Control*, vol. 7, no. 1, p. 137, Dec. 2018, doi: 10.1186/s13756-018-0430-1.

[42] G. Garau *et al.*, “Update of the Standard Numbering Scheme for Class B β-Lactamases,” *Antimicrob. Agents Chemother.*, vol. 48, no. 7, pp. 2347–2349, Jul. 2004, doi: 10.1128/AAC.48.7.2347-2349.2004.

[43] L. Lauretti *et al.*, “Cloning and Characterization of bla VIM , a New Integron-Borne Metallo-β-Lactamase Gene from a Pseudomonas aeruginosa Clinical Isolate,” *Antimicrob. Agents Chemother.*, vol. 43, no. 7, pp. 1584–1590, Jul. 1999, doi: 10.1128/AAC.43.7.1584.

[44] R. F. Potter, A. W. D’Souza, and G. Dantas, “The rapid spread of carbapenem-resistant Enterobacteriaceae,” *Drug Resist. Updat.*, vol. 29, pp. 30–46, Nov. 2016, doi: 10.1016/j.drup.2016.09.002.

[45] M. C. Persoon *et al.*, “Mortality related to Verona Integron-encoded Metallo-β-lactamase-positive Pseudomonas aeruginosa: assessment by a novel clinical tool,” *Antimicrob. Resist. Infect. Control*, vol. 8, no. 1, p. 107, Dec. 2019, doi: 10.1186/s13756-019-0556-9.

[46] G. Cabot *et al.*, “Overexpression of AmpC and efflux pumps in Pseudomonas aeruginosa isolates from bloodstream infections: prevalence and impact on resistance in a Spanish multicenter study,” *Antimicrob. Agents Chemother.*, vol. 55, no. 5, pp. 1906–1911, May 2011, doi: 10.1128/AAC.01645-10.

[47] P. Nordmann, T. Naas, and L. Poirel, “Global Spread of Carbapenemase-producing Enterobacteriaceae,” *Emerg. Infect. Dis.*, vol. 17, no. 10, pp. 1791–1798, Oct. 2011, doi: 10.3201/eid1710.110655.

[48] V. Miriagou *et al.*, “Sequence of pNL194, a 79.3-Kilobase IncN Plasmid Carrying the blaVIM-1 Metallo-β-Lactamase Gene in Klebsiella pneumoniae,” *Antimicrob. Agents Chemother.*, vol. 54, no. 10, pp. 4497–4502, Oct. 2010, doi: 10.1128/AAC.00665-10.

[49] L. Falgenhauer *et al.*, “Comparative genome analysis of IncHI2 VIM-1 carbapenemase-encoding plasmids of Escherichia coli and Salmonella enterica isolated from a livestock farm in Germany,” *Vet. Microbiol.*, vol. 200, pp. 114–117, Feb. 2017, doi: 10.1016/j.vetmic.2015.09.001.

[50] A. Makena *et al.*, “Comparison of Verona Integron-Borne Metallo-β-Lactamase (VIM) Variants Reveals Differences in Stability and Inhibition Profiles,” *Antimicrob. Agents Chemother.*, vol. 60, no. 3, pp. 1377–1384, Mar. 2016, doi: 10.1128/AAC.01768-15.

[51] T. Naas *et al.*, “Beta-lactamase database (BLDB) – structure and function,” *J. Enzyme Inhib. Med. Chem.*, vol. 32, no. 1, pp. 917–919, Jan. 2017, doi: 10.1080/14756366.2017.1344235.

[52] M. A. Toleman, K. Rolston, R. N. Jones, and T. R. Walsh, “bla VIM-7, an Evolutionarily Distinct Metallo-β-Lactamase Gene in a Pseudomonas aeruginosa Isolate from the United States,” *Antimicrob. Agents Chemother.*, vol. 48, no. 1, pp. 329–332, Jan. 2004, doi: 10.1128/AAC.48.1.329-332.2004.

[53] V. A. Simossis, “Homology-extended sequence alignment,” *Nucleic Acids Res.*, vol. 33, no. 3, pp. 816–824, Feb. 2005, doi: 10.1093/nar/gki233.

[54] M. I. Page and A. Badarau, “The Mechanisms of Catalysis by Metallo -Lactamases,”

Bioinorg. Chem. Appl., vol. 2008, pp. 1–14, 2008, doi: 10.1155/2008/576297.

[55] R. Salimraj *et al.*, "Crystal structures of VIM-1 complexes explain active site heterogeneity in VIM-class metallo-β-lactamases," *FEBS J.*, vol. 286, no. 1, pp. 169–183, Jan. 2019, doi: 10.1111/febs.14695.

[56] A. Makena *et al.*, "Comparison of Verona Integron-Borne Metallo-β-Lactamase (VIM) Variants Reveals Differences in Stability and Inhibition Profiles," *Antimicrob. Agents Chemother.*, vol. 60, no. 3, pp. 1377–1384, Mar. 2016, doi: 10.1128/AAC.01768-15.

[57] K. Bush and P. A. Bradford, "Interplay between β-lactamases and new β-lactamase inhibitors," *Nat. Rev. Microbiol.*, vol. 17, no. 5, pp. 295–306, May 2019, doi: 10.1038/s41579-019-0159-8.

[58] P. Markou and Y. Apidianakis, "Pathogenesis of intestinal Pseudomonas aeruginosa infection in patients with cancer," *Front. Cell. Infect. Microbiol.*, vol. 3, p. 115, Jan. 2014, doi: 10.3389/fcimb.2013.00115.

[59] M. V Edelstein *et al.*, "Spread of extensively resistant VIM-2-positive ST235 Pseudomonas aeruginosa in Belarus, Kazakhstan, and Russia: a longitudinal epidemiological and clinical study," *Lancet Infect. Dis.*, vol. 13, no. 10, pp. 867–876, Oct. 2013, doi: 10.1016/S1473-3099(13)70168-3.

[60] J. Morán-Barrio, A. S. Limansky, and A. M. Viale, "Secretion of GOB Metallo-β-Lactamase in Escherichia coli Depends Strictly on the Cooperation between the Cytoplasmic DnaK Chaperone System and the Sec Machinery: Completion of Folding and Zn(II) Ion Acquisition Occur in the Bacterial Periplasm," *Antimicrob. Agents Chemother.*, vol. 53, no. 7, pp. 2908–2917, Jul. 2009, doi: 10.1128/AAC.01637-08.

[61] S. M. Drawz and R. A. Bonomo, "Three Decades of β-Lactamase Inhibitors," *Clin. Microbiol. Rev.*, vol. 23, no. 1, pp. 160–201, Jan. 2010, doi: 10.1128/CMR.00037-09.

[62] N. R. Khanna and V. Gerriets, *Beta Lactamase Inhibitors*. StatPearls Publishing, 2022.

[63] D. M. Livermore, "Multiple Mechanisms of Antimicrobial Resistance in Pseudomonas aeruginosa: Our Worst Nightmare?," *Clin. Infect. Dis.*, vol. 34, no. 5, pp. 634–640, Mar. 2002, doi: 10.1086/338782.

[64] A. Potron, L. Poirel, and P. Nordmann, "Emerging broad-spectrum resistance in Pseudomonas aeruginosa and Acinetobacter baumannii : Mechanisms and epidemiology," *Int. J. Antimicrob. Agents*, vol. 45, no. 6, pp. 568–585, Jun. 2015, doi: 10.1016/j.ijantimicag.2015.03.001.

[65] D. Rawat and D. Nair, "Extended-spectrum ß-lactamases in gram negative bacteria," *J. Glob. Infect. Dis.*, vol. 2, no. 3, p. 263, 2010, doi: 10.4103/0974-777X.68531.

[66] D. L. Paterson, "Recommendation for treatment of severe infections caused by Enterobacteriaceae producing extended-spectrum β-lactamases (ESBLs)," *Clin. Microbiol. Infect.*, vol. 6, no. 9, pp. 460–463, Sep. 2000, doi: 10.1046/j.1469-0691.2000.00107.x.

[67] J. C. Vázquez-Ucha, J. Arca-Suárez, G. Bou, and A. Beceiro, "New carbapenemase inhibitors: Clearing the way for the β-lactams," *Int. J. Mol. Sci.*, vol. 21, no. 23, pp. 1–

32, 2020, doi: 10.3390/ijms21239308.

[68] R. M. Lu *et al.*, “Development of therapeutic antibodies for the treatment of diseases,” *J. Biomed. Sci.*, vol. 27, no. 1, pp. 1–30, 2020, doi: 10.1186/s12929-019-0592-z.

[69] S. J. Hecker *et al.*, “Discovery of Cyclic Boronic Acid QPX7728, an Ultrabroad-Spectrum Inhibitor of Serine and Metallo-β-lactamases,” *J. Med. Chem.*, vol. 63, no. 14, pp. 7491–7507, Jul. 2020, doi: 10.1021/acs.jmedchem.9b01976.

[70] N. Jones, B. Ray, K. T. Ranjit, and A. C. Manna, “Antibacterial activity of ZnO nanoparticle suspensions on a broad spectrum of microorganisms,” *FEMS Microbiol. Lett.*, vol. 279, no. 1, pp. 71–76, Feb. 2008, doi: 10.1111/j.1574-6968.2007.01012.x.

[71] T.-N. Phan, T. Buckner, J. Sheng, J. D. Baldeck, and R. E. Marquis, “Physiologic actions of zinc related to inhibition of acid and alkali production by oral streptococci in suspensions and biofilms.,” *Oral Microbiol. Immunol.*, vol. 19, no. 1, pp. 31–38, Feb. 2004, doi: 10.1046/j.0902-0055.2003.00109.x.

[72] J. A. Lemire, J. J. Harrison, and R. J. Turner, “Antimicrobial activity of metals: mechanisms, molecular targets and applications,” *Nat. Rev. Microbiol.*, vol. 11, no. 6, pp. 371–384, Jun. 2013, doi: 10.1038/nrmicro3028.

[73] J. Zhang, Y. Liu, Q. Li, X. Zhang, and J. K. Shang, “Antifungal Activity and Mechanism of Palladium-Modified Nitrogen-Doped Titanium Oxide Photocatalyst on Agricultural Pathogenic Fungi Fusarium graminearum,” *ACS Appl. Mater. Interfaces*, vol. 5, no. 21, pp. 10953–10959, Nov. 2013, doi: 10.1021/am4031196.

[74] N.-Y. T. Nguyen, N. Grelling, C. L. Wetteland, R. Rosario, and H. Liu, “Antimicrobial Activities and Mechanisms of Magnesium Oxide Nanoparticles (nMgO) against Pathogenic Bacteria, Yeasts, and Biofilms,” *Sci. Rep.*, vol. 8, no. 1, p. 16260, Dec. 2018, doi: 10.1038/s41598-018-34567-5.

[75] G. Vimbela, S. M. Ngo, C. Fraze, L. Yang, and D. A. Stout, “Antibacterial properties and toxicity from metallic nanomaterials,” *Int. J. Nanomedicine*, vol. Volume 12, pp. 3941–3965, May 2017, doi: 10.2147/IJN.S134526.

[76] C. Mollard *et al.*, “Thiomandelic Acid, a Broad Spectrum Inhibitor of Zinc-Lactamases,” *J. Biol. Chem.*, vol. 276, no. 48, pp. 45015–45023, 2001, doi: 10.1074/jbc.M107054200.

[77] T. R. Walsh, M. A. Toleman, L. Poirel, and P. Nordmann, “Metallo-Lactamases: the Quiet before the Storm?,” *Clin. Microbiol. Rev.*, vol. 18, no. 2, pp. 306–325, 2005, doi: 10.1128/CMR.18.2.306-325.2005.

[78] B. Ma *et al.*, “The antimicrobial peptide thanatin disrupts the bacterial outer membrane and inactivates the NDM-1 metallo-β-lactamase,” *Nat. Commun.*, vol. 10, no. 1, p. 3517, Dec. 2019, doi: 10.1038/s41467-019-11503-3.

[79] J. S. Sohier *et al.*, “Allosteric inhibition of VIM metallo-β-lactamases by a camelid nanobody,” *Biochem. J.*, vol. 450, no. 3, pp. 477–486, Mar. 2013, doi: 10.1042/BJ20121305.

[80] R. Woodman, J. T.-H. Yeh, S. Laurenson, and P. K. Ferrigno, “Design and Validation of a Neutral Protein Scaffold for the Presentation of Peptide Aptamers,” *J. Mol. Biol.*, vol. 352, no. 5, pp. 1118–1133, Oct. 2005, doi: 10.1016/j.jmb.2005.08.001.

[81] C. Tiede *et al.*, “Adhiron: a stable and versatile peptide display scaffold for molecular recognition applications,” *Protein Eng. Des. Sel.*, vol. 27, no. 5, pp. 145–155, May 2014, doi: 10.1093/protein/gzu007.

[82] E. Koutsoumpeli *et al.*, “Antibody Mimetics for the Detection of Small Organic Compounds Using a Quartz Crystal Microbalance,” *Anal. Chem.*, vol. 89, no. 5, pp. 3051–3058, Mar. 2017, doi: 10.1021/acs.analchem.6b04790.

[83] A. Lopata *et al.*, “Affimer proteins for F-actin: novel affinity reagents that label F-actin in live and fixed cells,” *Sci. Rep.*, vol. 8, no. 1, p. 6572, Dec. 2018, doi: 10.1038/s41598-018-24953-4.

[84] R. Sharma *et al.*, “Label-free electrochemical impedance biosensor to detect human interleukin-8 in serum with sub-pg/ml sensitivity,” *Biosens. Bioelectron.*, vol. 80, pp. 607–613, Jun. 2016, doi: 10.1016/j.bios.2016.02.028.

[85] J. I. Robinson *et al.*, “Affimer proteins inhibit immune complex binding to FcγRIIIa with high specificity through competitive and allosteric modes of action,” *Proc. Natl. Acad. Sci.*, vol. 115, no. 1, pp. E72–E81, Jan. 2018, doi: 10.1073/pnas.1707856115.

[86] K. Z. Haza *et al.*, “RAS-inhibiting biologics identify and probe druggable pockets including an SII-α3 allosteric site,” *bioRxiv*, p. 2020.06.04.133728, Jan. 2020, doi: 10.1101/2020.06.04.133728.

[87] A. Herbert, “Affimer Inhibition of New Delhi Metallo β-Lactamase 1,” 2020.

[88] L. De Faveri, “Modulation of New Delhi Metallo-β-Lactamase-1 activity using Affimers,” 2019.

[89] G. Kaplan and J. M. Gershoni, “A general insert label for peptide display on chimeric filamentous bacteriophages,” *Anal. Biochem.*, vol. 420, no. 1, pp. 68–72, Jan. 2012, doi: 10.1016/j.ab.2011.08.050.

[90] G. T. Hess *et al.*, “M13 Bacteriophage Display Framework That Allows Sortase-Mediated Modification of Surface-Accessible Phage Proteins,” *Bioconjug. Chem.*, vol. 23, no. 7, pp. 1478–1487, Jul. 2012, doi: 10.1021/bc300130z.

[91] R. M. Horton, Z. Cai, S. M. Ho, and L. R. Pease, “Gene splicing by overlap extension: tailor-made genes using the polymerase chain reaction. BioTechniques 8(5):528-535 (November 1990).,” *Biotechniques*, vol. 54, no. 3, pp. 129–133, Mar. 2013, doi: 10.2144/000114017.

[92] A. S. Khalil *et al.*, “Single M13 bacteriophage tethering and stretching,” *Proc. Natl. Acad. Sci.*, vol. 104, no. 12, pp. 4892–4897, Mar. 2007, doi: 10.1073/pnas.0605727104.

[93] J. Rakonjac, N. J. Bennett, J. Spagnuolo, D. Gagic, and M. Russel, “Filamentous Bacteriophage: Biology, Phage Display and Nanotechnology Applications,” 2011. doi: 011;13(2):51-76. Epub 2011 Apr 18.

[94] F. Karlsson, C. A. K. Borrebaeck, N. Nilsson, and A.-C. Malmborg-Hager, “The Mechanism of Bacterial Infection by Filamentous Phages Involves Molecular Interactions between TolA and Phage Protein 3 Domains,” *J. Bacteriol.*, vol. 185, no. 8, pp. 2628–2634, 2003, doi: 10.1128/JB.185.8.2628-2634.2003.

[95] A. A. S. Tang, C. Tiede, D. J. Hughes, M. McPherson, and D. C. Tomlinson, “Isolation of isoform-specific binding proteins (Affimers) by phage display using negative selection,” *Sci. Signal.*, vol. 10, no. 505, Nov. 2017, doi: 10.1126/scisignal.aan0868.

[96] D. J. Christensen, E. B. Gottlin, R. E. Benson, and P. T. Hamilton, “Phage display for target-based antibacterial drug discovery.,” *Drug Discov. Today*, vol. 6, no. 14, pp. 721–727, Jul. 2001, doi: 10.1016/s1359-6446(01)01853-0.

[97] M. Fairhead and M. Howarth, “Site-specific biotinylation of purified proteins using BirA.,” *Methods Mol. Biol.*, vol. 1266, pp. 171–84, 2015, doi: 10.1007/978-1-4939-2272-7_12.

[98] E. Gasteiger, A. Gattiker, C. Hoogland, I. Ivanyi, R. D. Appel, and A. Bairoch, “ExPASy: The proteomics server for in-depth protein knowledge and analysis.,” *Nucleic Acids Res.*, vol. 31, no. 13, pp. 3784–8, Jul. 2003, doi: 10.1093/nar/gkg563.

[99] T. (University of Leeds), Christian, “Kingfisher Flex protocol ‘Phage Display standard.’” pp. 9–11, 2019.

[100] M. C. F. Thomsen and M. Nielsen, “Seq2Logo: a method for construction and visualization of amino acid binding motifs and sequence profiles including sequence weighting, pseudo counts and two-sided representation of amino acid enrichment and depletion.,” *Nucleic Acids Res.*, vol. 40, no. Web Server issue, pp. W281-7, Jul. 2012, doi: 10.1093/nar/gks469.

[101] N. J. Yang and M. J. Hinner, “Getting Across the Cell Membrane: An Overview for Small Molecules, Peptides, and Proteins,” 2015, pp. 29–53.

[102] L. J. González, G. Bahr, T. G. Nakashige, E. M. Nolan, R. A. Bonomo, and alejandro J. Vila, “Membrane anchoring stabilizes and favors secretion of New Delhi metallo-β-lactamase,” *Nat. Chem. Biol.*, vol. 12, no. 7, pp. 516–522, Jul. 2016, doi: 10.1038/nchembio.2083.

[103] S. El-Andaloussi, T. Holm, and U. Langel, “Cell-Penetrating Peptides: Mechanisms and Applications,” *Curr. Pharm. Des.*, vol. 11, no. 28, pp. 3597–3611, Nov. 2005, doi: 10.2174/138161205774580796.

[104] N. Nekhotiaeva, A. Elmquist, G. Rajarao, M. Hällbrink, U. Langel, and L. Good, “Cell entry and antimicrobial properties of eukaryotic cell-penetrating peptides,” *FASEB J.*, vol. 18, pp. 394–396, Mar. 2004, doi: 10.1096/fj.03-0449fje.

[105] M. F. N. Abushahba, H. Mohammad, S. Thangamani, A. A. A. Hussein, and M. N. Seleem, “Impact of different cell penetrating peptides on the efficacy of antisense therapeutics for targeting intracellular pathogens OPEN,” 2016, doi: 10.1038/srep20832.

[106] J. S. Lee and J. Feijen, “Polymersomes for drug delivery: design, formation and characterization.,” *J. Control. Release*, vol. 161, no. 2, pp. 473–483, Jul. 2012, doi:

10.1016/j.jconrel.2011.10.005.

[107] X.-Y. Zhang and P.-Y. Zhang, “Current Nanoscience,” 2017, doi: 10.2174/1573413712666161018 1.

[108] F. Ahmed *et al.*, “Shrinkage of a rapidly growing tumor by drug-loaded polymersomes: pH-triggered release through copolymer degradation.,” *Mol. Pharm.*, vol. 3, no. 3, pp. 340–350, 2006, doi: 10.1021/mp050103u.

[109] R. Sharma *et al.*, “Adaptive Laboratory Evolution of Antibiotic Resistance Using Different Selection Regimes Lead to Similar Phenotypes and Genotypes,” *Front. Microbiol. | www.frontiersin.org*, vol. 1, p. 816, 2017, doi: 10.3389/fmicb.2017.00816.

[110] Avacta, “No immunogenicity issues for Affimer technology,” 2017. https://avacta.com/2017-05-18/.

[111] M. Krishna and S. G. Nadler, “Immunogenicity to Biotherapeutics – The Role of Anti-drug Immune Complexes,” *Front. Immunol.*, vol. 7, p. 21, Feb. 2016, doi: 10.3389/fimmu.2016.00021.